GEM TN-92-170

GEM Detector BaF_2 Precision EM Calorimeter Selection Report

California Institute of Technology; University of California, San Diego; Princeton University; Carnegie Mellon University; Brookhaven National Laboratory; Oak Ridge National Laboratory; Lawrence Livermore National Laboratory; Shanghai Institute of Ceramics; Beijing Glass Research Institute; Beijing Institute of High Energy Physics; Beijing University; Shanghai Institute of Nuclear Physics; Tongji University; Tsinghua University; University of Science and Technology, Hefei; Zhongnan Optical Instrument Facility; and Tata Institute of Fundamental Research

August 31, 1992

Abstract:

Answers to questions from the GEM Collaboration concerning the BaF_2 Precision EM Calorimeter option.

GEM DETECTOR
BaF_2 PRECISION EM CALORIMETER
SELECTION REPORT

By

California Institute of Technology
University of California, San Diego
Princeton University
Carnegie Mellon University
Brookhaven National Laboratory
Oak Ridge National Laboratory
Lawrence Livermore National Laboratory
Shanghai Institute of Ceramics
Beijing Glass Research Institute
Beijing Institute of High Energy Physics
Beijing University
Shanghai Institute of Nuclear Physics
Tongji University
Tsinghua University
Univ. of Science and Technology, Hefei
Zhongnan Optical Instrument Facility
Tata Institute of Fundamental Research

August 31,1992

THE BaF_2 COLLABORATION

G. Gratta, M. Gruenewald, D. Kirkby, W. Lu, R. Mount,
H. Newman, S. Shevchenko, X. Shi, R.Y. Zhu, D. Ma
California Institute of Technology, *Pasadena, California, U.S.A.*

D. Asner, J. Branson, H. Kobrak, R. Swanson
University of California, *San Diego, California, U.S.A.*

P. Denes, M. Ito, D. Marlow, P. Piroue, B. Sadeghi, D. Stickland
Princeton University, *Princeton, New Jersey, U.S.A.*

A. Engler, T. Ferguson, R. Kramer, R. Sutton, H. Vogel
Carnegie Mellon University, *Pittsburgh, Pennsylvania, U.S.A.*

J.A. Kierstead, P.W. Levy, S. Stoll, A. Weingarten, C.L. Woody
Brookhaven National Laboratory, *Upton, New York, U.S.A.*

M. Bauer, C. Britton, H. Cohn, J. Heck, F. Plasil, K. Read,
M. Rennich, A. Wintenberg
Oak Ridge National Laboratory, *Oak Ridge, Tennessee, U.S.A.*

B. Fuchs, W. Kway, C. Loomis, D. Makowiecki, T. Saito, C. Wuest
Lawrence Livermore National Laboratory, *Livermore, California, U.S.A.*

X.L. Fang, P.X. Gu, J.K. Guo, G.Q. Hu, S.K. Hua, Z.D. Ji, P.J. Li,
D.Z. Shen, G.S. Shen, E.W. Shi, W.T. Su, Z.Y. Wei, Y.Y. Xie, L. Xu,
Z.L. Xue, D.S. Yan, Z.W. Yin, X.L. Yuan, G.M. Zhao, Y.L Zhao,
W.Z. Zhong, R.M. Zhou
Shanghai Institute of Ceramics, *Shanghai, China*

G. Chen, Z.Z. Dai, X.Y. Dong, Y.C. Gao, T.Z. Li, G.T. Liu,
Z.Q. Liu, S.Q. Man, S.X. Ren, Z.L. Su, Y.T. Wang, O. Wen, H. Xiao,
H.Z. Yang, F.C. Zhang, F.Y. Zhang, J.Q. Zhang, J. Zhang, Y.N. Zheng
Beijing Glass Research Institute, *Beijing, China*

Xiang-zong Chui, Yuan-ning Gao, Wei-xin Gu, Yi-fan Gu, Ya-nan Guo, Yi-zhi Huang, Chun-hua Jiang, Jin Li, Zhi-gang LI, Cheng-sheng Mao, Ze-pu Mao, Hua-yi Sheng, Yun-yong Wang, Man Wang, De-ming Xi, Yi-gang Xie, Rong-sheng Xu, Chuan-song Yu, Da-hua Zhang, Bing-yun Zhang, Chang-chun Zhang, Jia-quan Zhang, Yu Zhang, Di-xin Zhao, Jing-wei Zhao, Bao-an Zhuang
Insitute of High Energy Physics, *Beijing, China*

Zu-he Bian, Ming-fu Cai, Yang-mei Fan, Rong-dian Han, Lu-yuan Hao, Xin-si Lin, Bao-an Liu, We Mei, Qi-cun Shi, Hui-min Wang, Zhong-min Wang, Shu-lan Wu, Shi-lin Xing, Ji-hua Xu, Ke-zun Xu, Xiao-liang Xu, Bing-xin Yang, Bang-jiao Ye, Xiao-qi Yu, Jie Zhang, Yong-zhao Zhou
University of Science and Technology, *Hefei, China*

L.Y. Chen, J. Du, M. Gu, J. Wang, L.M. Wang, X. Wu, K.H. Xiang, W.H. Zheng
Tongji University, *Shanghai, China*

Ji-gang An, Ke-jun Kang, Yuzheng Lin, Gui-lin Liu, Da-wei Mai, Wei-dou Ni, Ren-cheng Shang, Jing-jin Wang, Si-da Xu, Zhan Xu, Jing-yi Zhang
Tsinghua University, *Shanghai, China*

Dong-xing Jiang, Chu-xi Lai, Hong-tau Liu, Song-jiang Xia, Yan-lin Ye
Beijing University, *Beijing, China*

J.R. Bao, D.X. Cao, S.M. Chen, D.Z. Jiang, X.P. Li, S.H.Lin, H.Z. Liu, T.W. Rong, K.L. Sheng, L.R. Shen, H.H. Wan, F.H. Yu, W.H. Zheng, D.Z. Zhu, F.Y. Zhu
Shanghai Institute of Nuclear Research, *Shanghai, China*

Zhongnan Optical Instrument Facility, *Zhicheng, China*

T. Aziz, S. Banerjee, S. Ganguli, S. Gupta, A. Gurtu, R. Raghavan, K. Sudhakar, S. Tonwar
Tata Institute of Fundamental Research, *Bombay, India*

Contact Person:
Harvey B. Newman
256-48
High Energy Physics
Caltech
Pasadena, CA 91125

Phone (818)-356-6656
Fax (818)-795-3951

1 Introduction

The Barium Fluoride (BaF_2) calorimeter, composed of 16,000 crystal pairs, is one of the two options being pursued by the GEM Collaboration as a candidate precision electromagnetic (EM) calorimeter. The purpose of this report is to:

- Propose that GEM adopt the BaF_2 crystal system now, as its precision EM calorimeter. This is based on the increased physics discovery potential which the high electron and photon resolution brings to the experiment, together with the current state of understanding of the means of controlling the radiation damage, and precision calibration and monitoring of the system during running.
- Respond to GEM's Requirements for the BaF_2 technology, as formulated by the GEM Executive Committee (listed in Appendix A). Over the last year, substantial progress has been made on the R&D and the design of the Precision BaF_2 Crystal EM Calorimeter. We discuss our progress in demonstrating, through tests and simulations, that the calorimeter system will operate in the high radiation SSC environment, with sufficient uniformity, stability and calibration accuracy to reach the design resolution of $2.0\%/\sqrt{E} \oplus 0.5\%$.
- Summarize the status of the production plan, and the ability to manufacture the finished crystal pairs in China for GEM, at a fixed price of \$ 2.5/cc. The crystals will be mounted in a thin (100 μm wall) laser-welded titanium alloy structure, based on the experience of the L3 and Crystal Barrel detectors, with a minimum of inactive material between or in front of the crystals. The support structure also is planned to be manufactured in China.

The BaF_2 electromagnetic calorimeter's intrinsic energy resolution of $2.0\%/\sqrt{E} \oplus 0.5\%$ is comparable to the performance achieved by the L3 Collaboration with the BGO electromagnetic calorimeter [1], as demonstrated at test beams at Cornell in 1985 and at the CERN SPS in 1987 - 1989.

The speed, radiation hardness, fine granularity, uniform coverage and large acceptance of the BaF_2 calorimeter result in an excellent precision electromagnetic calorimeter for the SSC. The increased physics discovery potential which a precision EM calorimeter of this type can bring to a major SSC Detector has been widely recognized over the last five years. This is illustrated, in the context of the Standard Model, by its superior ability to detect the Intermediate Mass Higgs through its decays $H^0 \rightarrow \gamma\gamma$, $H^0 \rightarrow (\mu/e)\gamma\gamma + X$

(80 - 140 GeV), and $H^0 \rightarrow e^+e^-$ (140 - 170 GeV) [2]. Beyond the Standard Model, a BaF_2 calorimeter with the specified resolution would provide increased sensitivity for the detection of new narrow states decaying into multi-leptons and/or photons.

The program to develop a BaF_2 precision EM calorimeter was initiated in 1991 by an international collaboration of 13 institutions in the U.S., China and India, with partial support from the SSC Subsystem R&D and DoE/HEP programs. In the Fall of 1991, the GEM Collaboration [3] adopted the high precision BaF_2 EM calorimeter – in combination with a scintillating fiber hadron calorimeter (HCAL) – as one of the two principal approaches to calorimetry to be developed during 1992. (The other system is an integrated Liquid Argon system with a fine sampling "accordion" Liquid Argon, with the option of "Hybrid" system consisting of a Liquid Krypton EM section combined with a scintillating fiber HCAL).

During 1992, the Livermore National Lab in the U.S., and several additional major Chinese Institutions (Tsinghua University, the Zhongnan Optical Instrument Facility, the Shanghai Institute of Nuclear Physics and Beijing University) joined the BaF_2 Collaboration in GEM, and have substantially strengthened the BaF_2 development effort. Inter-regional coordination of the Chinese efforts on crystal manufacture and mechanical processing, through the Directorate of the Chinese Academy of Sciences, and at the ministerial level, also has begun within the last few months, with the net effect of substantially accelerating progress in these crucial parts of the BaF_2 project.

Within the last four months, Zhongnan and LLNL have rapidly advanced the state of development of mechanical processing (cutting, polishing and UV-reflective coating) of the crystals, and Tsinghua, LLNL, and ORNL have initiated the detailed engineering plan for the mechanical support. These advances, combined with the progress towards the production of appropriately radiation hard crystals at SIC and BGRI, and the discovery of the ability to control the damage effect in existing crystal by illumination with visible light (outside the range of sensitivity of the photodevices) indicate that the construction phase of the calorimeter could begin before the end of 1993, and could be completed by the end of 1997, as originally planned.

The development of a medium-scale production facility for full sized BaF_2 crystals progressed rapidly at the Shanghai Institute of Ceramics (SIC) and the Beijing Glass Research Institute (BGRI) during 1991, and an improvement program to produce crystals with the requisite radiation hardness was instituted in 1992. The crystal production facility, including a total of thirteen furnaces at the two sites, has been set up with major

funding provided by the Chinese Academy of Sciences and the Beijing Municipal government. As specified in Memoranda of Understanding signed between SIC, BGRI and Caltech in May 1991, and between SIC, BGRI and GEM in March 1992, and following a Letter of Intent signed between Zhongnan and the BaF_2 Collaboration, the Chinese institutes have agreed to provide finished mass-produced crystal pairs at a price of $ 2.5/cc.

The principal risk in choosing the higher-resolution BaF_2 crystal calorimeter for GEM is the radiation damage of the crystals. Radiation leads to the formation of light-absorbing "color centers", which reduce the transmission of light through the crystals, and hence the apparent light yield as measured by the photodevice. Conservative specifications for appropriately radiation hard crystals for GEM, expressed in terms of the transmission through the crystals after 1 MegaRad (see Reference [4]) are listed in Appendix B (also see Reference [5]).

In order to assess the risk, and to assist in the understanding and hence the solution of the radiation damage problem a "BaF_2 Panel" of internationally recognized experts on radiation damage in crystals was formed by GEM and the SSC Laboratory. Following a review of the progress towards rad-hardness achieved up until January 1992 by SIC and BGRI in China, the Panel found that the rapid progress in producing large crystals with improved radiation hardness, and the increased understanding of the principal causes of radiation damage were very promising. Based on this progress, and the fact that there are no fundamental barriers to producing crystals with the required specifications, the Panel strongly encouraged the GEM Collaboration to proceed with a program of R&D that could lead to radiation hard crystals. In addition to ongoing R&D in China and the U.S., the Panel recommended [6] a program of work designed to accelerate the progress, so that crystals with the specified radiation hardness could be produced within the required time-frame. Following the Panel's recommendations in its February Report [6], work on improvements in crystal processing, impurity and defect analysis in the crystals, radiation damage measurements with photons, neutrons and hadrons, and analysis and simulations of the response to electromagnetic showers, including possible time-dependent systematic effects was initiated as quickly as possible [5,7].

Following its last meeting in August 1992, the Panel concluded [8] that BaF_2 is intrinsically radiation hard: the radiation damage effect is definitely caused by point defects which are related to impurities in the crystals, including oxygen and hydrogen. Following irradiation tests by Woody *et al.* [9,10], it was established that the damage induced by neutrons and charged hadrons, as well as photons could be completely removed by ther-

mal annealing. This led to a strong recommendation by the Panel to pursue annealing with light as a means of controlling the radiation damage effect. This recovery effect was previously understood for BaF_2 crystals [11,12,13]), but work by a Panel member (M. Strathman) revealed that the light intensity required could be very small, making a system for light annealing *in situ* practical. After presentation of this recommendation to the GEM Caollaboration Council by the Panel, work on light annealing began immediately at BNL, LLNL, and West Virginia University. An engineering conceptual design for annealing the crystals in place, while running at the SSC, was started at ORNL and UCSD. As discussed in this report, results of the tests show that the damage at the SSC can indeed be controlled in this way, using light piped through miniature fiber bundles to each crystal pair, as the transparency of the crystals can be kept at values well above the GEM specifications (Appendix B).

Additional progress in producing large crystals with improved radiation-hardness, was achieved by SIC in the week following the August Panel meeting.

We completed the construction of the first, pre-production BaF_2 array consisting of 7×7 large crystal-pairs in 1991. The crystal-pairs were projective, and had the full length (50 cm), but were of somewhat reduced transverse size. The array was read out with UV-selective phototubes, to select the fast BaF_2 scintillation components. A beam test of the prototype array at an electron, muon and pion beam at Fermilab (experiment T-849) was completed by January 1992. The results of the analysis, presented at the GEM Tucson meeting in March, demonstrated a resolution for 68 GeV electrons of $0.77^{+0.12}_{-0.18}\%$, which was limited by the Fermilab beam momentum resolution – determined to be $0.5 \pm 0.2\%$. The result, which includes the effect of residual light collection nonuniformity (due to our simple first-round wrapping and optical coupling techniques), is consistent with the specified resolution at this energy of 0.6%.

In response to the Requirements set by the GEM Executive Committee (Appendix A.), recent progress will be presented, in this report and at the meetings prior to the GEM calorimetry decision, on:

- Work underway to improve the production of full-sized crystals (25 cm long) at the Shanghai Institute of Ceramics (SIC) and the Beijing Glass Research Institute (BGRI) in China.
- Production of small and medium size high purity crystals, aimed at improving the radiation hardness, at LLNL and Optovac.

- Radiation damage tests of large BaF_2 crystals at BNL using photons, neutrons and hadrons.

- Demonstration of the stability and linearity of a crystal and photodevice, using a cosmic ray tower and a UV light monitoring system constructed at UCSD.

- The plan for annealing the crystals during running, in such a way that the transparency is kept stably at an absorption length well above 1 meter, in excess of the specification of 0.95m set by GEM Executive Committee in March. By this method, the contribution to the constant term of the energy resolution caused by radiation-induced non-uniformities in the crystals is expected to be limited to the level of $\leq 0.15\%$. This will be achieved by monitoring the crystal transparency using the pulsed UV monitoring system (flash lamp or laser), with a short term sensitivity to changes of transmission of much better than 1%[1].

- The development of crystal pairs with light collection controlled to a maximum deviation from uniformity along the crystal of 5%, to maintain the design resolution. This includes the development of graded thin multilayer coatings of MgF_2 and Aluminum, with high reflectivity in the region of the BaF_2 fast component (220 nm) at LLNL, together with simulations and lab tests at ORNL and LLNL.

- The plan for calibration of the BaF_2 calorimeter. The absolute calibration scale will be maintained by reconstruction of inclusive $Z^0 \rightarrow e^+e^-$, with the possible additional use of $\Upsilon \rightarrow e^+e^-$ decays. Additional physics calibrations (under development) include the use of isolated minimum ionizing particles (MIPS) and electrons from b decays. The UV hydrogen lamp (190 - 250 nm) or UV laser and quartz fiber monitoring system mentioned above will be used to monitor the gain and light transmission variations on a daily basis. An additional monitoring tool is an "RFQ system", producing an intense flux of 6-7 MeV photons.

- The plan for manufacture of prototypes and then the full calorimeter, including crystal mass production at SIC and BGRI, and mechanical processing (precision cutting, lapping, polishing and application of a UV-reflective coating) at the Zhongnan Optical Instrument Factory and BGRI, resulting in the delivery of completed crystal pairs from China, at a fixed price of \$ 2.5/cc. Production of a titanium alloy support structure, is planned to be laser welded at Tsinghua University. Site

[1]Long term stability at the 0.1 - 0.2% level has been achieved in the L3 Xenon lamp system, as discussed in Section 7.3.

visits to SIC, BGRI and Zhongnan Optical Instrument factory took place in July and August to fix the engineering details and the production steps.

- Monte Carlo simulations at ORNL and Caltech, aimed at demonstrating that the BaF_2 system's resolution can be maintained, with a constant term not to exceed 0.6%. This study includes the effects of the estimated residual non-uniformity, and the estimated short and long term instabilities of the system: due to the estimated level of changes in crystal response over time, or gain shifts in the readout system.

This report summarizes some of the work, and references individual Status Reports (July, August 1992) submitted by member groups of the BaF_2 Collaboration on each of the topics listed above, for further details. Given the rapid state of development of the design and the light-annealing study, and the ongoing progress in growing crystals with improved radiation hardness, the latest work necessarily will be presented at the GEM meetings at the beginning of September.

Contents

1 Introduction **4**

2 BaF_2 Calorimeter Physics Capabilities **15**

3 The BaF_2 and Scintillating Fiber, and Liquid Argon/Krypton Calorimetry Choices for GEM **16**

4 Selection of the High Resolution BaF_2 Calorimeter For GEM **20**

5 BaF_2 EM and Scintillating Fiber HCAL Design **21**

6 BaF_2 EM Calorimeter Design **21**

6.1 Recent Progress Demonstrating the Manufacturability of the BaF_2 Calorimeter 25

7 BaF_2 Calorimeter Performance **27**

7.1 Position Resolution 27

7.2 Energy Resolution 30

7.2.1 Light Yield and Photostatistics: a_1 31

7.2.2 Electrical Noise: a_0 32

7.2.3 Physics Noise and Geometry Effects: b_S and b_G 32

7.2.4 Light Collection Nonuniformity: b_{NU} 33

7.2.5 Nonlinearities of the Photodevice, and Short Term Instabilities b_{NL} 34

7.2.6 Remaining Intercalibration Error b_C 35

7.2.7 The Energy Resolution of CLEO II CsI Calorimeter 36

7.2.8 Summary of the Computed BaF_2 Energy Resolution 37

7.3 The Energy Resolution of the L3 BGO Calorimeter 39

7.3.1 Energy Resolution in L3 39

7.3.2 Corrections to the L3 Data Included In The Resolution 44

7.3.3 Conclusions on the L3 BGO and GEM BaF_2 Resolutions 45

8 Radiation Damage in BaF_2 Crystals **50**

8.1 Summary of Progress on Radiation Damage During 8/92 50

8.1.1 Further Results on Radiation Hard Crystals From China 51

8.1.2 Annealing In Situ With Light, To Obtain Radiation Hard Crystals in GEM 51

9 Intercalibration Methods **59**

9.1 Calibration By Inclusive $Z^0 \rightarrow e^+e^-$ Reconstruction 59

9.2 MIP Calibration 60

9.3 RFQ Calibration 63

9.3.1 L3 RFQ Operation and Status 63

9.3.2 RFQ Operation Mode for GEM 64

9.3.3 Installation Plan for the RFQ Installation in GEM 67

9.3.4 RFQ Calibration Electronics Readout In GEM 69

9.3.5 Availability of a Low Cost RFQ for GEM 70

9.4 UV Flash Lamp Monitoring System (UCSD) 70

9.5 UV Laser Monitoring System (CMU) 71

10 Results of the 1991 BaF_2 Beam Test **72**

11 Detector Quality Control and Acceptance Testing **73**

12 Conclusion: The BaF_2 GEM Calorimeter 74

List of Figures

1 The significance in $H \rightarrow \gamma\gamma$ searches, as a function of SSCY for $M_H = 80, 90, 100, 120, 140, 150$ and 160 GeV, for 3 resolutions: BaF_2, LAr and typical Sampling. 17

2 The significance in $H(t\bar{t}/W) \rightarrow \gamma\gamma\ell X$ searches, as a function of SSCY for $M_H = 80, 90, 100, 120, 140, 150$ and 160 GeV, for 3 resolutions: BaF_2, LAr and typical Sampling. 18

3 The GEM BaF_2 and Scintillating Fiber Hadron Calorimeter System . . . 22

4 Design of the GEM BaF_2 Electromagnetic Calorimeter 23

5 Definition of the crystal coordinate system and $\Sigma_5, \Sigma_9, and\ \Sigma_25$ for the L3 center of gravity analysis 28

6 Distribution of the center of gravity. The curves represent the full GEANT Monte Carlo and the crosses the L3 data for Bhabha events. 29

7 PMT linearity measurement of the R2490, measured at Hamamatsu. . . . 35

8 Energy Resolution of (a) the L3 BGO calorimeter, measured at CERN test beams with 4000 crystals, and (b) the BaF_2 calorimeter, calculated with a GEANT simulation. 38

9 Comparison of the reconstructed energy distribution of an electron or positron in Bhabha events. (a) Real data (b) Monte Carlo (c) Comparison of the data with the convoluted Monte Carlo. 40

10 Schematic view of the Xenon monitoring system for the L3 BGO. 41

11 The amplitude for a typical BGO crystal, relative to the corresponding reference PMT, during a calibration period. 42

12 Comparison of the structure in θ of the gain changes measured at LEP using Bhabha events, with respect to the gains measured at the CERN X3 test beam. 43

13 The mean reconstructed energy using the impact Σ_5, Σ_9, and Σ_{25} matrices as a function of the impact point parameter ρ. 46

14 (a) The distribution of the light uniformity factors R. (b) The energy correction as a function of the incoming energy for various R values. . . . 47

15 The light collection correction for 50 GeV showers, relative to 10 GeV showers in the L3 BGO. 48

16 Transmittance of the latest 25 cm long BaF_2 crystal produced by SIC, which shows a light attenuation length of 41 cm after 1 MegaRad irradiation. 52

17 Radiation damage and recovery of crystal SIC703 (20 cm long) with exposure to light from a Mercury lamp. 53

18 Energy resolution versus maximum deviation from light collection uniformity (%). 55

19 Radiation damage and recovery of crystal SIC703 (20 cm long) with exposure to light directed through optical fibers. 56

20 Normalized ADC distribution of a crystal at different energies. 65

21 Variation of the normalized peak positions from BGO crystals. 66

22 Installation scheme for the RFQ calibrator in GEM. 68

List of Tables

1 Time Factor to Discover an 80 GeV Higgs as a Function of a and b . . . 16

2 Features of the BaF_2 Calorimeter 24

3 Summary of Contributions to the Energy Resolution of the BaF_2 Calorimeter (In Percent) 37

4 Absorption length L_{att} (cm) measured after irradiation and recovery of SIC703, with exposure to light directed through filters and optical fibers. 54

5 Number of Events Versus Precision of the Peak Position Determination, in the MIPs Calibration. 61

6 Minimum Required Time to Calibrate Crystal, With a 100 Percent Efficient MIPs Trigger. 62

7 Measured and Calculated Equivalent Photon Energy Expected from an RFQ Beam Pulse on Target. 66

2 BaF_2 Calorimeter Physics Capabilities

High precision electromagnetic (EM) calorimeters will have unique physics discovery potential at the SSC – within and **beyond** the Standard Model. GEM has thus been designed as a **Precision Lepton and Photon Detector**, where the calorimetry system is the centerpiece of the experiment. One of the principal goals of GEM's experimental design – and its R&D program – is to achieve the best feasible EM resolution, combined with good resolution for hadron jets and missing E_T.

An important potential discovery for the GEM electromagnetic calorimeter (EMC) is the Higgs boson in a mass range between 80 and 180 GeV through its $\gamma\gamma$, $\ell + \gamma\gamma + X$, and $ZZ^* \rightarrow 4\ell$ decay modes [2]. While the 4ℓ decay mode will allow GEM to detect the Higgs with a mass heavier than 140 GeV, the $\gamma\gamma$ decay mode will cover a gap between 140 GeV and the upper limit for Higgs detection at LEP Phase II (80 GeV) [14].

H$\rightarrow \gamma\gamma$ detection places stringent requirements on the overall detector design, especially on the design of the EM calorimeter. Because of the small production cross-section and the narrow decay width of the Higgs boson in this mass range, and because of the large irreducible $\gamma\gamma$ background and QCD jet background, the discovery potential is directly related to the reconstructed $\gamma\gamma$ mass resolution, and the ability of the detector to reject background.

A simple parametrization of the energy resolution of a calorimeter can be expressed as:

$$\frac{\delta E}{E} = \frac{\mathbf{a}\%}{\sqrt{E}} \oplus \mathbf{b}\% \tag{1}$$

where **a** and **b** are two constants and E is the energy being measured, in GeV. Table 1 [2] lists the time factor required to discover a narrow $\gamma\gamma$ resonance, such as the Standard Model Higgs using the $H^0 \rightarrow \gamma\gamma$ decay mode, as a function of **a** and **b**, normalized to the BaF_2 resolution **a**=2.0 and **b**=0.5. Because of the high statistics of the background, this ratio corresponds to the width of the reconstructed invariant mass peak.

Figure 1 (Reference [2], p. 46) shows the significance of the Higgs signal in the $H^0 \rightarrow \gamma\gamma$ search, as a function of the number of SSC years of running at design luminosity (1 SSCY = 10^{40}cm^{-2}). Bands are shown for EM calorimeters with the resolutions of BaF_2 $(2/\sqrt{E} \oplus 0.5)\%$, Liquid Argon $(7.5/\sqrt{E} \oplus 0.5)\%$, and a standard sampling calorimeter $(15/\sqrt{E} \oplus 1)\%$. The upper bound of each band in the figure corresponds to the irreducible background $\gamma\gamma$ background only, while the lower bound corresponds

Table 1: Time Factor to Discover an 80 GeV Higgs as a Function of a and b

a	2.0	3.0	5.5	7.5	10	15
b=0.5	1.0	1.1	1.5	1.9	2.4	3.4
b=.75	1.4	1.5	1.7	2.1	2.6	3.6
b=1.0	1.8	1.8	2.1	2.4	2.8	3.8
b=1.5	2.6	2.6	2.8	3.1	3.4	4.2
b=2.0	3.4	3.5	3.6	3.8	4.1	4.8

to the total QCD background, as discussed in Section 4.2 of [2].

Figure 2 (Reference [2], p. 56) shows the significance of the Higgs signal in the search using the rarer decay channels $Ht\bar{t} \rightarrow \gamma\gamma\ell X$ and $HW \rightarrow \gamma\gamma\ell X$ as a function of the number of SSCY, for the same six Higgs masses and EM calorimeter design resolutions. The upper bound of each band in the figure corresponds to the background level calculated in [2], while the lower bound corresponds to the background scaled up by a factor of two. It is clear from the figure that higher resolution corresponds to shorter discovery time.

The above table and figures illustrate the advantage in discovery potential which is provided by a calorimeter with a very high intrinsic EM resolution (small **a**) as well as a small systematic term (**b**), as compared to an EM calorimeter with lower resolution.

Beyond the Standard Model, the high resolution of the BaF_2 calorimeter also could be of great advantage in the detection of SUSY Higgs, where $\tilde{H} \rightarrow \gamma\gamma$ is likely to have a lower production cross section than in the Minimal Standard Model, or in the detection of new narrow resonances in Intermediate Mass range which decay to multi-electron or multi-photon final states.

3 The BaF_2 and Scintillating Fiber, and Liquid Argon/Krypton Calorimetry Choices for GEM

The high resolution, speed, and radiation resistance requirements, and the need to complete the R&D and engineering design of the optimal calorimetry system which fits within the budgetary constraints in 1992, have pointed the way towards two comple-

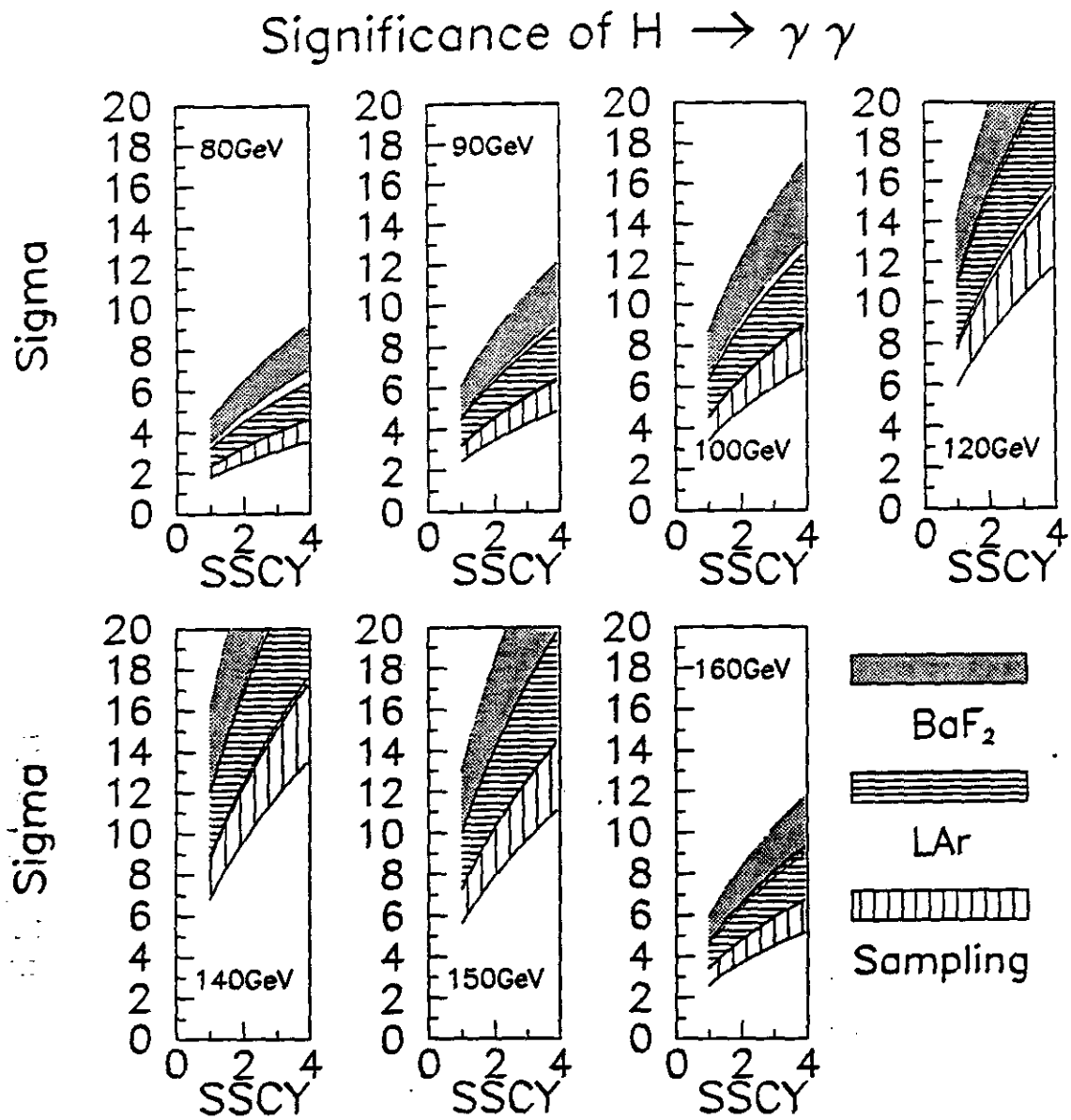

Figure 1: The significance in $H \rightarrow \gamma\gamma$ searches, as a function of SSCY for $M_H = 80, 90, 100, 120, 140, 150$ and 160 GeV, for 3 resolutions: BaF_2, LAr and typical Sampling.

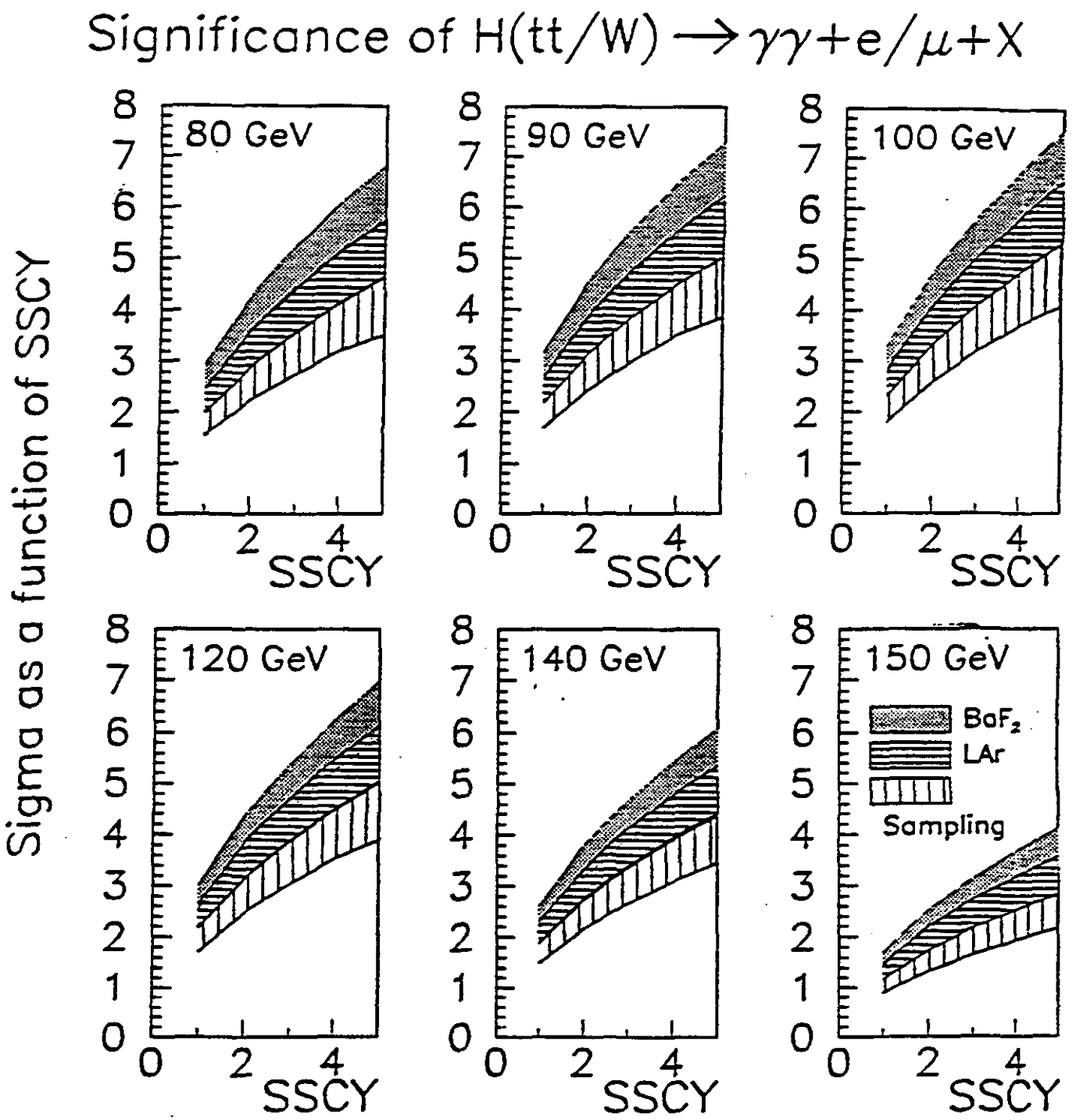

Figure 2: The significance in $H(t\bar{t}/W) \rightarrow \gamma\gamma\ell X$ searches, as a function of SSCY for $M_H = 80, 90, 100, 120, 140, 150$ and 160 GeV, for 3 resolutions: BaF_2, LAr and typical Sampling.

mentary systems[3]:

- A BaF_2 crystal high precision EM section, followed by a scintillating fiber hadron calorimeter (HCAL).
- A Liquid Argon (LAr) calorimeter with a fine sampling accordion EM section. The resolution may optionally be improved by the use of Liquid Krypton (LKr), in the EM section of a "Hybrid" system which has a scintillating fiber HCAL.

The advantages of the BaF_2 and scintillating HCAL approach are summarized below.

- **BaF_2 PRECISION CRYSTAL EM; With SCINTILLATOR HCAL**
  - Higher intrinsic EM resolution: $\sigma_E/E = (2.0/\sqrt{E} \oplus 0.5)\%$.
  - High uniformity for the EM section, leading to nearly complete rapidity coverage with high resolution for the detection of new high mass particles decaying into photons or electrons. The support structure, based on the proven carbon fiber-epoxy composite design [1] used by L3, and experience by the Crystal Barrel at CERN with thin titanium alloy foil structures, presents a minimum of dead material in front or between the crystals.
  - Higher EM and HCAL speed, resulting in a somewhat higher signal to noise ratio in an isolation cone (due to less "pileup" from uninteresting beam-beam collisions accompanying the event of interest) when searching for events containing isolated electrons or photons.
  - Effective ("tunable") compensation: the intrinsically non-compensating EM section (e/π response ratio predicted to be in the range of 1.3 - 1.5, based on laboratory tests) can be compensated by adjusting the $e/\pi \approx 1$ in the hadron calorimeter behind the BaF_2. This leads to a small constant term (below 2%) in the resolution for jets[5].
  - Higher density: one can obtain more absorption lengths for a given calorimeter radius, while maintaining the jet resolution.
  - Projective geometry, for clean EM/HCAL matching and calorimetric cluster reconstruction.

As noted in the BaF_2 Engineering Design/Cost Update report [15], a comparison of he features favoring the choice of the scintillating fiber HCAL, with those in favor of a BaF_2 EM calorimeter indicates an excellent match between the electromagnetic and hadron calorimeter technologies.

It is the special features of the BaF_2 which, if successfully implemented and combined with a high resolution muon system, would give the GEM experiment its unique physics discovery potential, and which would distinguish its physics reach substantially from the SDC experiment. This has been illustrated extensively through the simulation studies of R.Y. Zhu et al. over the last three years [2], on the search for the Higgs in the 80 - 140 GeV range through its decays into two photons, two photons accompanied by an isolated lepton (electron or muon), or four leptons, as discussed further below.

4 Selection of the High Resolution BaF_2 Calorimeter For GEM

At the time of submission of the GEM Letter of Intent [3], the GEM Executive Committee found that the higher capability BaF_2 system carried with it a higher risk. The principal issue, and the central focus of the 1992 BaF_2 R&D program, is radiation damage in mass produced crystals. Related issues are the light collection uniformity, stability of response, and precision calibration of the system, so that the high resolution of the BaF_2 system will be maintained *in situ*. The R&D program also has included the completion of the most urgent engineering tasks, which are needed to develop the BaF_2 's engineering design to a level that will demonstrate the manufacturability of the calorimeter at reasonable cost, in time for submission of the GEM Technical Design Report in early 1993.

After a review of the R&D status, and the remaining issues for the BaF_2 and the LAr/LKr calorimetry systems in February 1992, the GEM Executive Committee specified a set of requirements for each calorimeter technology. These requirements are listed in Appendix A.

Between March and August 1992, rapid advances have taken place in the understanding and means of controlling the radiation damage, and in the development of the detailed manufacturing plan and quality control for the the crystals. Substantial progress has also taken place on the design of the mechanical support, and the conceptual design of the detector assembly procedure.

The manufacturing plan includes both the technical specifications and procedures for producing finished polished crystal pairs and the calorimeter support in China, and the determination of the institutional roles in China for the final development, production, and quality control of the BaF_2 calorimeter system. If the BaF_2 technology is selected, coordination of the inter-regional Chinese involvement in the construction of the BaF_2 detector, through the leadership of the Chinese Academy of Sciences, and at the ministerial level, will help ensure that finished crystal pairs are produced for the GEM experiment at the fixed price of $ 2.5 per cc.

Given the recent developments on control of the radiation damage, the current state of understanding of the related stability and calibration issues, and the strength of the international collaboration which is prepared to construct the calorimeter on schedule, it is the opinion of the members of the BaF_2 Collaboration that the BaF_2 crystal system is the superior EM calorimeter choice for GEM. This statement is based on BaF_2 crystals of existing quality from China. It is expected that ongoing improvements in the radiation hardness of crystals produced at SIC and BGRI, will further strengthen and provide additional support for this contention, in the near-term future.

5 BaF_2 EM and Scintillating Fiber HCAL Design

The design of the BaF_2 EM calorimeter and scintillating fiber hadron calorimeter system is shown in Figure 3 [15]. The BaF_2 calorimeter layout is shown in Figure 4.

6 BaF_2 EM Calorimeter Design

Barium Fluoride (BaF_2) is a unique high density inorganic scintillator with three emission spectra peaking at 195 nm, 220 nm and 310 nm, with decay time constants of 0.87, 0.88 and 600 nsec respectively [16]. The intensity of the fast components have no temperature dependence — which should give a BaF_2 calorimeter greater intrinsic stability than the L3 BGO calorimeter — while the slow component increases with decreasing temperature at a rate of $-2.4\%/^\circ C$ [17]. The speed of the fast components enable the detector to be gated in a single beam crossing at the SSC.

The BaF_2 EM calorimeter consists of two parts:

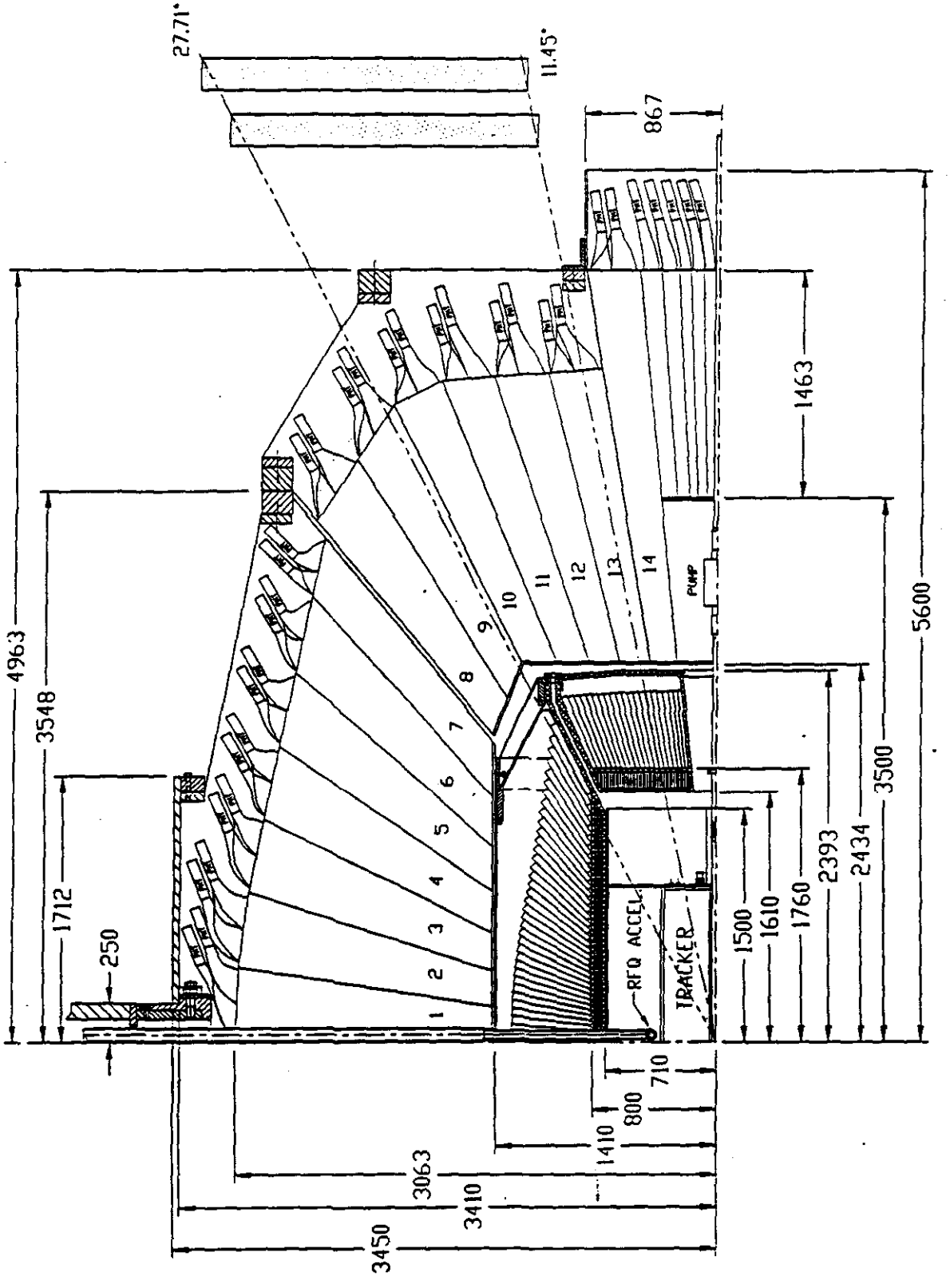

Figure 3: The GEM BaF_2 and Scintillating Fiber Hadron Calorimeter System

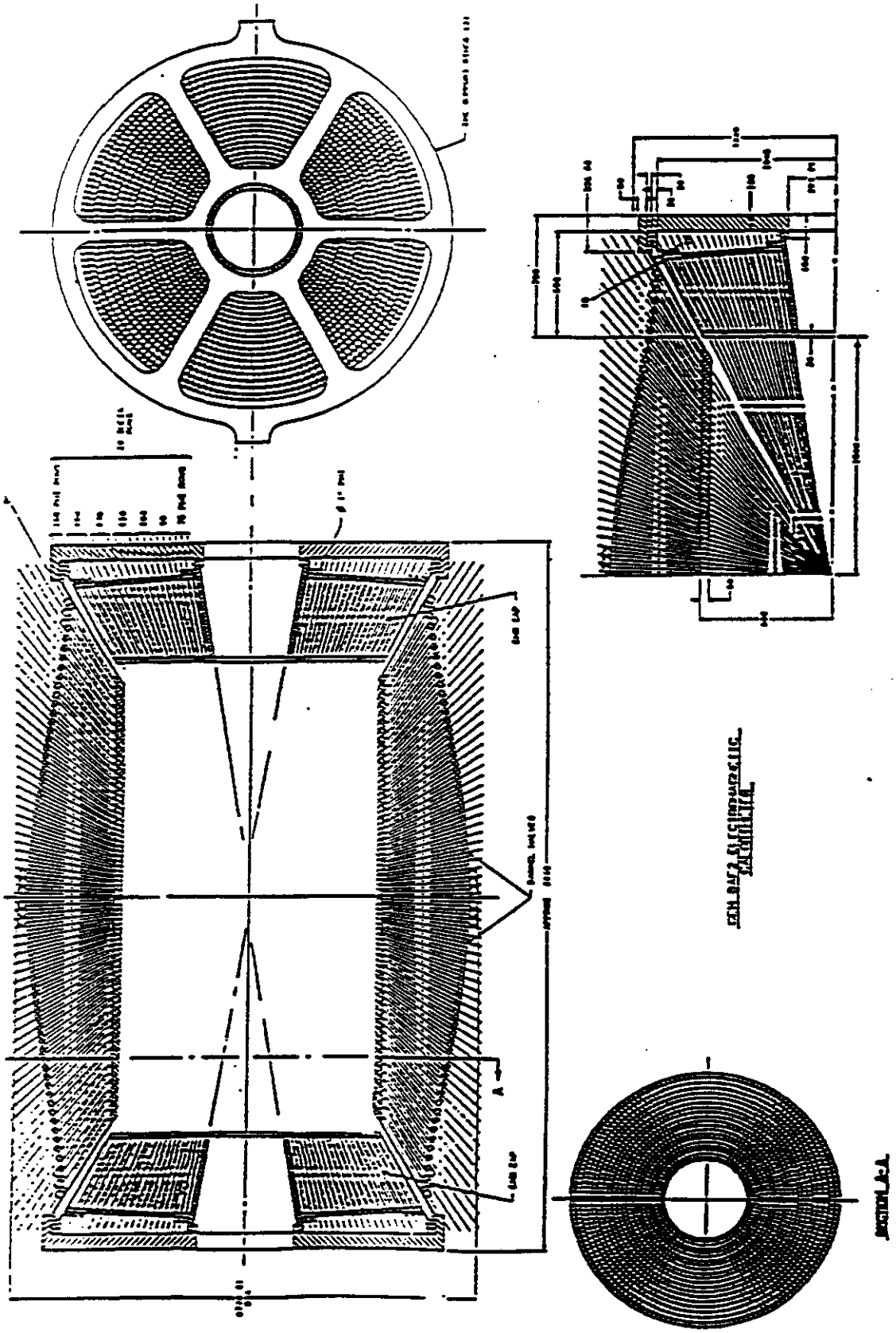

Figure 4: Design of the GEM BaF_2 Electromagnetic Calorimeter

- A central barrel calorimeter with an inner radius of 75 cm and an outer radius of 140 cm, covering a rapidity range of $|\eta| \leq 1.35$.
- Two endcaps, located at z=± 160 cm, covering a rapidity range of $1.35 \leq |\eta| \leq 3$, where only the range of $|\eta| \leq 2.5$ covered by tracking is considered active for precision electromagnetic measurements.

Table 2 shows the basic parameters of the GEM BaF_2 calorimeter.

Table 2: Features of the BaF_2 Calorimeter

Detector	Barrel	Two Endcaps
Crystal Front/Rear Face (cm^2)	3.1 × 3.1 / 5.1 × 5.1	2.3 × 2.3 / 3.0 × 3.0
Crystal Pair-Length (cm)	50	50
Crystal Pair-Number	10,880	5304
Crystal Volume (m^3)	8.4	2.4
Assembly Weight (t)	43.0	14.4

The BaF_2 calorimeter [15] has the following features:

- **Segmentation:** $\Delta\eta \approx \Delta\phi \approx 0.04$
- **Time Resolution:** gating time in less than 16 *ns* (a single beam crossing)
- **Position Resolution:** δx and $\delta y \approx 1.0$ mm.
- **Energy Resolution:** $(2.0/\sqrt{E} \oplus 0.5)\%$;
- **Radiation Resistance:** ≥ 1 MRad Per Year.

The inner radius of the BaF_2 calorimeter, combined with its Moliere radius and tranverse segmentation, make its design extremely close to the L3 BGO in terms of electromagnetic shower-sharing among the crystals. The ratio of the inner radii between the L3 and BaF_2 systems, and the corresponding ratio of the Moliere radii are both 1.45. As verified with simulations and a beam test, the percentage of the shower energy contained in subarrays of 3 × 3 and 5 × 5 crystals in the barrel region, are equal for the two systems to within ≈ 1%. We are therefore able to adapt many of the L3 shower reconstruction and identification algorithms directly, for studies of physics signals involving events with isolated electrons and photons.

The BaF_2 calorimeter follows the proven uniform and extremely light structural design used in the BGO calorimeter [1], which has allowed L3 to achieve very high resolution. Each crystal is housed in a precisely dimensioned, laser welded, thin-walled (100 μm) titanium alloy cavity, and is compressed by small fixtures mounted in each cavity against an inner core consisting of carbon fiber composite. The thinner cell walls and higher design tolerances will lead to potentially higher intrinsic resolution than the L3 BGO calorimeter.

A finite element analysis at ORNL [15], performed on a similar design based on carbon fiber composite cells with 300 μm walls, showed that in spite of its thinness, the structure is stable against the tensile and torsional loads provided by crystal weight and compression, with a large safety factor.

The use of titanium/aluminum/vanadium alloys has the advantage of making the structure easier to manufacture, while maintaining the same overall structural strength and stability as the carbon fiber structure. Tsinghua University has the capability, and has proposed to manufacture such a titanium structure in China at reduced cost. A 7×7 cell prototype also has been proposed [18], and preparations for the prototype construction are underway[2].

The use of a metallic support structure also has the advantage of providing a better ground for the electronics. This will result in less difficulty in achieving the intrinsic low noise level of the electronics, as compared to a carbon fiber structure with a thin (few micron) deposited metallic coating.

6.1 Recent Progress Demonstrating the Manufacturability of the BaF_2 Calorimeter

Substantial progress has been made by ORNL and LLNL, to ensure that the crystal calorimeter can be constructed on schedule, meeting all crystal dimension, crystal surface quality and coating, and mechanical support requirements. Preparation of finished crystal-pairs, construction of the mechanical support, and quality control and inspection throughout the manufacturing process in China, in addition to assistance from China in the assembly of the BaF_2 detector at the SSC Lab, are expected to result in overall reduced costs.

[2] A site visit by engineers J. Heck and B. Fuchs to China is underway [19], as of this writing. Site reports, including welding test results and detailed plans for construction of this prototype, are expected by early September 1992.

Specific points of progress in the manufacturing process, illustrating relatively low engineering risk based on expertise at LLNL and ORNL combined with L3 experience in crystal calorimeter construction, include:

- Redesign of the crystal dimensions to include three 90° angles, providing mutually perpendicular reference surfaces that greatly simplify the manufacturing procedure and dimensional control.

- Precise specifications of the crystal dimensions at ORNL, working together with LLNL, Caltech, and the Zhongnan Optical Instrument Facility. The engineering design of the crystal mechanical processing procedure, including cutting, lapping, and polishing of the crystals after growth has been developed at LLNL [19] and ORNL.

- A program of tests of diamond turning, ion beam milling, and polishing with diamond powders was carried out at LLNL. Polishing using a wheel of synthetic pitch impregnated with diamond was chosen, as it is relatively inexpensive, it produced a highly flat (one-tenth wave) smooth (to 10 - 20 Angstroms rms) surface, and it is readily adaptable to mass-production in China. Use of a special final polishing pass [19] has been shown to produce an exceptionally high quality, crystalline surface, which will ensure the long term life of the UV-reflective coating. The lack of subsurface damage was verified by ion beam channeling measurements at Charles Evans & Associates. Transfer of this technology to the Zhongnan Optical Instrument Facility has begun, with a site visit in August.

- The design of a polishing machine using the synthetic pitch method, fixtures for processing several crystals at once, and the specification of the lapping and polishing process, has been completed at LLNL [19], in cooperation with ORNL. The fixtures have been ordered, and the machine will be brought into operation at LLNL in late August and early September.

- A prototype mounting system with the crystals under axial compression and the support structure under tension has been designed at ORNL. The structure will use thin titanium alloy foils, as in the final calorimeter.

- Improvement of a Chinese oven installations has begun. The base pressure in one of the Chinese ovens has been improved from the 10^{-5} to the 10^{-6} Torr range, by installation of a cold trap. Following a site visit at SIC by M. LeBeau (chief engineer for the L3 BGO) and C. Wuest, together with a representative from

Leibold Hong Kong in mid-July, a program was initiated to improve the seals, increase the pumping speed with a new higher capacity vacuum pump, insititute systematic leak testing procedures, install a mass spectrometer for residual gas analysis, and improve the quality and placement of the vacuum gauges.

- Production engineering of the BaF_2 calorimeter is underway at ORNL and LLNL. This includes the design of the standard operating procedures, the development of a complete project plan for BaF_2 crystal mass production, and the design and construction plan for the support structure. The project plan will encompass all crystal production, mechanical processing, surface treatment, quality control and testing, preparation and mounting steps. The goal is to provide a first round picture of the production process for the BaF_2 calorimeter, as required by GEM management by the end of August. This work also is required now in order to have a project plan of sufficient completeness ready by the time of the Technical Design Report.

Further details on the crystal production are contained in the LLNL reports on surface preparation and crystal coating [19]. Additional information on the calorimeter layout, support, and assembly are contained in the report on the BaF_2 Calorimeter Manufacturing Plan, and the BaF_2 Engineering Design/Cost Report (Updates), which are both in preparation at ORNL.

7 BaF_2 Calorimeter Performance

An analysis of the expected performance of the full-size BaF_2 calorimeter is summarized in the following sections.

7.1 Position Resolution

The position of an electromagnetic shower, i.e. the coordinate of the impact point of an electron or a photon at the energy-weighted longitudinal position in an electromagnetic calorimeter, is usually measured by using the center of gravity method. The position resolution of a calorimeter thus depends on its structure, especially the lateral cell size. For a calorimeter organized in pointing towers, the position resolution as a function of

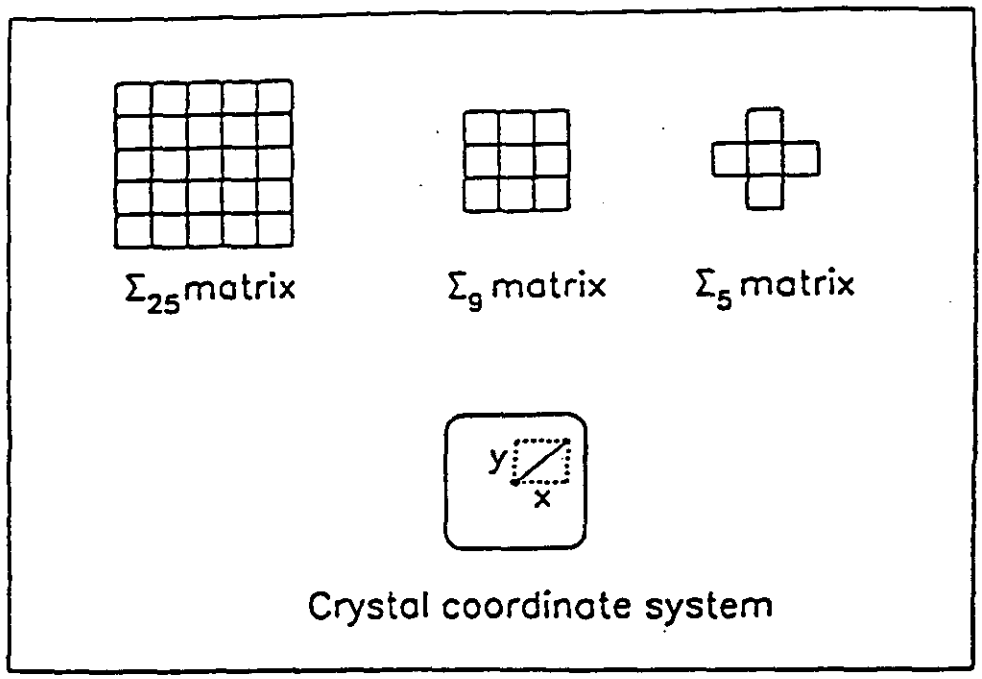

Figure 5: Definition of the crystal coordinate system and Σ_5, Σ_9, and Σ_25 for the L3 center of gravity analysis

energy has been parametrized as [4]:

$$\delta x(\mathrm{mm}) = \frac{3}{\sqrt{E}} e^{0.4D} \tag{2}$$

where E is the energy of the particle being measured in GeV, and D is the cell size in radiation lengths. The position resolution of the BaF_2 calorimeter, calculated according to Eq. 2 for a 20 GeV electron or photon, is 1.2 mm.

This position resolution will not compromise the discovery potential of the BaF_2 calorimeter [2].

The full potential of a crystal calorimeter for determination of the shower position can be much better appreciated by considering a detailed analysis using LEP data. For more difficult physics cases, where photon pointing using longitudinal segmentation is required, high resolution on the individual coordinate measurements in each segment could be useful.

A recent analysis using electrons measured in the L3 BGO calorimeter [20] from $e^+e^-(\gamma)$ events at the the Z^0 ($E \approx 45.5$ GeV) at LEP, has shown that significantly higher position resolution can be obtained. Using the summed pulse heights in submatrices of 5, 9 and 25 BGO crystals ($\Sigma_5, \Sigma_9, \mathrm{and}\Sigma_{25}$, as shown in Figure 5, M. Merck has shown that resolutions $\delta x \leq 0.65$mm may be obtained using Σ_9, and Σ_{25}), or $\delta x \leq 0.85$ mm using Σ_5, while Eq. 2 predicts 1.0 mm for this case with BGO. The resolution near the edges of a BGO crystal are significantly better than the maximum errors quoted above

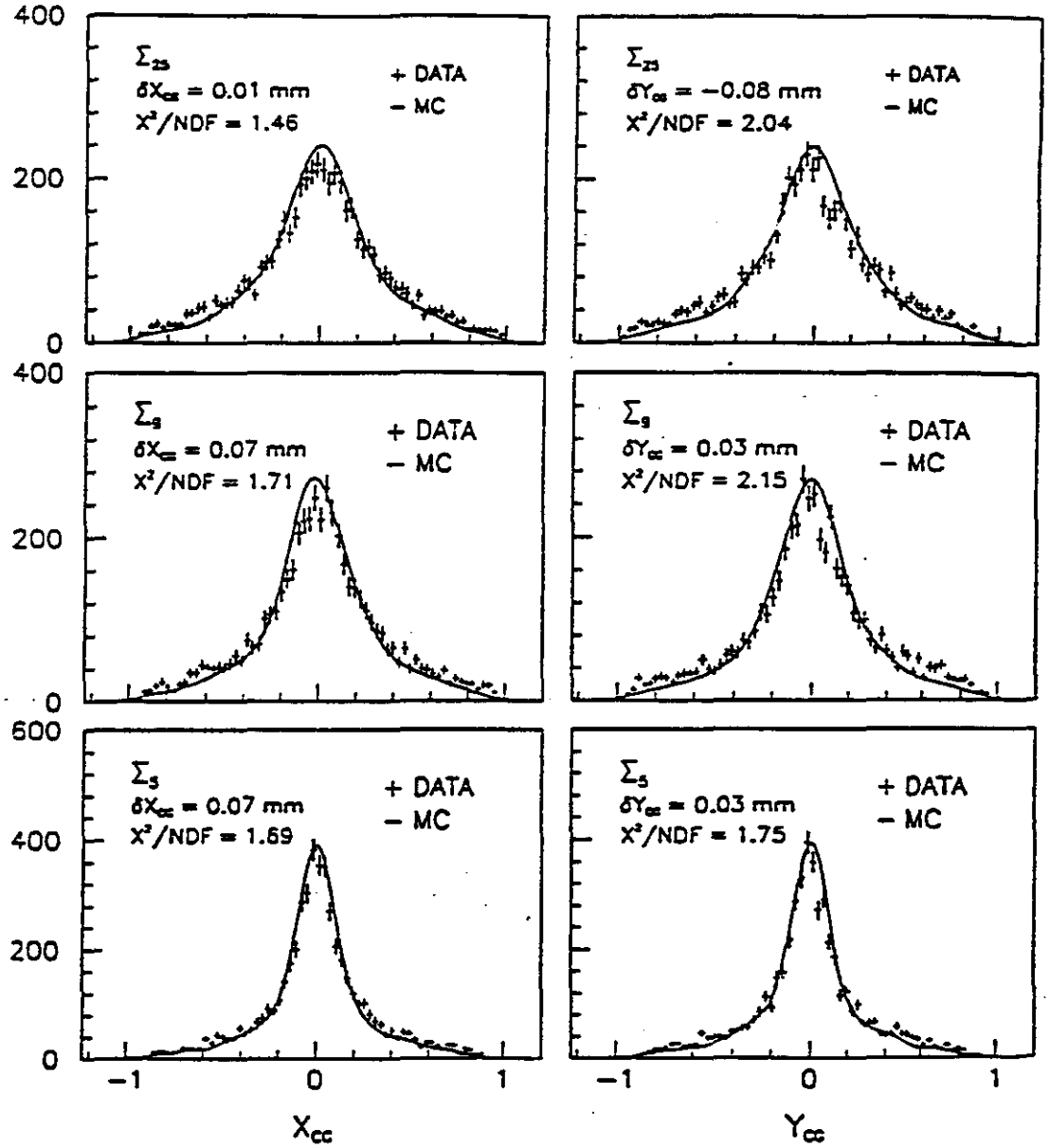

Figure 6: Distribution of the center of gravity. The curves represent the full GEANT Monte Carlo and the crosses the L3 data for Bhabha events.

(see Reference [20] p. 67). The distributions in the x center of gravity X_{CG}, and Y_{CG}, before unfolding the familiar 'S' curve, are shown in Figure 6. The agreement between data and the GEANT Monte Carlo is excellent: confirming the resolution and showing that the fits to the data are unbiased, down to the level below 0.1 mm.

7.2 Energy Resolution

The energy resolution of an electromagnetic calorimeter can be parametrized as:

$$(\frac{\delta E}{E})^2 = (\frac{\mathbf{a_0}}{E})^2 + (\frac{\mathbf{a_1}}{\sqrt{E}})^2 + \mathbf{b}^2 \tag{3}$$

where

- $\mathbf{a_0}$ is the contribution from electrical noise, summed over a few Moliere radii around the maximum of the lateral shower distribution;
- $\mathbf{a_1}$ is the 'stochastic constant' from photoelectron statistics;
- the systematic term **b** has the contributions:

$$\mathbf{b}^2 = \mathbf{b_S}^2 + \mathbf{b_G}^2 + \mathbf{b_{NU}}^2 + \mathbf{b_{NL}}^2 + \mathbf{b_C}^2 \tag{4}$$

  - $\mathbf{b}_S$ represents "physics noise" due to intrinsic fluctuations of the electromagnetic shower
  - $\mathbf{b}_G$ represents the geometry effects, including shower leakage at the front, side and back of the detector and inactive material between cells;
  - $\mathbf{b_{NU}}$ the effect of the nonuniformity of light response
  - $\mathbf{b_{NL}}$ represents the effects of nonlinearities and and very short term time-instabilities in the photodevice and/or readout system, which cannot be calibrated out.
  - $\mathbf{b_C}$ represents the residual intercalibration error, after the other contributions to **b** have been taken into account.

At low energy, the dominant contribution to the energy resolution is the noise term ($\mathbf{a_0}$), which decreases quickly with increasing energy. The sampling term ($\mathbf{a_1}$) dominates in the range of medium to high energies until a high energy limit is reached, where the systematic term (**b**) dominant.

For the L3 BGO detector, measured at the CERN SPS, the energy resolution was parametrized in a similar (but not identical) fashion [20], where the constant **b** included a term added in quadrature for the momentum spread of the incoming beam particles, which was parametrized as $1.25\%/\sqrt{E}$. With this parametrization, the stochastic constant $\mathbf{a_1}$ was estimated to be 0.5%, and the precision of the intercalibration constants (including the last three terms in **b** described above) was found to be 0.4%.

7.2.1 Light Yield and Photostatistics: a_1

It is not extremely difficult to build a homogeneous electromagnetic calorimeter with a small a_1 term. A photoelectron (p.e.) yield better than 10 p.e./MeV would be enough to provide an a_1=1%.

Following R&D studies in 1989-1990, we chose the recently developed Hammamatsu R4406 vacuum phototriode equipped with 'solar blind' K-Cs-Te or Rb-Te photocathodes [21] as the readout device. Both cathodes have about 10% quantum efficiency at 220 nm and provide suppression of the slow component by a factor of nearly 10. After suppression of the slow component by these photocathodes, the photoelectron ratio of fast-to-slow components (F/S) is typically 1.6/1 to 2/1.

The R4406 triode also has a gain of more than 50% of its nominal value when operating in a 1 Tesla magnetic field with an angle of 45° or less to its axis [21]. The synthetic silica (quartz) window has very high radiation resistance against photon and neutron doses [22]. Another choice of photodevice is a proximity focused few stage phototube, recently developed by Hamamatsu [23], (with several prototypes scheduled for delivery at Caltech in October 1992) which has gain of >30 under 0.8 tesla magnetic field. A detailed analysis has shown that typically 50 p.e./MeV have been obtained from 25 cm long BaF_2 crystals by using K-Cs-Te photocathodes.

The light yield of 50 cm long crystals has been measured at Caltech with γ ray sources and at Fermilab with an electron beam. The photoelectron yield was measured to be 20-50 p.e./MeV with Cs-Te or Rb-Te photocathodes, with good light response uniformity [4] obtained by simple wrapping. With the use of an efficient UV reflective coating [19] for uniform light collection, we conservatively estimate a lower limit of 30 p.e./MeV. This corresponds to $a_1 \leq 0.6\%$, which does not contribute significantly to the resolution for electrons and photons above 5 GeV.

Note: We are also continuing to consider the use of UV-selective solid state photodevices, with the necessary radiation resistance (MegaRads), linearity (0.1%), dynamic range (10^5), low noise and magnetic field immunity. As an example, Advanced Photonix has proposed a temperature compensated avalanche photodiode (APD) with a quantum efficiency reaching 80% in the UV (by a proprietary process), and with a gain of a few hundred [24]. High quantum efficiency UV-sensitive silicon photodiodes, and stable temperature-compensated APD's have each been developed by Advanced Photonix, and the combination of the two technologies to meet our needs would take an estimated 6

months of R&D. An APD has been tested up to 0.4 MegaRads, with no observable effect. The use of such a device would open the possibility of a modified design incorporating longitudinal segmentation (photon pointing).

7.2.2 Electrical Noise: a_0

Because of its small capacitance (10 pf) and small dark current (0.1 nA), it is not difficult for the R4406 vacuum phototriode and the front electronics described in previous section to provide an electrical noise level of 2000 electrons per channel [25]. A recent study by P. Denes [26] using a fast/slow ratio F/S = 1.6 has shown that for a 'shape and capture' front end electronics scheme, it is possible to reach typical noise levels of 1000 - 1500 electrons, with times to the peak of 1 bunch crossing (16 ns) or less.

In reality, one needs to sum over a few Moliere radii to reconstruct an electromagnetic shower. In the case of using 3 × 3 crystals, which contains 95% of the shower energy according to GEANT simulations [27], the intrinsic electrical noise will be 4000 - 6000 electrons without channel-to-channel correlations. Assuming the minimum gain of the R4406 phototube is 6, i.e. 50% of its nominal gain of 12 in the worst magnetic field situation[28], the signal corresponds to 180,000 – 300,000 electrons/GeV with a K-Cs-Te photocathode. This means an a_0 term of 1.3% to 3.5% for a 3 × 3 crystal readout, if the existing R4406 is used. The a_0 term can be reduced to the range of 0.25 – 0.6% if the proximity focused few stage tube (with gain 30) is used.

For the typical value of a_0 = 2%, shown in Section 7.2.8, the contribution of the electrical noise term is negligible at energies above 10 GeV.

7.2.3 Physics Noise and Geometry Effects: b_S and b_G

A detailed GEANT simulation was carried out to estimate the effect of shower leakage and non-active material for the BaF_2 design [4]. The simulation was calculated for an array composed of 121 (11 × 11) BaF_2 crystals with standard size: 3 × 3 cm^2 at the front, 5 × 5 cm^2 at the back and 50 cm long. Effects included in the simulation were:

- 250 μm carbon fiber walls between crystals;
- shower leakage because of summing a limited number (3 × 3 or 5 × 5) crystals; and

- 0.30 radiation lengths of dead material, representing the beam pipe, tracker, and carbon fiber mechanical support, at the front of the BaF_2 array.

The results of this GEANT study are summarized in Section 7.2.8 below.

7.2.4 Light Collection Nonuniformity: b_{NU}

Good light collection uniformity longitudinally along the crystal axis is important to maintain the high resolution, and the linearity over a wide energy range, for a precision crystal calorimeter. This has been studied in detail by K. Shmakov [7], and by R. Zhu [4] and W. Lu at Caltech. For a wide variety of possible uniformity shapes, and for random inhomogeneities, it was determined that a 5% nonuniformity over the 50 cm length of a crystal pair causes a contribution to this constant term in the resolution of 0.25% (also see Section 8.1.2).

Given our experience at Caltech, recent simulation studies by Shmakov (ORNL) [7], and the use of efficient UV-reflective coating being developed by Livermore [19], we expect to control the uniformity to this level overall[3].

The uniformity of the crystals will be controlled by light annealing *in situ*, and by monitoring with the UV flash lamp or laser system. The attenuation length of the crystals will be kept at a value of the absorption L_{att} well above 1 meter, in excess of the GEM specifications set for the BaF_2 technology (Appendix B).

As shown in L3, and by Shmakov [5,7] for the BaF_2 case, the optimum resolution is obtained, for a finite crystal length and a given energy, with a small nonuniformity that compensates for energy leakage from the back of the crystal (also see Section 7.3.2). The optimum uniformity for the BaF_2 case has a magnitude of 3-4% for a 100 GeV photon. Hence, if we start at a typical attenuation length of 2 meters, and the radiation-induced reduction of absorption length is controlled by light annealing, no degradation of the resolution will occur [7].

In the summary of contributions the resolution that follows, we therefore include an overall a contribution to the resolution from initial and radiation-induced non-uniformities[4] of 0.25%.

[3]This refers to Δ, the maximum deviation from uniformity over the lengh of the crystal, as defined by Shmakov.

[4]See Section 8.1.2.

7.2.5 Nonlinearities of the Photodevice, and Short Term Instabilities b_{NL}

The grid-mesh low gain photodevices from Hamamatsu have been shown, in our cosmic ray tests at UCSD, and during the FNAL beam test of our BaF_2 prototype matrix, to be much more stable than standard high gain tubes.

The R4480 PMT, whose gain (typically 10^3) depends on the input voltage (while the R4406 which we will use in the final system does not) showed an rms fluctuation of $\leq$ 0.15% [29] during our final data taking at Fermilab T-849. This measurement included fluctuations in the readout system, and temperature variations in the hall at Fermilab (in December) which were considerably larger than those that will be encountered underground at the SSC. Taking this into account, we assign a 0.1% contribution for short term gain fluctuations. It is important to note that given a light calibration system matching the L3 Xenon system's short term accuracy (0.1 to 0.15%), one can keep this effect down to the 0.1% level, where the calibration systems' contribution to the overall error is itself considered in a separate section of this report.

The R4406 tubes have been specified by Hammamatsu as being linear to 2% up to 100 mA, with their standard base, where 22 mA corresponds to 2 TeV (for our typical 30 p.e./MeV). At 2 TeV the non-linearity is below 0.5%, and is expected to be measured and stable to better than 0.1%.

For the recently developed proximity focused R2490 series phototubes developed by Hamamatsu fo Caltech, very recent data has shown the tubes to be linear to within 0.1% up to output currents of 1 Ampere. This is illustrated in Figure 7.

Another example of a very linear, stable tube for which lab data is available is the Hamamatsu R4598 (with a gain of 10^3 to 10^4) designed for the KTeV experiment [30]. This tube has been shown to have a nonlinearlity of essentially 0 to 10 mA, below 0.5% up to 40 mA, below 1% up to 80 mA, with a maximum nonlinearity of 2% at 200 mA. As shown in the KTeV Design Report, the nonlinearity is a smooth curve which can be calibrated out, and careful calibration is needed only at the upper part of the dynamic range.

Using the R2490 and R4598 data, the estimated residual error due to calibration of the nonlinearity is $\approx$ 0.1% up to the top end of the GEM digital readout system's range.

Since the goal resolution for the digital readout system is 0.2%, for both GEM candidate technologies, the sum of these effects added in quadrature would be 0.24% at

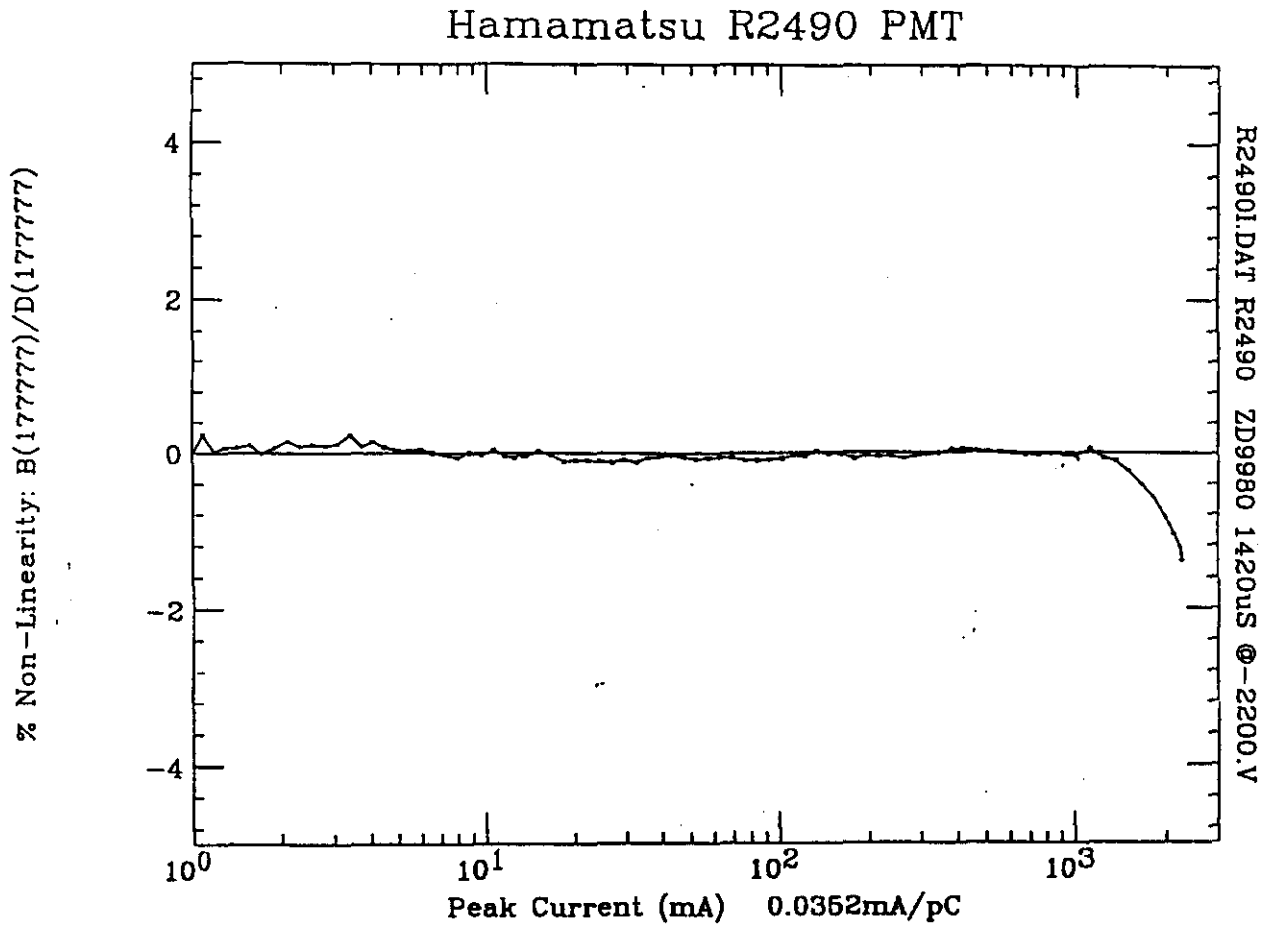

Figure 7: PMT linearity measurement of the R2490, measured at Hamamatsu.

very high energies (near 2 TeV). For lower energies, such as the range up to 500 GeV shown in Table 3 below, the estimated error is 0.1% to 0.15% from short term phototriode instabilities, below 0.1% from intrinsic tube non-linearities, and 0.1% to 0.15% from the digital readout, for a total of approximately 0.2%.

7.2.6 Remaining Intercalibration Error b_C

While running at the SSC, where inclusive Z^0's are produced copiously, the limitations on the resolution which have been experienced in L3 (described at the end of Section 7.3) do not apply, and the high resolution is achievable. Recently, H. Yamamoto has demonstrated that monthly calibrations of individual BaF_2 crystals are possible, to a statistical accuracy of 0.3%, using the mass reconstruction of inclusive $Z^0 \rightarrow e^+e^-$ events [31]. The estimated systematic accuracy of this calibration over the long term, using many data sets, is expected to be extremely low. We include a systematic contribution of 0.1%, to account for the differences in using electrons (rather than photons in a similar energy range) in the calibration procedure.

Combining the $Z^0 \rightarrow e^+e^-$ physics calibration data with our UV flasher system, RFQ system[5], and other physics reactions such as isolated MIPS – all to track the gains from day to day – a feasible goal is a long term crystal by crystal calibration with an average intercalibration error of 0.25%.

The goal for the BaF_2 in GEM of 0.25% can be compared to the absolute calibration accuracy already achieved by CLEO II [32]. This is summarized in the following section. KTeV also has a goal of below 0.25% for periodic calibration and gain monitoring.

As discussed in some detail in Section 7.3 below, and emphasized elsewhere for other precision experiments [30,32] the ultimate resolution can only be achieved – in any large system – following extensive offline analysis using physics reactions during the experiment[6]. The key to the final calibration accuracy is the intrinsic resolution of the system itself, which allows one to make the necessary energy, position and scale corrections to the required precision. The quality of the calibration also depends on the energy range calibrated, compared to the final range of energies to be covered by the experiment (this has important implications for GEM test beam plans, independent of its EM calorimeter choice).

It is important to note that many of the effects considered separately above are commonly included in the "intercalibration error", measured at a test beam or in an experiment[7]. Hence an earlier analysis [4] of the BaF_2 resolution listed a reasonable overall "intercalibration" error of 0.4%.

As a result, it appears feasible that the overall design resolution of the BaF_2 system may be achieved, with the one proviso that the radiation damage effects are controlled (see Section 8).

7.2.7 The Energy Resolution of CLEO II CsI Calorimeter

The CLEO II collaboration achieves similar monitoring precision as does L3, but, has more copious physics processes available to provide a better absolute calibration [32]. They use Xenon flash lamps to monitor the time dependence of their photodiodes. For absolute calibration over a wide energy range, CLEO uses three physics processes:

[5]Discussed further in Section 9.3.

[6]For example, KTeV plans to record 40,000 Ke3 decays per CsI block per week, resulting in a final energy scale precision of ±0.04%.

[7]The additional tests and detailed considerations to separate out the effects listed in Appendix A. are often not needed.

- 1) π^0 decays below 2 GeV,
- 2) photon energies in $ee\gamma$ events above 500 MeV, and
- 3) back to back $\gamma\gamma$ events at the beam energy.

Their calibration procedure has maintained an absolute run-to-run gain of $\pm 0.25\%$ as checked by Bhabha energies and π^0 masses over time. They quote a calibration accurate to 1.% at 25 MeV, 0.5% at 100 MeV, and 0.2% at 5 GeV.

Table 3: Summary of Contributions to the Energy Resolution of the BaF_2 Calorimeter (In Percent)

E (GeV)	5	10	100	500
Electrical Noise	0.4	0.2	0.02	0.004
Photoelectrons	0.2	0.14	0.045	0.02
GEANT b_S and b_G	0.60	0.43	0.30	0.36
Nonuniformity b_{NU}	0.25	0.25	0.25	0.25
Nonlinearity b_{NL}	0.2	0.2	0.2	0.2
Intercalibration b_C	0.25	0.25	0.25	0.25
Total	0.85	0.64	0.51	0.54

7.2.8 Summary of the Computed BaF_2 Energy Resolution

Table 3 summarizes the BaF_2 resolution, including the contributions from electrical noise, photoelectron statistics, intrinsic resolution from GEANT simulation, residual nonlinearities and short term instabilities of the readout, and the intercalibration (as specified above). The result of the energy resolution is shown in Fig. 8b. It can be parametrized as $2\%/\sqrt{E} \oplus 0.5\%$, which is also shown in Fig. 8b as a solid line.

As a comparison, Fig. 8a shows the energy resolution measured with 4000 BGO crystals in a CERN test beam [1]. In the energy range beyond 20 GeV, the dominant contribution to the energy resolution is the systematic intercalibration error. The resolution of the L3 BGO calorimeter can also be parametrized as $2\%/\sqrt{E} \oplus 0.5\%$, which is also shown in the Fig. 8a as a solid line.

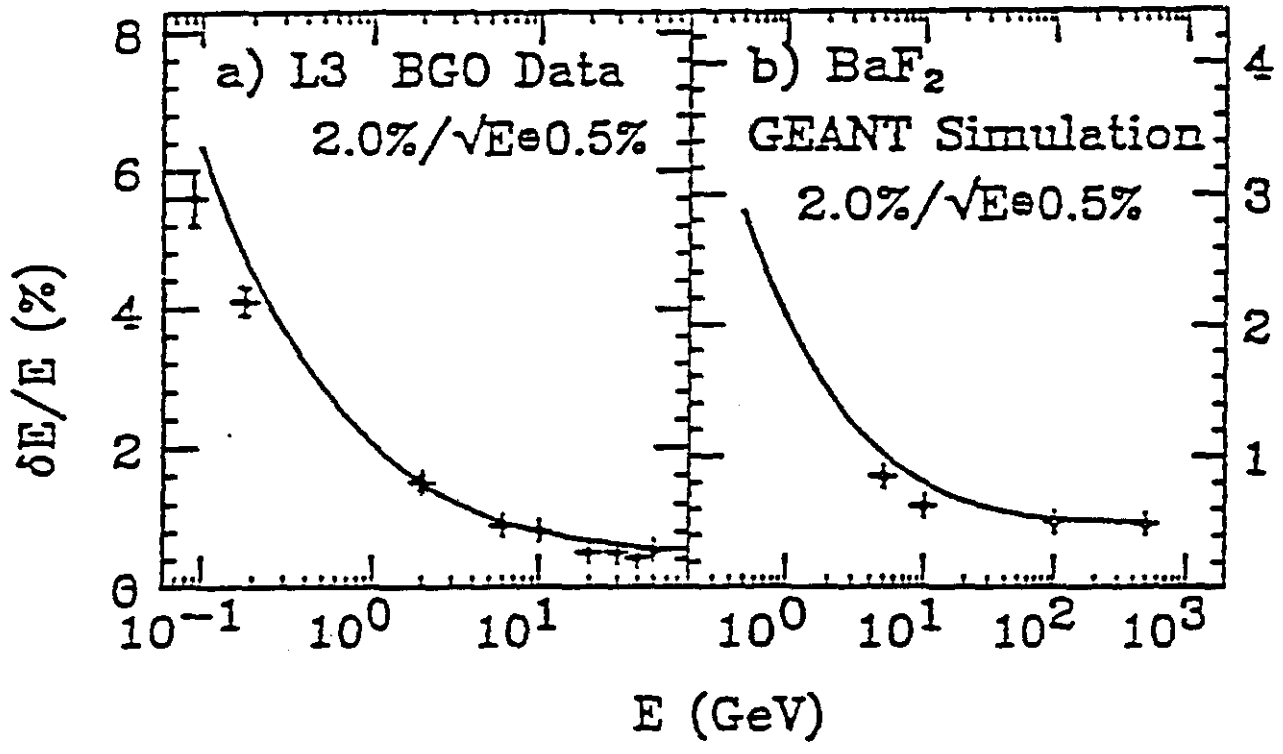

Figure 8: Energy Resolution of (a) the L3 BGO calorimeter, measured at CERN test beams with 4000 crystals, and (b) the BaF_2 calorimeter, calculated with a GEANT simulation.

More detailed information on the energy dependence of the various terms, and their correlations, can only be estimated by more extensive simulations (see for example [7]). The accuracy of such simulations, given the early stage of the experiment and the quotation of errors to an accuracy of 0.1% and below – prior to the commencement of detector construction – must be considered with great care.

It is important to note that the parametrization mentioned above is not just an "intrinsic" resolution, but includes many of the effects (material in front and between crystals, energy leakage) which affect the resolution of a real calorimeter system. As discussed above and quoted for other large crystal calorimeter systems [30], the "intrinsic" resolution [30] due to photostatistics and shower fluctuations can reach:

$$(\frac{\delta E}{E})_{intrinsic} = \frac{0.5\%}{\sqrt{E}} + 0.3\%.$$

7.3 The Energy Resolution of the L3 BGO Calorimeter

In order to check the computations summarized above, and to further verify if the design resolution of the BaF_2 calorimeter is achievable once the radiation damage problem is controlled – by light annealing or further improvements in crystal quality – recent detailed studies on the electron energy resolution of the L3 BGO calorimeter at LEP [20,33] have been reviewed. These analyses use Bhabha scattering events $e^+e^- \rightarrow e^+e^-(\gamma)$ events at the Z^0 peak, where the electron energy is $E \approx 45.5$ GeV – apart from radiative effects which contribute $\approx 0.7\%$ to the resolution peak, and a low energy tail.

The aspects of these studies which are relevant to the expected BaF_2 energy resolution — on the effects of residual systematic errors after precise corrections for nonlinearities, position corrections, uniformity of light response, and the ability to track the crystal gains with a Xenon lamp and light fiber monitoring system — are summarized below.

7.3.1 Energy Resolution in L3

The energy distribution obtained from Bhabha events is shown [20] in Figure 9, both for real events and for Monte Carlo events. The data peak is wider than the Monte Carlo peak, because the Xenon lamp monitoring system correction factors are only known to 0.7% [34]. The Monte Carlo resolution of 1.14% corresponds to a BGO calorimeter with the performance measured at the CERN X3 test beam (in agreement with GEANT simulations), convoluted with radiative effects. The data resolution shown, of 1.35%, includes all Bhabha events; even those where the cluster used to reconstruct the electron contains a dead crystal (typically 1.0% of the crystals). Eliminating these clusters from the sample results in typical resolutions of 1.2%.

In order to compare the data to the Monte Carlo, a Gaussian with a width of 0.7% is convoluted with the Monte Carlo distribution, resulting in strikingly good agreement, as shown in the figure Figure 9c. One can also simply subtract the resolutions shown in the top parts of the figure in quadrature, confirming that the residual systematic error due to the intercalibration error is 0.7%. This 0.7% constant term has also been obtained in an analysis using a more restricted sample of only collinear Bhabhas (by C. Tully at Caltech), which has been presented at the GEM Calorimeter Group meeting in Tucson [35].

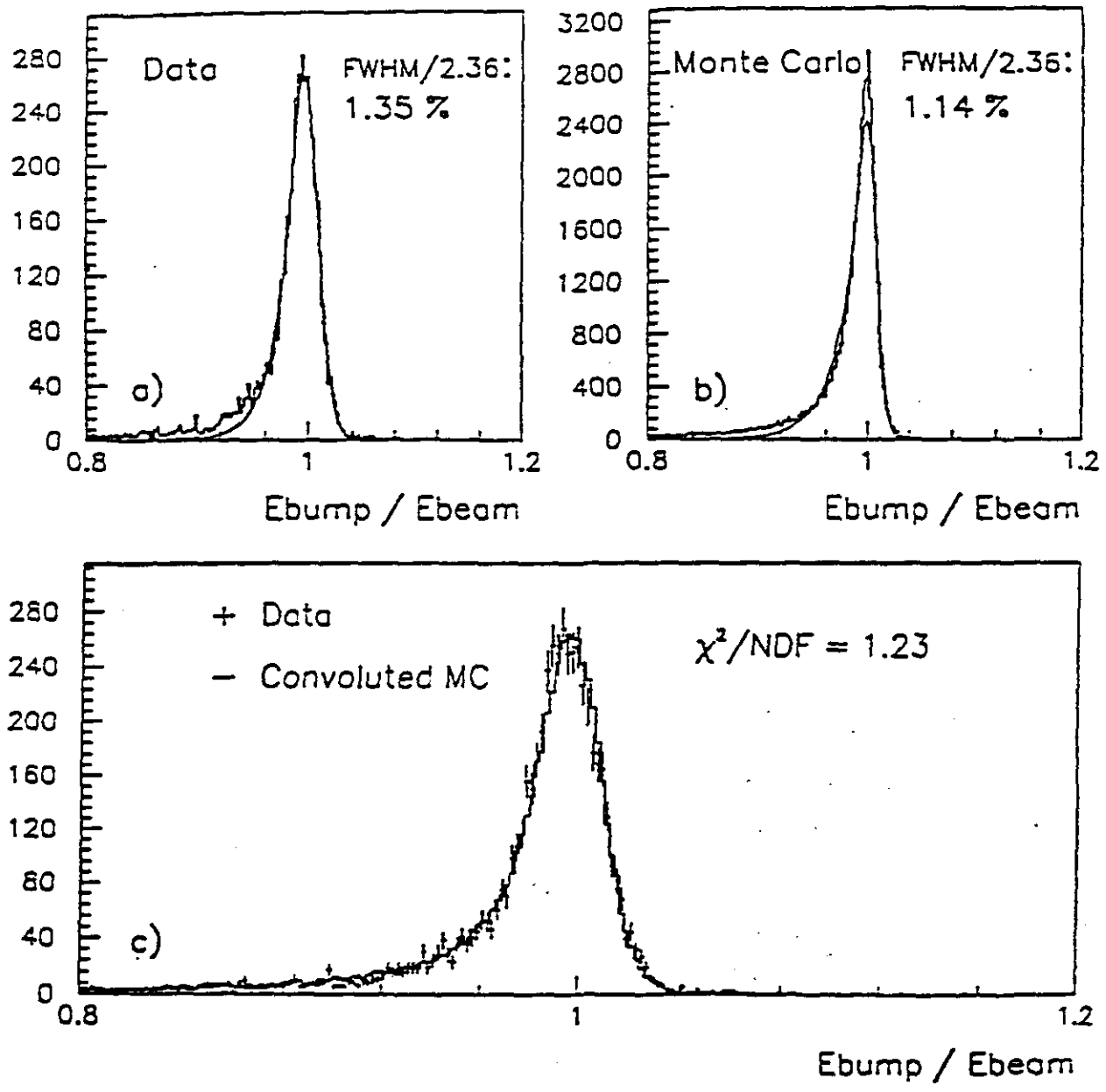

Figure 9: Comparison of the reconstructed energy distribution of an electron or positron in Bhabha events. (a) Real data (b) Monte Carlo (c) Comparison of the data with the convoluted Monte Carlo.

It is extremely important to note that the 0.7% constant term is the result of the lack of physics reactions to calibrate the detector at LEP. The Xenon lamp system itself, which has internal normalization monitors, as shown in Figure 10, has been measured [34,33] to be stable to typically 0.2% during 30 day calibration periods in 1990, and to 0.14% over a typical period of 45 days in 1991 during LEP data taking [36]. This is illustrated in Figure 11. The determination of the Xenon system stability is done by comparing the variation of the pulse heights observed with the lamp pulses in the BGO crystals, compared to the reference photomultiplier tubes. The longer-term stability of the entire system is 0.4% to 0.5% per year [36].

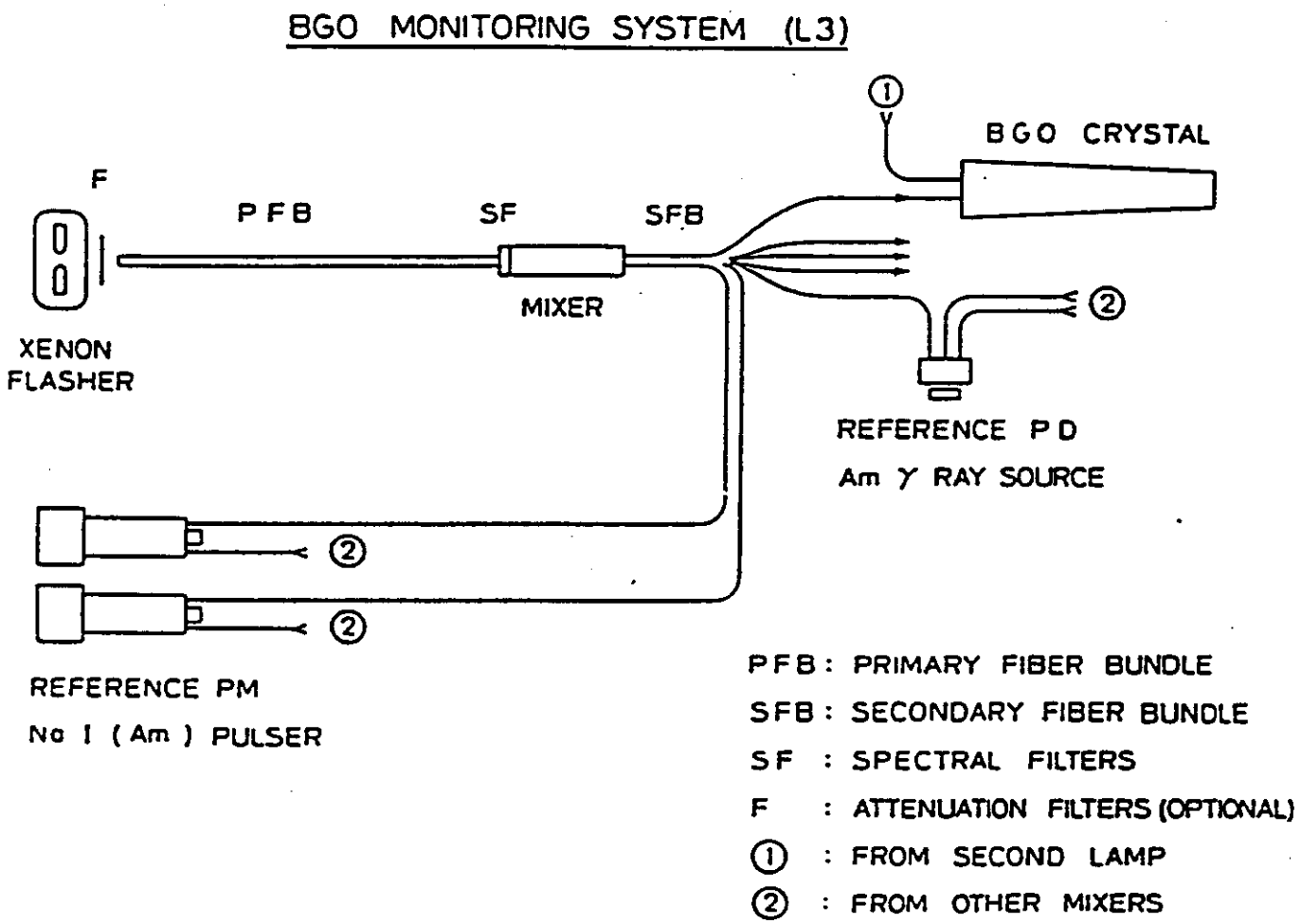

Figure 10: Schematic view of the Xenon monitoring system for the L3 BGO.

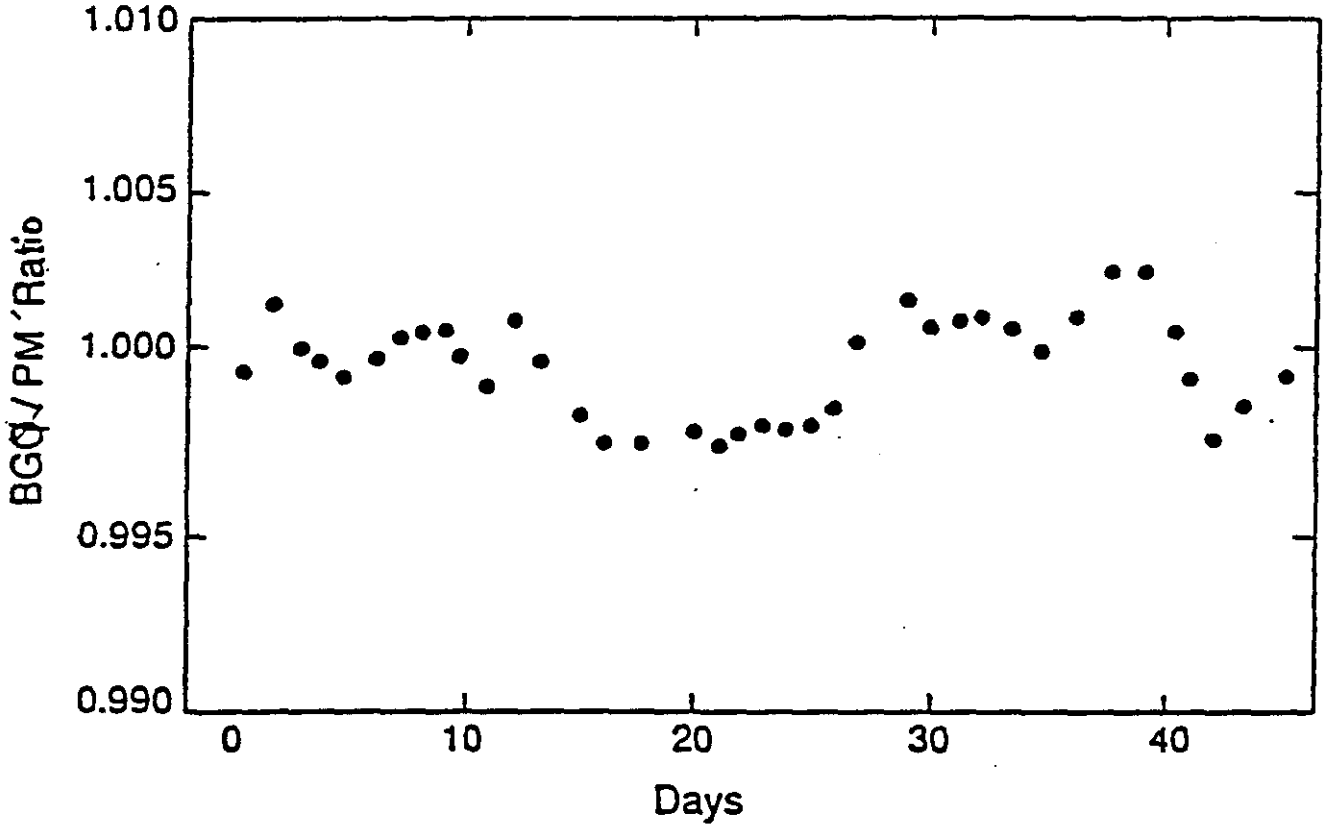

Figure 11: The amplitude for a typical BGO crystal, relative to the corresponding reference PMT, during a calibration period.

However, the absolute calibration of the Xenon monitoring system was lost due to having to transport it from the CERN SPS to LEP (and temporarily disconnect the fiber bundles). This calibration has been recovered for regions of the detector by using collinear Bhabha events and fitting the gains, to an accuracy of 0.2%. However, the number of Bhabhas obtained at LEP – approximately 22,000 events in the barrel region in 1991 - July 1992, or 1.5 electrons per crystal per year – does not allow tracking of the gains of individual crystals.

The accuracy of the Xenon lamp system in tracking the average gain of rings of crystals at fixed polar angles θ with respect to the beam line is shown in Figure 12.

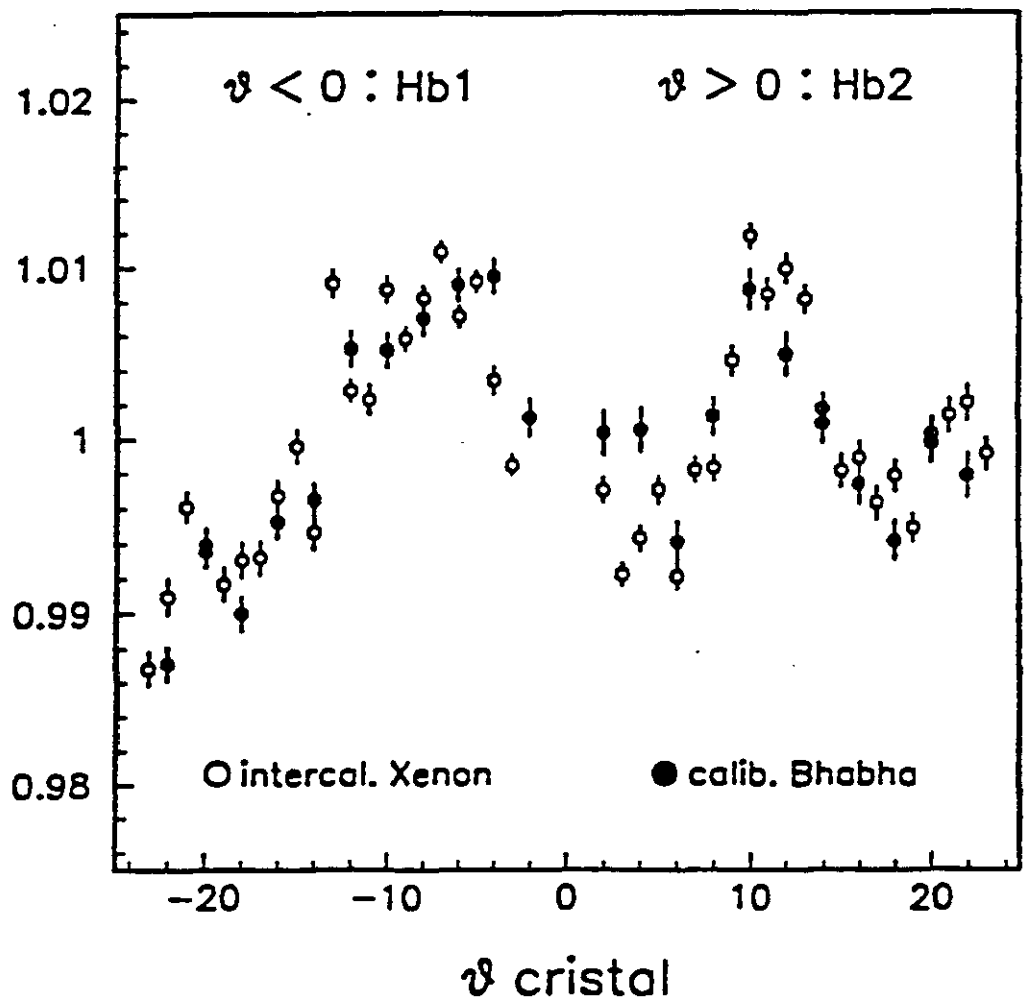

Figure 12: Comparison of the structure in θ of the gain changes measured at LEP using Bhabha events, with respect to the gains measured at the CERN X3 test beam.

Internal montoring of the system shows [36] that the intensity of light out of each mixer is calibrated to 0.1 - 0.15%, and that the BGO resolution is thus limited by the lack of a physics calibration reaction *in situ*, due to the spread in the light intensity out of the individual fibers.

In summary, the L3 BGO resolution of 1.3% observed for electrons in Bhabha events (1.2% without clusters containing the few inoperative crystals) can be explained fully in terms of:

- 0.6% from the design performance of the calorimeter, as observed at the CERN X3 test beam. This already includes an intercalibration error from crystal to crystal measured at the beam of 0.4%.[8]. The rear leakage contribution to the resolution, estimated as 0.13% [20] is implicitly included. The contributions from front leakage (albedo) and transverse leakage beyond the summed cluster of crystals have been determined to be negligible.
- 0.7% from radiative effects in Bhabha events at the Z^0 peak at LEP.
- 0.8 ($\pm$0.1)% from the Xenon monitoring error.

7.3.2 Corrections to the L3 Data Included In The Resolution

The resolution quoted above already includes some systematic effects, which have been corrected out. The residual errors associated with these corrections are summarized below.

Impact Point Correction

The energy response has been parametrized in terms of the impact point ρ relative to the center of the crystal, where

$$\rho = X_{rec}^2 + Y_{rec}^2$$

and where X_{rec} and Y_{rec} are the positions reconstructed by the L3 center of gravity method discussed in Section 7.1, using the crystal pulse heights alone. X_{rec} and Y_{rec} are normalized to the local transverse crystal size. The parametrization is obtained by fitting

[8] A significant part of this intercalibration error is the result of the temperature sensitivity of the BGO light output to temperature of -1.55% per degree C. In contrast, the BaF_2 fast components have negligible temperature dependence over a wide range around room temperature.

a simple second order polynomial $F(\rho)$ for Σ_9 (3×3) or Σ_{25} (5×5). The reconstructed energy is then obtained by multiplying the raw energy sum by the ratio $F(0)/F(\rho)$. The accuracy of this correction procedure is illustrated in Figure 13 (where most of the events occur within $\rho = 1$). The residual error due to this correction, after averaging over a large number of events is $\approx 0.2\%$.

Energy Dependent Light Uniformity Correction

The light collection uniformity in each L3 BGO crystal is obtained by a simple coating of NE560 white paint $\approx 50\mu$m thick. The uniformity has been checked with a cosmic telescope ("bench"), and the light collection efficiency as a function of the longitudinal position along the crystal $L(x)$ has been parametrized in terms of a third order polynomial.

In a rigorous treatment the efficiency function L(x) would be convoluted with the parametrized shower shape at each energy. A simplified analysis, which illustrates the energy dependence for different light nonuniformities, uses the ratio R defined as:

$$\mathrm{R} = \frac{(\mathrm{L}(\mathrm{x}_0) - \mathrm{L}(\mathrm{x}_\mathrm{L}))}{\mathrm{L}(\mathrm{x}_\mathrm{L})}$$

where x_0 is a point at the front (small end) of the crystal, and x_L at the back. The distribution of the measured R values is shown in Figure 14a. The curves cross at 10 GeV by definition, as this is the chosen reference point.

The average R is -10% with an rms spread about the mean of $\approx$ 4%. As shown in Figure 14b, this results in very little energy dependence in the range from 5 to 50 GeV.

Figure 15 shows that the actual non-linearity correction, from 10 to 50 GeV is 0.25%, with a residual rms error of 0.08%. The results in the figure are obtained using the rigorous analysis described above [20].

7.3.3 Conclusions on the L3 BGO and GEM BaF_2 Resolutions

From the above discussion, it is clear that the L3 BGO calorimeter would be operating at design resolution now, if a large enough sample of electrons and/or photons from useful "calibration reactions" such as Bhabha events were available per unit time. This problem will soon be alleviated, at least in part, by installation of the L3 RFQ system this Fall, but it will be very difficult to recover the full precision without a sufficient number of high energy electrons or photons of known energy in each crystal.

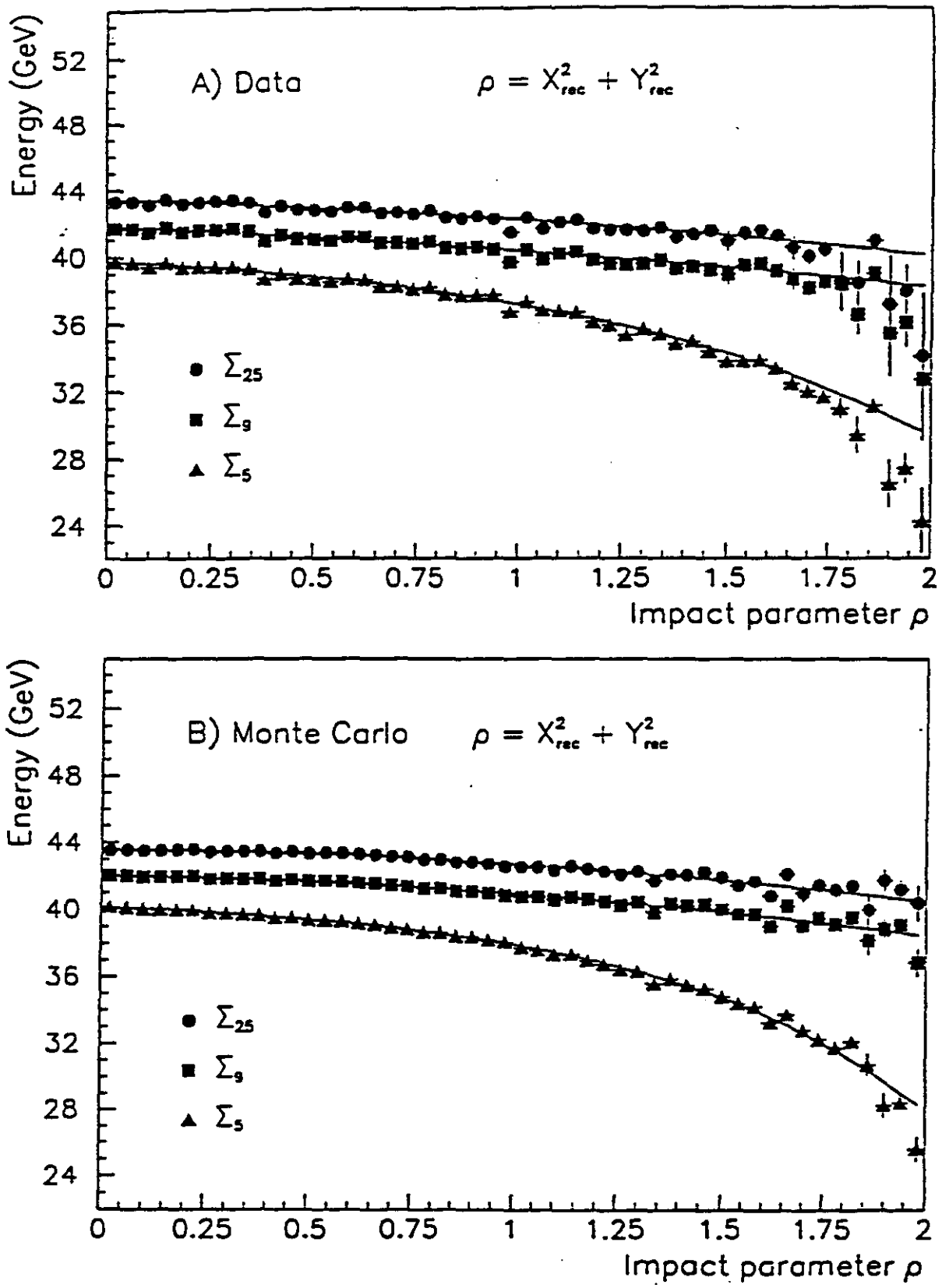

Figure 13: The mean reconstructed energy using the impact Σ_5, Σ_9, and Σ_{25} matrices as a function of the impact point parameter ρ.

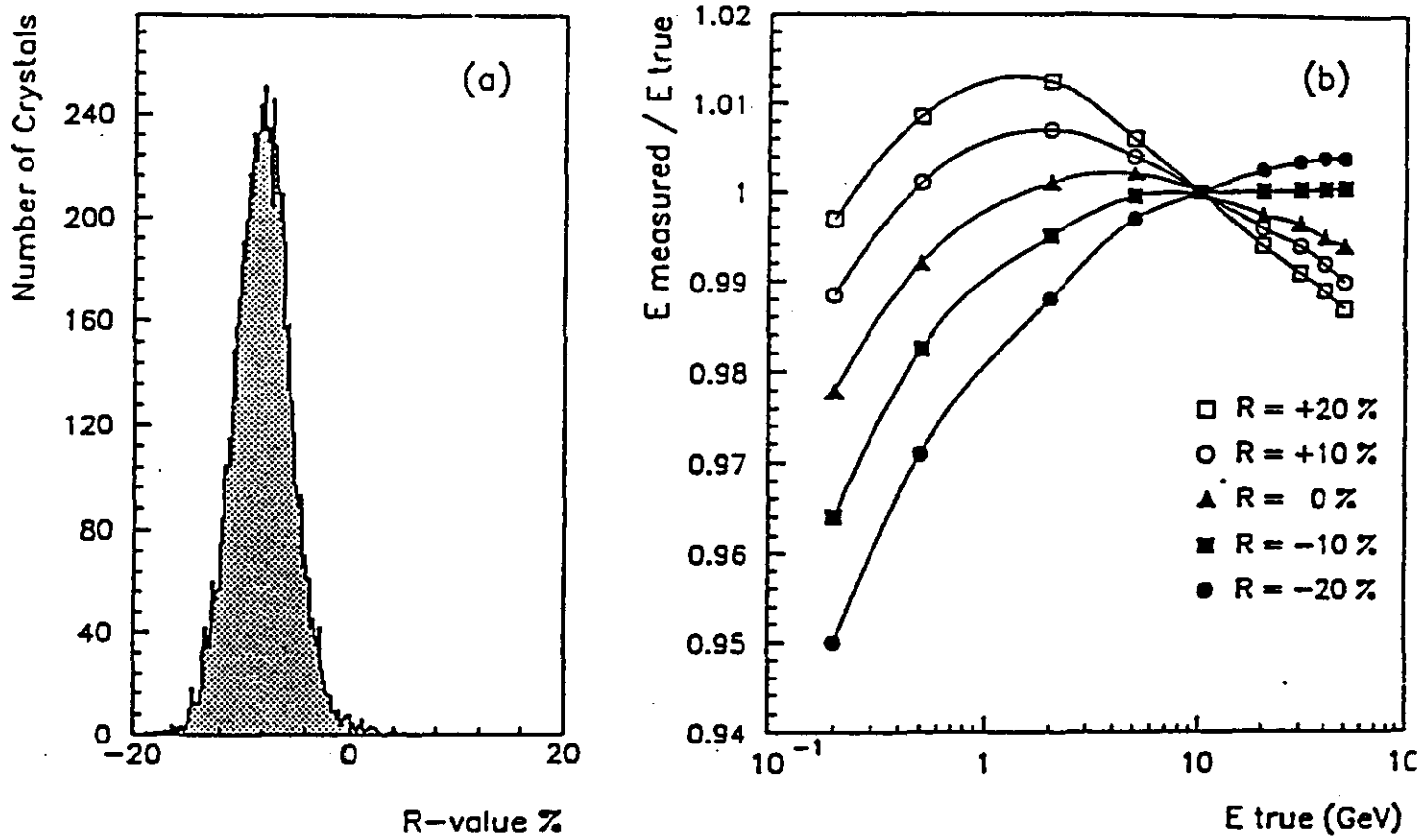

Figure 14: (a) The distribution of the light uniformity factors R. (b) The energy correction as a function of the incoming energy for various R values.

As mentioned above, and discussed further in Section 9.1, the in situ reconstruction of the Z^0 invariant mass in $Z^0 \rightarrow e^+e^-$ decays will reduce this problem greatly. By precision monitoring combined with continual calibrations using the inclusive Z^0 and (possibly) other physics reactions, and by analyzing these constants as time-series over the long term, we expect to reach the design resolution of the entire BaF_2 system.

The one proviso to this is the control of the radiation damage problem. Extremely rapid strides in understanding how to control the radiation damage *in situ* are being made right now (from day to day) using annealing of the crystals with visible light, as discussed further in Section 8.

In comparing the BGO and BaF_2 resolutions, one has to take into account the differences in the two detectors. The BaF_2 crystals are 24.5 X_0 versus 21.5 X_0 for the

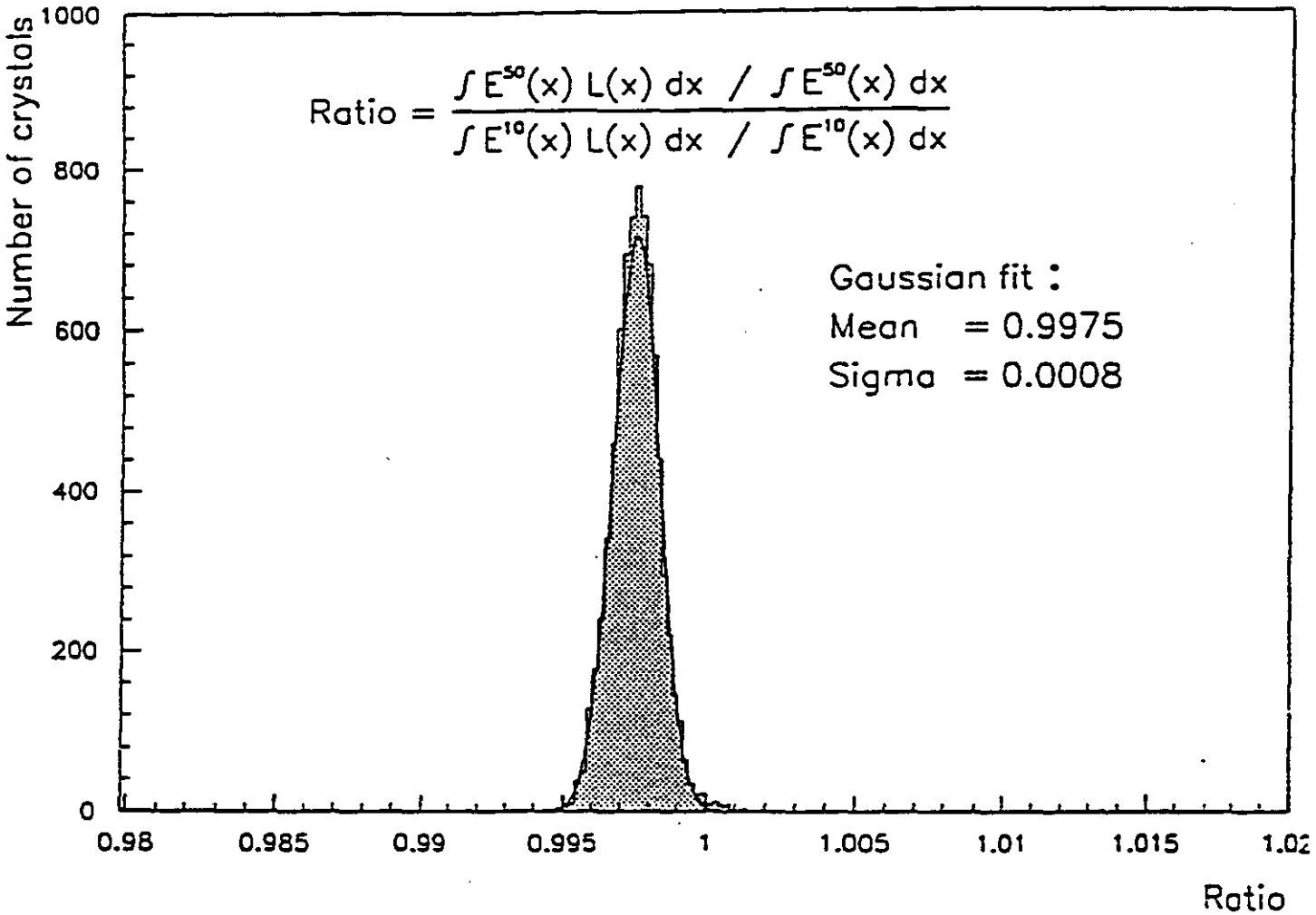

Figure 15: The light collection correction for 50 GeV showers, relative to 10 GeV showers in the L3 BGO.

BGO. As a result the contribution of the rear energy leakage to the BGO resolution (0.18%) is approximately equal to the corresponding contribution for the BaF_2 at 500 GeV[9].

It is widely recognized[10]. that transverse leakage beyond 3 X 3 in either the L3 BGO or the BaF2 case, contributes a negligible amount to the shower fluctuations, once the longitudinal fluctuation contribution to resolution is kept this small.

It is also important to note that the BaF_2 system will be manufactured 8-10 years

[9]This is based on parametrisations derived by Merk [20], and by the precise shower shape curves he computes, using GEANT 3.14 with very low energy cutoffs: 100 keV for electrons and 10 keV for photons.

[10]See C. Fabjan's Chapter on Calorimetry in T. Ferbel's book on Experimental Techniques in HEP.

later than the BGO, with the BGO experience in mind. This will lead to a number of engineering improvements, that will help the overall resolution. The BGO crystals are 300 ± 100 microns undersized, because of the early cutting technology used at SIC. That is, the Shanghai Institute of Ceramics ultimately achieved the dimensional accuracy desired (100 microns), with the aid of technology developed by M. LeBeau at LAPP (Annecy), – but larger tolerances were allowed to make sure the crystals fit. As a result, the distance between BGO crystals is typically 800 ± 150 microns. The GEM specification is 550 microns between crystals, based on the tolerances agreed to by the Zhongnan Optical Instrument Facility (ZOIF) in July (see Appendix C), and including 300 microns of carbon fiber wall. Using a 100 micron titanium wall, as now planned, LLNL's superior crystal cutting and polishing methods, as well as the extremely thin coatings which have been developed and are in use at LLNL and ZOIF, the closer spacing should be attainable with high confidence. Overall the improved engineering (and experience) will help the BaF_2 system achieve better resolution, in some respects[11] than the BGO.

The improved engineering (precision cutting and coating) will also help reduce the systematics associated with the impact point correction and the energy dependence of the light nonuniformity corrections, below the already small levels experienced for the L3 BGO[12].

[11]See the discussion of b_G in Section 7.2.3.
[12]See Sections 7.3.2 and 7.3.2.

8 Radiation Damage in BaF_2 Crystals

The BaF_2 R&D program on radiation damage closely follows the guidelines set by the BaF_2 Expert Panel [6], and is focused on meeting the milestones set by the GEM Executive Committee in February 1992 following its review of the BaF_2 Expert Panel Report (Appendix A.). The milestones on radiation resistance of the crystals, aimed at demonstrating the BaF_2 calorimeter's ability to maintain its stability and thus its high resolution *in situ*, and the means by which the milestones will be met include:

- Demonstration of substantial improvement in 20-25 cm long BaF_2 crystals, with an attenuation length $\lambda > 60$ cm after 1 MegaRad:
  This is being addressed by the continual production of full sized crystals at SIC and BGRI in China, following improved materials-preparation and crystal growth techniques.

- Production of small rad-hard crystals with $\lambda > 95$ cm after 1 MegaRad, meeting the GEM final specifications (see [4]):
  This is being addressed by a program of work underway at Optovac and LLNL in the U.S., including growth of crystals from pure raw materials, with specially treated or pure metal crucibles, control of the oven vacuum (with residual gas analysis) and the growth cycle.

Using pretreatment of the crystal raw materials, improved oven vacuum, and control of the oven growth cycle, SIC and BGRI have committed to deliver 5 full size crystal-pairs approaching the GEM final specifications.

8.1 Summary of Progress on Radiation Damage During 8/92

Substantial new results, indicating that the radiation damage of BaF_2 crystals of **EXISTING** quality can be controlled in situ in GEM – to the level required to maintain the high resolution – have very recently been obtained in August 1992. By annealing the crystals with blue light in situ, the transparency of the crystals can be maintained with a transparency which is comparable to the best crystals before irradiation. This has been demonstrated in detail, as reviewed below.

A brief summary of the BaF_2 Panel's conclusions up to its August Report [8,6], and

results on the understanding and means towards eliminating the radiation damage effect in BaF_2 crystals during the manufacturing process are given in Appendix D.

8.1.1 Further Results on Radiation Hard Crystals From China

Additional progress in producing large crystals with improved radiation-hardness was achieved by SIC in the week following the August Panel meeting.

- A 25 cm long new crystal from SIC has achieved a transmission of 48.6% (at 220 nm) after irradiation to 1 MegaRad, as measured at Caltech. This corresponds to an absorption length of 41 cm, as shown in Figure 16.
- One key new factor in the improved quality of the crystals is the systematic elimination of $Ba(OH)_2$ microcrystals during the manufacture of the BaF_2 powder which is the raw material used for crystal growth. This allows the Chinese institutes to use material from more than supplier, to obtain crystals with radiation hardness which is similar to the quality shown in the figure.

It is important to note that the improvement at SIC was accomplished under very adverse conditions (very high ambient temperature, unstable control electronics) within the Jiading plant, which would not apply in an actual mass production situation.

8.1.2 Annealing In Situ With Light, To Obtain Radiation Hard Crystals in GEM

The work by Woody in July *et al.* [9,10] that established that the damage from all types of particles can be removed by thermal annealing (see Appendix D), other data from BNL, and the work of M. Strathman of the Expert Panel, led to a strong recommendation by the Panel to pursue annealing with light as a means of controlling the radiation damage [8]. This recovery effect was previously understood for BaF_2 crystals [11,12,13]), but recent work by M. Strathman [37,38] and Woody revealed that the light intensity required could be very small, making a system for light annealing *in situ* practical. After presentation of this recommendation to the GEM Collaboration Council by the Panel, work on light annealing began immediately at BNL, LLNL, and West Virginia University. An engineering conceptual design has been started at ORNL and UCSD.

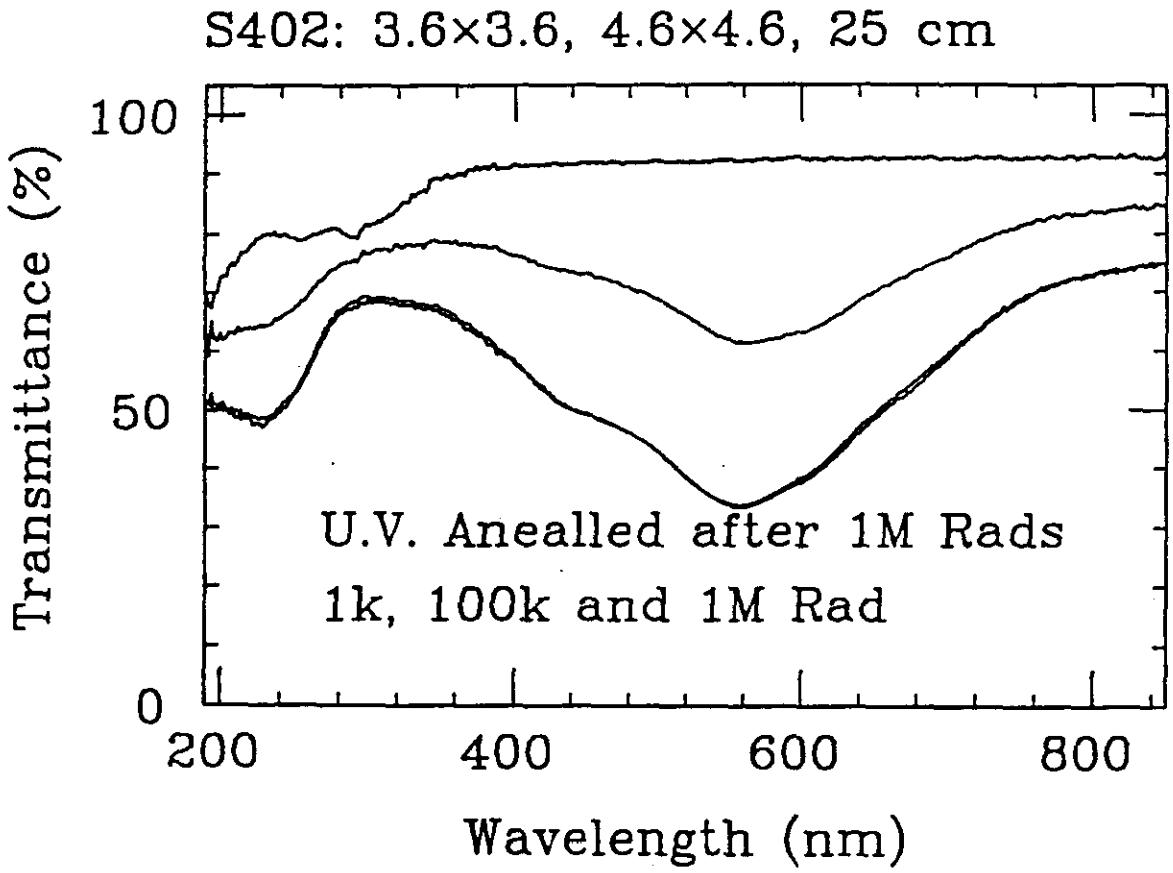

Figure 16: Transmittance of the latest 25 cm long BaF_2 crystal produced by SIC, which shows a light attenuation length of 41 cm after 1 MegaRad irradiation.

The initial series of tests results (some of which were presented at the August 9 GEM Calorimeter Group Meeting), indicate that the damage at the SSC can indeed be controlled in this way. Several groups have been able to maintain BaF_2 crystals with absorption lengths well above the GEM specifications (see Appendix B), at low and very high dose rates, by illuminating them after or during irradiation. Results up to August 24 include:

- Tests at BNL [39] were made with the 20 cm long crystal "SIC703" which had previously been subjected to $\approx$ 2 MegaRads of hadrons at the AGS, followed by 1 MegaRad of Co^{60} γ's. The absorption length was $\approx$ 40 cm (at 220 nm) after

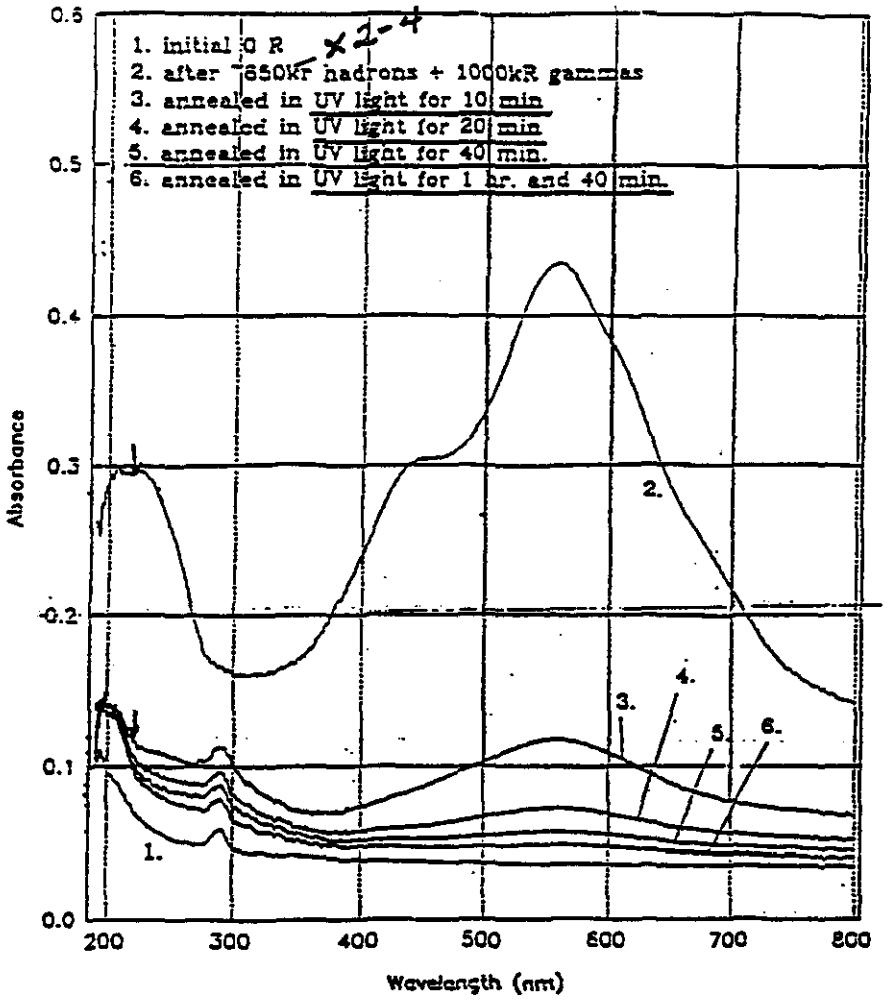

Figure 17: Radiation damage and recovery of crystal SIC703 (20 cm long) with exposure to light from a Mercury lamp.

irradiation. The crystal was placed 10 cm from a small (relatively low intensity) Hg lamp. The results measured in their spectrophotometer, expressed in terms of the absorbance

$$A = \log_{10}(I_{in}/I_{out}),$$

which includes the 10% loss at the two air/BaF_2 interfaces, are shown in Figure 17. The absorption length L_{att} recovered to 120 cm, well in excess of GEM's specifications for heavily irradiated crystals (see Appendix B.) after only 10 minutes' exposure to the lamp. Further recovery, reaching $L_{att} > 150$ cm after less than one hour's exposure, was observed.

Table 4: Absorption length L_{att} (cm) measured after irradiation and recovery of SIC703, with exposure to light directed through filters and optical fibers.

Before	After 500 Rad	3 Hr/> 420nm	3 Hr/> 300nm	3 Hr/> 180nm
250	104	120	144	160

- Further detailed measurements were made at BNL, using very low light intensities transmitted to the crystal through a small bundle of 7 quartz optical fibers. The light was not optically coupled into the fibers in any way: the lamp was allowed to shine on one end of the bundle, and the fibers were allowed to fan out and touch the end of the BaF_2 crystal at he other end of the bundle. The crystal was thermally annealed, and exposed to 500 Rads, before illuminating with light. A filter cutting off the wavelengths above 420 nm, was placed between the fiber bundle for the first three hour of light exposure, followed by three hours with a 300 nm cutoff, then a 180 nm (effectively no) cutoff. The results are summarized in Table 4, where the absorption length before irradiation, after irradiation, and after each successive three hour exposure to light are shown. The original curves from the spectrophotometer, showing the smooth reduction in absorbance A, for all wavelengths down to 190 nm (down to the end of the range covered by the spectrophotometer) are shown in Figure 18.

  The detailed data shows no apparent acceleration of recovery with the shorter wavelengths, and recovery throughout the whole spectrum (in the far UV as well) when the crystal is illuminated with long-wavelength light only.

  It is important to note that a change of attenuation length from an initial value of 2 meters to 1.5 meters corresponds to a change in transmittance over 50 cm of 6%. The absorption length can therefore be controlled precisely by monitoring the crystal transparency using the pulsed UV monitoring system (flash lamp or laser), with a short term sensitivity to changes of transmission of much better than 1%[13]. In this way, the uniformity of the light response curve over the length of a crystal-pair will be controlled near the optimum value (see Section 7.2.4) to 2-3%. As shown in Figure 19 [5,7], the contribution to the constant term of the energy resolution caused by radiation-induced non-uniformities in the crystals (for a variety of shapes of non-uniformity) is expected to be $0.1 - 0.15\%$.

[13]Long term stability at the 0.1 - 0.2% level has been achieved in the L3 Xenon lamp system, as discussed in Section 7.3.

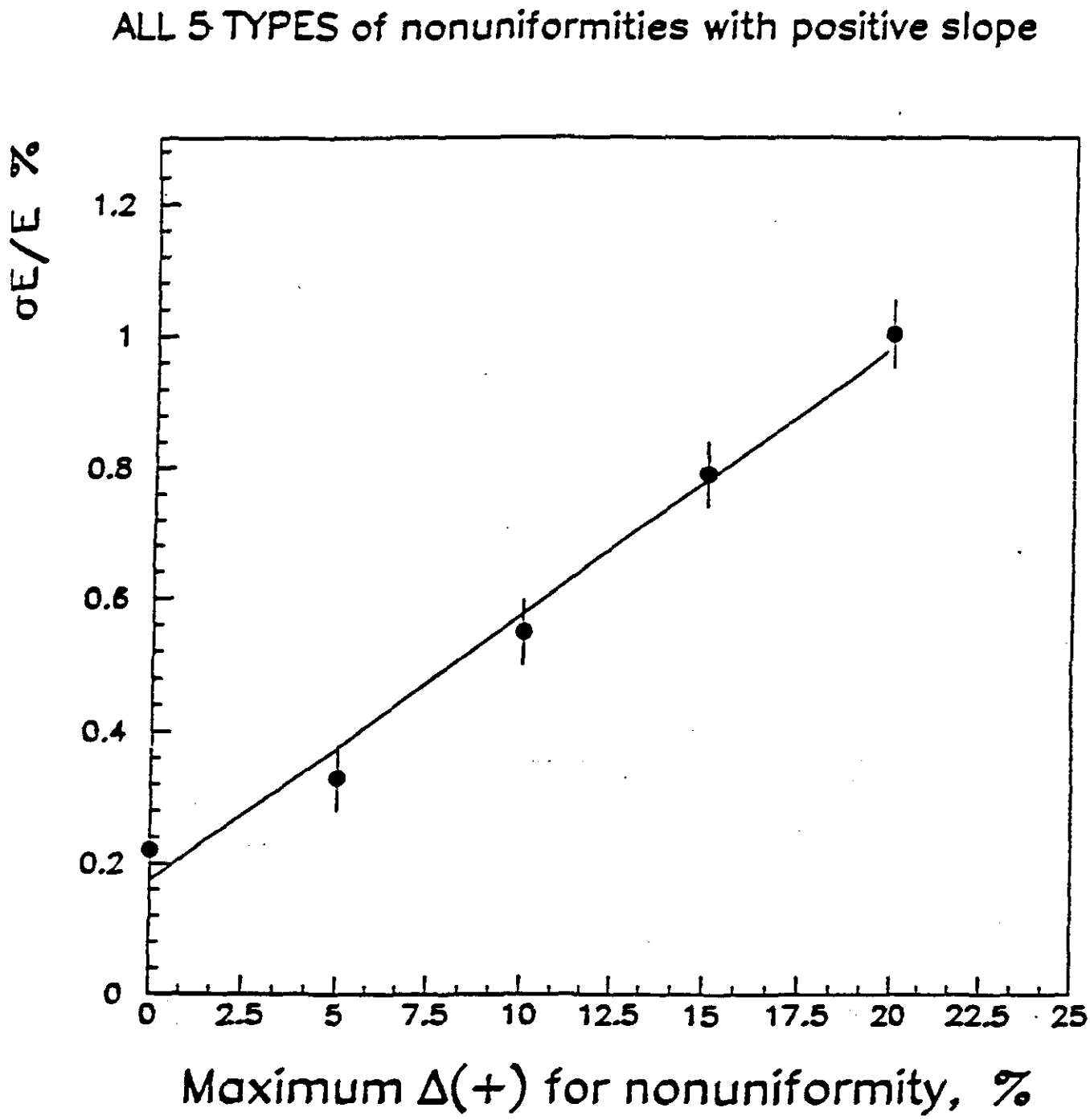

Figure 18: Energy resolution versus maximum deviation from light collection uniformity (%).

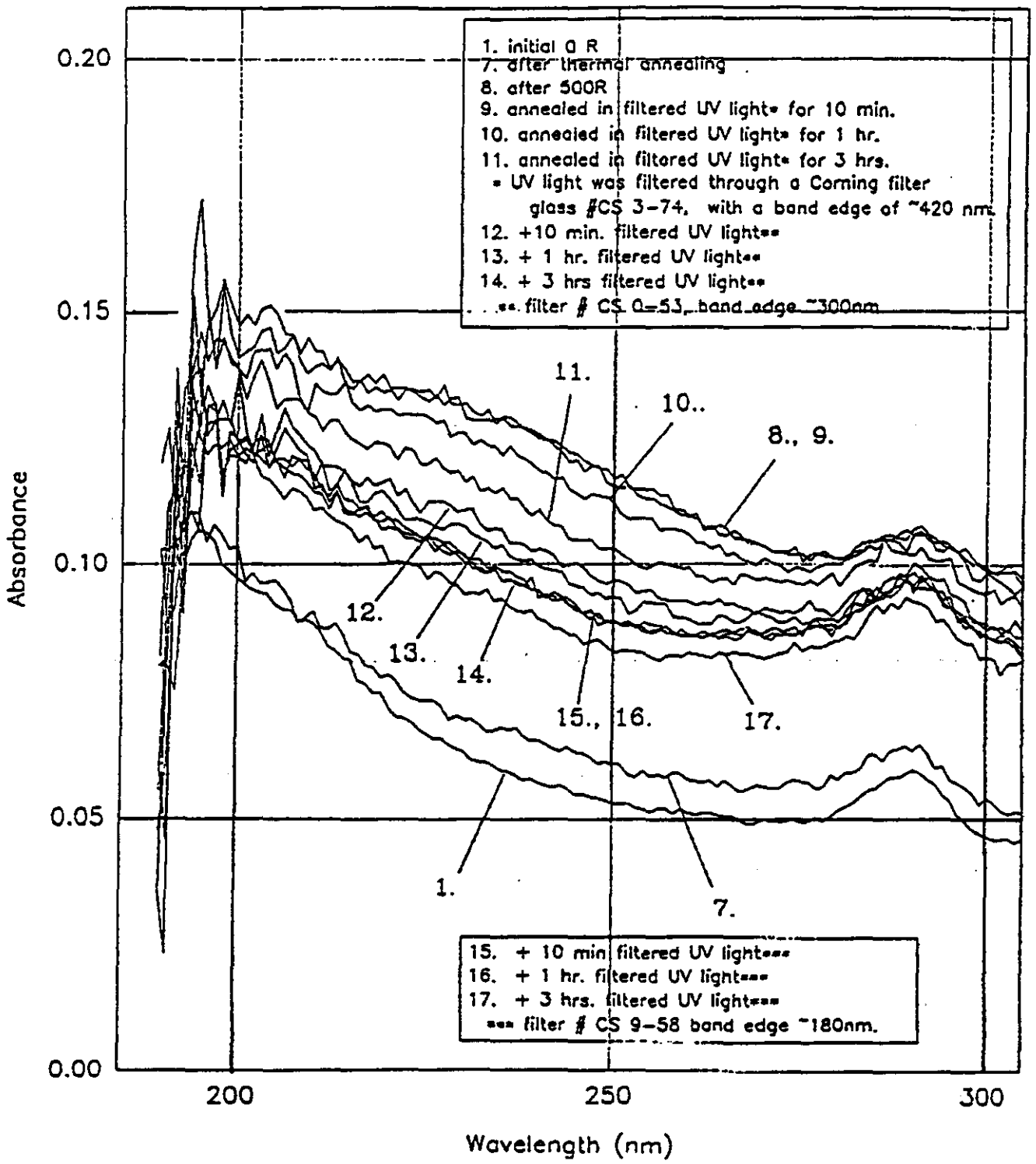

Figure 19: Radiation damage and recovery of crystal SIC703 (20 cm long) with exposure to light directed through optical fibers.

- Preliminary measurements at West Virginia University confirmed the effect seen at BNL: one gets the same recovery with or without cuttoffs for wavelengths shorter than 340nm.

- A 25 cm long crystal from SIC recovered from L_{att} = 35 cm to 100 cm using only RED light (700 nm), in a first test at Caltech.

- Two one inch BaF_2 cubes brought back from SIC in July were irradiated to 84 KRad at LLNL [51], at a rate of 3 KRad/hour (an order of magnitude higher rate than expected at the SSC at $\eta = 2.5$). One cube was in the dark and the other cube was illuminated with a small mercury lamp during irradiation. The light source was a miniature Pen-Ray mercury lamp with a rating of a 0.004 Watts/cm^2 at a distance of 1 inch the 254 nm line. The results are that the unilluminated, irradiated crystal lost 7.1% of its transparency, while the illuminated, irradiated crystal lost only 1.4% of its transparency at 220 nm (from 88.9% to 87.5%). This means that the small amount of illumination reduced the damage effect by a factor of 5. After 4 days in a dry atmosphere under room fluorescent lights, the transmission increased to 88.5 cm. Using Reference [52], recently formulated by R, Zhu and D. Ma to compute the attenuation lengths L_{att} accurately, the corresponding values of L_{att} are respectively 201 cm, 89 cm, and 148 cm. [14].

  LLNL is now testing crystals with filtered light, and with a tungsten lamp coupled with a silica fiber to a cube for *in-situ* irradiation/illumination.

- In tests performed at Caltech within the last ten days, R. Zhu *et al.*have shown that 10 hours of bleaching with blue light (400 nm) at modest intensity can bring the crystals to a stable light attenuation length of 180 cm (quite sufficient for our purposes) after irradiation to 1 MegaRad.

A more extensive, quantitative study of the flux and frequency range of light required to anneal the crystals *in situ* has been carried out by R.Y. Zhu and D.A. Ma at Caltech [53]. This study is summarized in Appendix G., which is attached to this report. The conceptual design of the light-annealing system for GEM is now underway, with mounting fixtures designed at ORNL, and light systems (standard lamps and fibers) being designed at IHEP and UCSD. The light intensity per crystal required to keep the crystals at a stable attenuation length of 1.5 meters ranges from a few milliWatts per cm^2 at $\eta = 0$ to

[14]With 1 inch long crystals, the absolute transmission measurement must be accurate to much better than 1% if an absorption length of 2 meters is to be precisely determined. The estimated error on the 201 cm absorption length in this test is currently $\approx \pm 20cm$.

50 milliWatts at $\eta = 2.5$, at SSC design luminosity. This is has been checked, at LLNL and by UCSD, to be 4 to 5 orders of magnitude below the DC power handling capacity of several types of standard quartz fibers. Latest results will be presented at the GEM meetings at the beginning of September, 1992.

The very encouraging results summarized above have led to several schemes, all of which appear to be practicable with standard lamps and fiber bundles, or other devices for illumination of all GEM crystals *in situ*. These include:

- Use of standard Hg or quartz Halogen lamps together with appropriate filters, or lasers equipped with beam expanders, in a continuous illumination mode. Since K-Cs-Te or RbTe photocathodes have quantum efficiencies below 10^{-4} for wavelengths longer than 400 nm, neither the DC currents, nor the electronic noise in a fast gate, would disturb the operation of the BaF_2 at all[15].
- Use of a pulsed UV lamp or laser (e.g. 308 nm) between runs or with data taking briefly gated off.

As of this writing, the first method appears easiest to implement, with ample light supplied through fibers to each crystal to allow annealing *in situ* up to the 10^{34} range.

[15]The RbTe photocathode's efficiency has recently been measured to be 1 μA/Watt at 400 nm.

9 Intercalibration Methods

Precise, frequent calibrations *in situ* are vital to maintain the high resolution of a precision detector. As shown in table 3, one of the the dominant contributions to the resolution of BaF_2 calorimeter at high energies is the intercalibration term (b_C, presented in Section 7.2).

The methods of calibration which will be used to precisely set the gain constant for each crystal of the BaF_2 calorimeter are:

- Absolute calibration by reconstruction of the Z^0 invariant mass [54] from its decay to e^+e^-[16].
- Daily gain monitoring using inclusive isolated minimum ionizing particles (MIPS), as currently under study at ORNL (also see [7]).
- Daily monitoring with a UV flash lamp and fiber system developed at UCSD, or a UV laser-based system which is being developed at CMU.
- An additional daily calibration with high intensity bursts of radiative capture photons, using a Radiofrequency Quadrupole Accelerator, as a cross check on the above methods.

9.1 Calibration By Inclusive $Z^0 \rightarrow e^+e^-$ Reconstruction

The primary means of calibrating each crystal in the BaF_2 calorimeter in GEM is the reconstruction of the Z^0 invariant mass, in inclusive $Z^0 \rightarrow e^+e^-$ events. It is important to note that the electrons involved in this calibration are very similar in energy to the photons from the Higgs in $H^0 \rightarrow \gamma\gamma$, where M_{Higgs} is in the 80 - 140 GeV range. An accuracy of 0.3% can be reached by using 150 electrons/crystal, which will be accumulated within 1 month of running at the standard SSC luminosity [54].

[16]Other higher rate physics reactions such as $\Upsilon \rightarrow e^+e^-$ and the copious electrons from b-decay are also under study.

9.2 MIP Calibration

The high flux of minimum ionizing particles (MIP) produced by the collider can also be used as a calibration source[7]. A MIP (mainly sailthrough pions) passing through a single 50 cm long BaF_2 crystal-pair longitudinally, deposits an average of ≈ 0.35 GeV. Since 50 cm of BaF_2 represents 1.7 absorption lengths, the probability of non-interaction for a pion is ≈ 18 %.

These signals will be extremely useful for a "relative calibration" of the response from crystal to crystal, that can be used together with the $Z^0 \rightarrow e^+e^-$ calibrations, and other monitors (discussed below), to maintain the precision of the BaF_2 system as a whole.

To look at MIP signals, A. Savin [7] simulated minimum bias events (MBE) and moderately high E_t events with Pythia 5.6. A P_t cut of 1.9 GeV was used. The number of interactions per crossing w as taken as 1.6 (Poisson-distributed), and the z-coordinate of the vertex Gaussian distributed with $\sigma_z = 4.0$ cm. No tracker information was used in the event analysis.

A GEANT simulation including the 0.8 Tesla magnetic field was performed. All particles were propagated through the BaF_2 EM calorimeter (with simplified geometry), but the transport for MIPs used accurate crystal geometry. No transport through the hadron calorimeter was performed, but the energy of each hit at the entrance of the HCAL was recorded.

To accumulate a sample of MIPs for calibration, one can use two methods. One is to use the MBE events which are routinely recorded. Each physics trigger event at 10^{33} will be accompanied by an average of 1.6 MBE events. The rate of these events (at a typical trigger rate recorded of 100Hz) is low, but this will allow us to undestand the MIPs events obtained, in detail.

The second method uses a dedicated trigger, which is straightforward to implement by branching off at Level 2 in the readout system, and sending data above a P_t cut to a crate of dedicated processors. This technique would allow us to acquire the 3000 MIPs per crystal which is needed for calibration accurate to 0.3% (see below) in a short time. The processors would then select isolated MIPs by a straighforward nearest neighbor algorithm. Extrapolating from the L3 RFQ system of similar (1990 vintage) design, we expect to get an absolute minimum of 1 kHz and more likely > 10 kHz throughput from these processors, which simply acquire digital data, histogram and find the mean.

Table 5: Number of Events Versus Precision of the Peak Position Determination, in the MIPs Calibration.

Number of Events	Precision of Peak Position (%)
100	1.72
400	0.97
800	0.65
1600	0.40
2400	0.29
3600	0.18
4800	0.14
7200	0.093
9600	0.075

The following criteria were used to select hadrons which traverse only one crystal, have relatively large E_t, and do not shower in the crystal.

- A single crystal has an amplitude in the range 0.25 - 0.50 GeV.
- The sum of the 8 crystals surrounding the one with the MIP-hit has an energy less than 95 MeV.
- The maximum amplitude in any of 8 crystals surrounding the one with the MIP-hit is below 70 MeV.
- There is a hit in the hadronic module behind the corresponding crystal.

Once this selection is made, the mean pulse height per MIP is 0.35 GeV. The energy distribution of MIPs, defined in this way, is well described by a Gaussian with a width $\sigma \approx 8$ %, plus a linear background.

To determine the statistics required for a calibration accuracy of 0.3%, events were generated according to the Gaussian + linear distribution obtained from the GEANT simulation. The number of events required to achieve a given statistical accuracy is listed in Table 5 [7].

Table 6: Minimum Required Time to Calibrate Crystal, With a 100 Percent Efficient MIPs Trigger.

$\mid \eta \mid$	MIPS Rate Per Crystal Crystal Per 10^5 Crossings	Minimum Time Required (Sec)
0.	2.6	1.15
1.	2.6	1.15
2.	13.0	0.23
2.5	54.	0.056
3.0	96.	0.031

As shown above, calibrating each crystal to a precision of 0.3 % will require approximately 3000 MIPs. Taking into account the η dependance of the event rate, Savin has calculated the minimum possible time of calibration, for a 100% efficient trigger, as summarized in Table 6 below.

With a dedicated 1 kHz (to 10 kHz) trigger, the required time for 0.3 % calibration accuracy is $\leq$ 32 (3.2) hours in the barrel, and $\leq$ 6 (0.6) hours in the Endcap. Taking into account that MBEs are present in all triggered events, and that triggered events should have higher P_t (and MIP rate too) than MBEs, the real calibration time may be 1.5 - 2 times less. It is thus very conservative to forsee a MIPs calibration accurate to 0.3% being obtained at least once per day during running. A separate MBE calibration trigger branching off at Level 1 may decrease the required time to a much smaller value.

Using a matrix of 5 $\times$ 5 crystals, with an upper limit of 200 MeV on neighboring crystals, gives a somewhat cleaner MIPs spectrum at low η, but decreases the total rate by factor of 1.75. This selection criterion may be applied to the low - η region.

For high luminosity it is possible to use a higher threshold cut of 200-300 MeV on the neighboring crystals in the region $2.7 \leq \eta \leq 3.0$, to increase the rate of selected MIPs.

The luminosity has some small influence on the peak position, because there is more pileup at higher luminosity. Changing from $\mathcal{L} = 10^{33}$ to $\mathcal{L} = 10^{34}$ has an effect of $\approx 1\%$ in the extreme lower end of the Endcap ($\eta = 2.5 - 3.0$), and less than 0.3% in the Barrel. One need only determine the luminosity with a precision of $\pm 2 \times 10^{33}$, to maintain the MIPs calibration accuracy to 0.3%.

9.3 RFQ Calibration

An additional calibration technique, which was developed for L3 and which we have proposed for GEM, is based on a Radio Frequency Quadrupole accelerator (RFQ) [40,42].

Depending on the type of target, this calibration scheme can be run in two different modes.

9.3.1 L3 RFQ Operation and Status

The first mode, developed for L3, uses a lithium target: the reaction $^7Li(p,\gamma)^8Be$ produces a flux of 17.6 MeV photons which can be used to calibrate the thousands of electromagnetic calorimeter cells at once, with an absolute accuracy of better than 1% in 1–2 hours. The feasibility of this calibration mode has been proven in an experimental test of a 4×5 L3 BGO crystal array [40]. An absolute calibration precision of 0.7% was achieved in the test. While the low energy photon calibration, method itself is not directly relevant to an SSC electromagnetic calorimeter, the L3 RFQ system is in many ways the "forerunner" (a lower energy working model) of the RFQ system proposed for GEM.

Caltech and the World Lab also have developed a gas neutralizer with a measured beam neutralization efficiency of 52%, meeting the calculated expectations. The L3 RFQ system is now running at the full rep-rate of 150 Hz, with a neutral H^0 beam which is focused on a target 7 meters after the neutralizer. A similar neutralizer will be used in GEM, with the beam focused at a distance of 12 meters.

The L3 RFQ system has been fully tested at the surface hall, and during a brief period down in Point 2 at LEP. It is now ready to be permanently installed in L3 September 15. In response to questions from GEM, we summarize the recent history of the RFQ at CERN, and its current status, as reported by Giorgio Gratta:

> The RFQ system arrived at the beginning of December, 1991, and was reassembled before the Christmas shutdown of CERN. We had the chance for a first (short) test run, which was successfully carried out before the New Year. We spent the time until February recommissioning the system. A major part of the work was the replacement of cables and the ion source housing made of PVC, and of other materials which were judged by the CERN Safety Group to present an undue

hazard in case of fire down in LEP Point 2. (This was not specified in a preliminary Safety Review in June 1990).

During this period we also prepared the necessary lifting jigs, mechanical supports, and other infrastructure. At the end of February the RFQ machine was lowered, reconnected, and its basic operation was successfully tested. Unfortunately, the LEP shutdown schedule was altered, because of other work on L3 in preparation for the 1992 data taking. At no time was the L3 magnetic field turned on, so that we could not test the RFQ system's operation in the leakage field (previously mapped) outside L3's magnet doors.

In addition, the temperature monitoring and protection circuit on the compressor for one of the cryopumps failed, causing the pump to shut down repeatedly (and causing noise to the L3 trigger). It was then decided to bring the machine back up to the LEP surface hall at Point 2 in May, and spend the Summer making sure that the system would work with full intensity in the L3 leakage field. This also allowed us to improve and verify the long term reliability of the system.

The RFQ system now runs very reliably. The magnetic field problems (for the beam transport and vacuum gauges) have been solved in a straightforward way, and tested extensively with a large magnet installed expressly for this purpose in the L3 surface hall. A good part of the beampipe has been redesigned and rebuilt, resulting in better downstream vacuum and higher beam intensity on target. We are now ready for installation in the L3 experiment on Sept 15.

9.3.2 RFQ Operation Mode for GEM

The second mode of RFQ operation [40,41], designed for use at the SSC uses a fluoride target: the reaction $^{19}F(p,\alpha)^{16}O^*$, and the subsequent decay of the excited oxygen nucleus $^{16}O^*$, produces hundreds to thousands of 6 MeV photons per millisteradian per beam pulse. These photons, functioning as a synchronized "equivalent high energy photon" of up to 25 GeV (per millisteradian subtended by a calorimeter cell, relative to the target), serve as a relative calibration source for all of the BaF_2 crystals. Using this system, a gain-monitoring precision of 0.3% can be reached, for a typical GEM crystal, wihin a few minutes.

It should be noted that since the radiative capture photons have a conversion length of $\approx$ 3 cm in BaF_2 , that 90% of the photons are absorbed in the first 7 cm. This

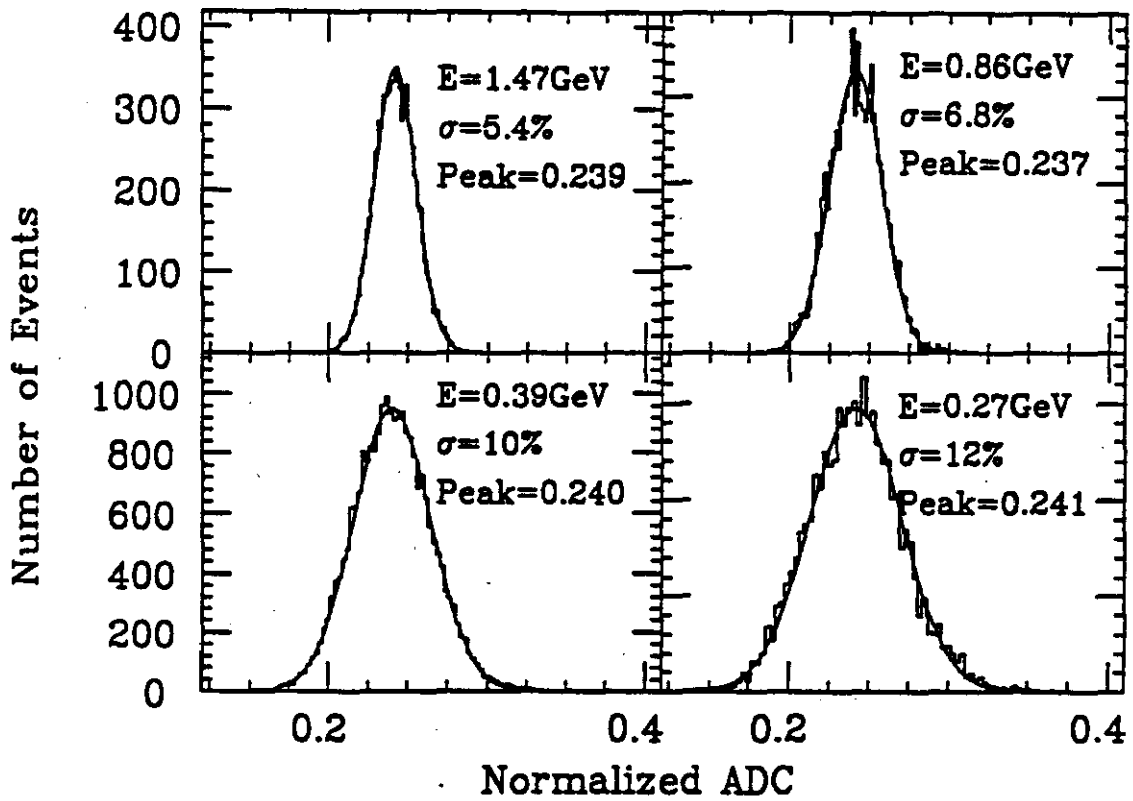

Figure 20: Normalized ADC distribution of a crystal at different energies.

makes the RFQ monitoring complementary both to the monitoring with MIPs, and to monitoring with the UV flasher system.

The feasibility of the RFQ monitoring mode with a fluoride target has been proven in another experimental test with 4 BaF_2 counters and a 7×7 L3 BGO crystal array [40]. Figure 20 shows the normalized ADC distributions of a crystal for runs with different beam intensities. The clean Gaussian distribution, and the correlation between the r.m.s. width and the total energy deposited in the crystal is clearly seen.

Figure 21 shows the deviation of the peaks of 49 BGO distributions, normalized to the sum of BGO energy in the 7×7 matrix, for several runs. This distribution has a gaussian shape with a standard deviation of 0.34%. The coresponding distribution with the BaF_2 counters had a standard deviation of 0.29%. In GEM, a series of calibrations over a longer time period, and correlation with the RFQ machine parameters to control systematics, is expected to give an accuracy which is better than the results of these early tests.

The equivalent photon energy (EPE), defined as the sum of the energies of photons

Table 7: Measured and Calculated Equivalent Photon Energy Expected from an RFQ Beam Pulse on Target.

Proton Energy (MeV)	2.0	2.5	3.0	3.5	3.85
EPE_{meas} (GeV)	1.5	13	22	30	37
EPE_{cal} (GeV)	2.6	14	24	33	38

from one beam pulse hitting one crystal detector, was measured at AccSys with a LiF target. Up to 2.38 GeV/0.1μCoulomb/1.6msrad was observed for a 1.92 MeV beam. There are much stronger fluorine resonances between 2.0 and 4.0 MeV [50], beyond the 1.92 MeV beam energy used in the test. By using a 3.85 MeV RFQ and a CaF_2 target, which would have no neutron production as a by-product below 4.05 MeV [50], an EPE of 30 GeV/0.1μCoulomb/1.6msrad or more is expected. Table 7 lists the EPE's measured with a CaF_2 target bombarded with a proton beam from a Van de Graaff at Caltech. The expected equivalent photon energies, calculated with an integration of the resonances [50], are also listed in the table. It is clear that with a 3.85 MeV proton beam up to 25 GeV per millisteradian per 0.1 μCoulomb on target can be achieved.

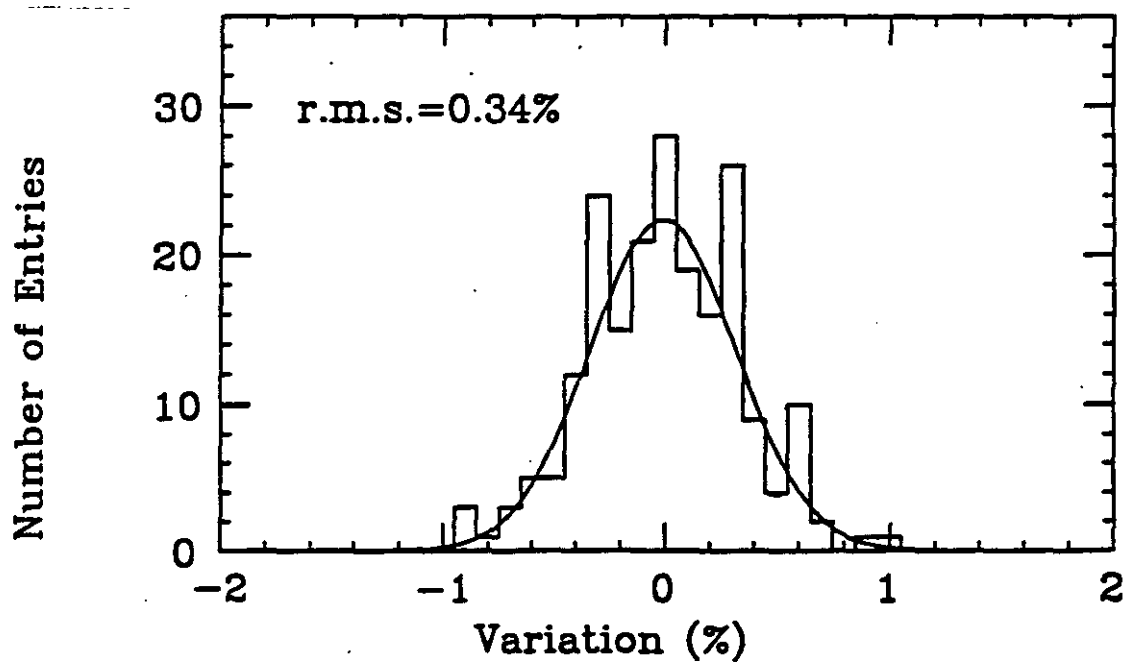

Figure 21: Variation of the normalized peak positions from BGO crystals.

9.3.3 Installation Plan for the RFQ Installation in GEM

AccSys and ORNL have developed a plan, and preliminary drawings, for installation of the RFQ system in GEM. The installation scheme is shown schematically in Figure 22.

The present plan for RFQ calibration is to use an AccSys Model PL-4 linac system operating with an H^- beam that is stripped to H^0 in a gas neutralizer, for transport into the central region of the detector, through the GEM magnetic field. The beam pipe enters at $\eta = 0$ through the Central Detector Support ("Membrane"), with a 6 cm diameter beam pipe terminating in a target (of the same diameter) in the central tracker region, outside the Silicon strip part of the tracker. Four BaF_2 crystals are removed for this purpose.

The H^- beam peak current design value is 30 to 40 mA, based on an existing H^- ion source design (see Appendix E). The RFQ beam is pulsed at $\approx 30Hz$ in 10μsec square pulses[17] The pulsing rate is chosen so that minimal target cooling will be required. Given the computed beam profile and the neutralizer efficiency measured in the L3 system, we have set a conservative figure of 10 mA peak current on target (15 to 20 mA expected). This corresponds to 100 nanoCoulombs per pulse, or $\approx 25GeV$ Equivalent Photon Energy (EPE) for a typical barrel BaF_2 barrel crystal (3.1×3.1 cm^2 at the front face), situated at a distance of 1 meter from the target. The minimum EPE (for the small crystal in the innermost ring of an endcap) is ≈ 1.5 GeV. At full machine intensity, we can expect $200GeV$ or more in the closest crystals.

Detailed simulations and precise tests [40] have shown that the average energy deposited by a photon in one crystal is 4 MeV, and that the fluctuations from pulse to pulse follow a Poisson distribution with an average of N objects, where N $\approx$ 250E(GeV). There are no tails on the pulse height distribution, as observed during our tests, over at least three orders of magnitude. The fluctuations in pulse height from one pulse to the next are very small, for a typical crystal. The beam on target is normally stable to within $\approx 1\%$ from pulse to pulse, for short periods. However, by normalizing to the beam intensity on target for each pulse (e.g. by looking at the total pulse height in the BaF_2 calorimeter) one can determine the relative response of each crystal to a statistical precision of better than 0.1% in a two minute run.

The accelerator system parameters, performance specifications, accelerator layout,

[17]This is updated from the July 27 AccSys proposal in Appendix E, which used the shorter pulse width and higher repetition rate associated with the L3 RFQ operation mode.

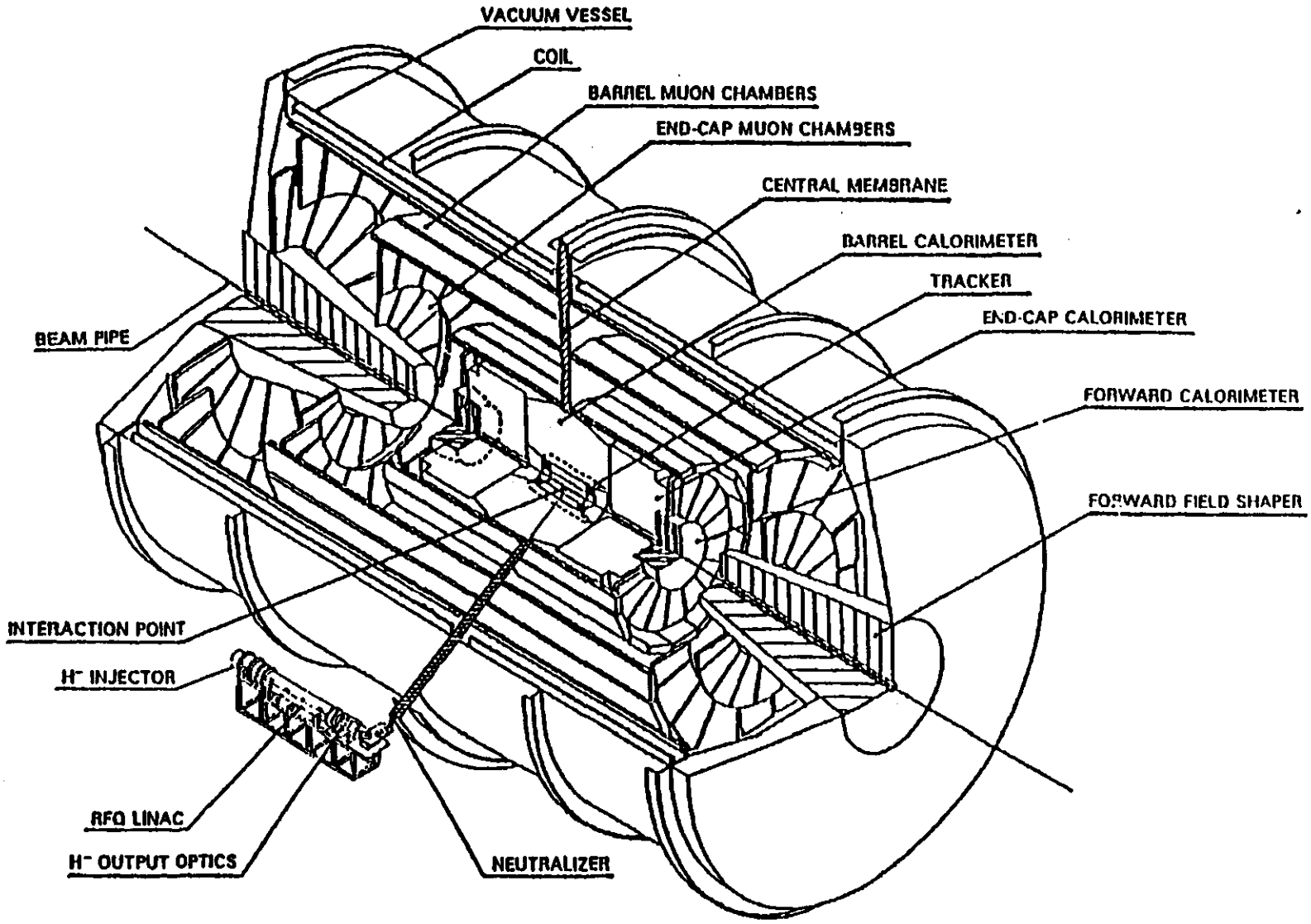

Figure 22: Installation scheme for the RFQ calibrator in GEM.

H^- ion source design, beam transport plan, and charged beam transport computations, up to the neutralizer, are summarized in Appendix E.

The details of the RFQ gain-monitoring procedure, including the relative pulse height expected in each crystal, and the systematics associated with beam stability and other factors which might affect the time-stability of this method, are now under study by A. Savin (ORNL) [7]. A report by H. Newman also will be presented at the GEM meetings in September.

9.3.4 RFQ Calibration Electronics Readout In GEM

(Report By Peter Denes.)

The RFQ system for GEM produces a long (10μsec) photon pulse, whose average distribution is used to monitor the gain of the BaF_2 crystals. As the photons are produced at random throughout this interval, additional electronics is required in the readout chain to acquire the RFQ signal. The proper way to acquire this signal is to add one more tap to the preamp split, and to fully integrate the entire 10μsec RFQ pulse with a separate, slow, gated integrator. This task is comparatively easy, as wide dynamic range is not required, and the electronic noise is negligible due to the long integration time. In this respect, the signal acquisition is essentially identical to the L3 BGO readout system. Such electronics is easily incorporated in a digital pipeline readout system in one of the two following scenarios:

Scenario I: Multiple ADCs –
If multiple ADCs are required to span the dynamic range, then the RFQ calibration channel consists of a separate gated integrator and CMOS ADC. The ADC outputs are then multiplexed into the standard readout. The analog electronics and slow ADC will cost approximately $ 50/channel [18].

Scenario II: Single ADC with Analog Multiplexer –
In this scenario, the multiple gain stages following the preamp are multiplexed into a single 60 MHz ADC with an analog multiplexer. The gated integrator would simply be one more input to the analog multiplexer. The ADC then simply runs normally at 60 MHz, sampling the rising integrator output every 16 ns, and one particular bucket, after

[18]This additional cost is offset by the lack of a small storage ring compressor, which is no longer needed to shorten the RFQ pulse. The price of this compressor was included in the cost estimate given by AccSys Technology, in the BaF_2 cost estimates through July 1992.

the RFQ pulse is terminated, is read out by the standard readout chain. In this case, the additional cost is simply the gated integrator, which should be less than $10/channel.

Note that a separate gain monitoring channel facilitates the use of optical pulse calibration monitoring. As experience from the L3 BGO has demonstrated, the difference in pulse shapes between the scintillation light and the optical calibration pulse may produce systematic gain shifts. These shifts would be eliminated with the use of a slow calibration channel. [19].

9.3.5 Availability of a Low Cost RFQ for GEM

Two RFQ systems with exactly the specifications required for the GEM calibration system at the SSC, built for the U.S. Navy (for a different application), are currently being commissioned at AccSys Technology, Inc. One of the accelerators is expected to be available by the Fall of 1992 for a full energy test of our technique at 3.85 MeV, using BaF_2 counters. At least one of the accelerators could be purchased (used) at very low cost by 1995, once the Navy's test program is completed.

The time required to complete, test and deliver a new RFQ accelerator, beam transport and neutralizer [41] is estimated to be 1.5 years. A complete RFQ system for GEM, including the downstream beam pipe and target, could thus be available by 1995.

9.4 UV Flash Lamp Monitoring System (UCSD)

A monitoring system consisting of a low pressure UV flashtube (Hamamatsu L3530-01), filter (Oriel 53320) with a bandpass matching the BaF_2 fast scintillation components (220 ± 25 nm), a diffuser consisting of a 50 cm long BaF_2 crystal-pair, and 0.5 mm quartz fibers, has been built at UCSD. The system provides 3 nsec pulses, as seen by an R4480 phototube with a RbTe photocathode. Very large pulses can be generated, up to the limitations of the existing phototube bases, according to the orientation and distance of the ends of the quartz fibers from the glass envelope of the UV tube.

The UV flashtube system was used in the last month to test the charge gain and linearity of the ORNL preamp, and the number of photoelectrons and the linearity of the phototube, in preparation for the tests of BaF_2 crystals in the UCSD cosmic ray

[19] Using the second scenario, a net cost savings of $\approx$ $0.5 M may be foreseen, by elimination of the pulse compressor storage ring.

tower. During running, the gains obtained with cosmic muons are being cross checked against the results obtained with the UV lamp system.

One possible plan for UV monitoring of the entire BaF_2 calorimeter with a system of this type includes 150 - 300 fibers per tube (a total of 50 - 100 flashtubes). In order to monitor changes in the flashlamp intensities, 50 - 100 BaF_2 crystals will have fibers from two lamps. In order to maintain the gain monitoring precision and global linearity, an option is being studied with two sets of flashlamps, 2 fibers per crystal, and 50 - 100 crystals having fibers from 4 flashlamps.

This system will be used to monitor the gain between calibrations using inclusive $Z^0 \rightarrow e^+e^-$ production, and other physics calibrations. In addition, if annealing of the crystals with light is implemented, this system will be used to control the transparency (absorption length) in the crystals, so that the light collection uniformity and hence the high resolution can be maintained during running.

Further information may be found in the UCSD status report, to be presented at the GEM meetings in early September.

9.5 UV Laser Monitoring System (CMU)

CMU has designed, and is developing a UV laser light monitoring system for the BaF_2 calorimeter. This will monitor the crystal transmission and photodetector response, in a way which is analogous to the Xenon lamp + light fiber system used in L3. The CMU system uses laser light pulsed at a rate of several tens of Hertz and several nsec pulselength, to monitor the transmission of the crystals and the photodetector response. The laser light will be transported through pipes filled with inert gas to minimize transmission loss, to a point near the calorimeter. The light will then be fanned out to UV-transmitting fibers which will transmit the light to the individual crystals. After testing the concept and design with a frequency-doubled 266 nm system available at CMU, the prototype system was constructed using a compact, low cost KrF (248 nm) laser.

In the longer term, excimer lasers in the 220 nm range could also be used, which are available at moderate cost.

10 Results of the 1991 BaF_2 Beam Test

The first BaF_2 test beam run was carried out successfully, entirely by GEM physicists, using the first prototype matrix of 49 BaF_2 crystals of reduced size at Fermilab (Experiment T-849) during December 1991.

A brief summary is given below. A more detailed report on the analysis and results is contained in Appendix F.

We triggered on a 4×4 cm^2 beam spot of particles identified as electrons in a transition radiation detector. The beam had a momentum spread of about 3 GeV FWHM and an angular spread of about 1.7 mrad. The analysis so far has concentrated on electrons spread rather uniformly over the 20×20 mm^2 front face of the central crystal.

The beam momentum was measured with a spectrometer composed of bending magnets and drift chambers. Previous experiments have obtained a momentum resolution of 1% in this beam. Following our improvements of the beam line, we achieved a momentum resolution of $0.5 \pm 0.2\%$.

We developed a clean set of beam cuts based mainly on the beam spectrometer, but including a cut on position matching between the coordinate determined by projecting the fitted trajectory onto the BaF_2 matrix, and the coordinate determined from the BaF_2 matrix itself. We also required that we see only one particle (one local energy maximum) in the crystal array. These "clean beam" cuts accepted 10% of the electron triggers. We removed remnant pions from the sample by requiring that we don't see a large amount of energy in a backup calorimeter. These cuts do not bias our resolution measurement.

For the FNAL run, we recorded pulse heights with a standard Fastbus ADC. We set all of the BaF_2 counters to have approximately the same output per MeV of energy deposition using straight through muons. To keep the central crystal within the range of the ADC, the gains were set to give one ADC channel per 30 MeV of deposited energy. The pedestal RMS spreads were about 1 ADC channel for all of the crystals. Since concluding the data-taking, we have found that electronic "noise" – including the trivial effect arising from the differential linearity of an ADC, which is important when the pedestal width is typically 1 channel – contributes 0.4% to our energy measurement at 68 GeV. This effect could easily be removed by splitting the signal so that one channel can record the pulse height with a higher gain. (This is part of the plan for the 1993 beam test, as discussed below).

We determined the energy in the BaF2 matrix by summing the energies in each crystal. The individual crystal energies were computed by subtracting the pedestal from the ADC value and multiplying by a gain correction factor. The gains of the counters were determined from the electron data. No energy corrections based on position or other variables were applied.

We have determined the RMS error on the difference between the energy measured in the BaF_2 and the energy measured in the beam spectrometer to be 1.0%. This number comes from a Gaussian fit to the measured energy distribution. The fit is made over the energy region ± 2.25 standard deviations away from the peak. This method gives a very fair estimate of the energy resolution, disregarding only a few percent of the events which are in the tails.

If we unfold our estimate of the beam momentum resolution of 0.5% and the 0.4% contribution due to the trivial electronic noise described above, we obtain a BaF_2 resolution $0.77^{+0.12}_{-0.18}\%$ at 68 GeV. This is consistent with the resolution expected from a GEANT simulation of 0.6%.

From the uniformity measurements made with the muon beam, we know that the nonuniformity of light collection in these crystals made a significant contribution to the energy resolution. Our best estimate of this contribution is 0.6%, and definitely not less than 0.5%. If we remove the effect of the nonuniformities, the BaF_2 resolution lies in the range of 0.0 and 0.7%.

We expect to be able to make substantial improvements in our next test beam run with improved crystals from China, a larger size matrix of full size crystals, thinner beam chambers and counters, a calibration system for gain-monitoring, and better (lower noise, higher dynamic range) electronics.

11 Detector Quality Control and Acceptance Testing

IHEP(Beijing) and USTC(Hefei) have agreed to take resonsibility for quality control and acceptance testing of the BaF_2 crystal pairs in China. This includes a detailed measurement of the light yield and light response uniformity profile, to be performed using transverse muons in a Cosmic Ray Test Stand, designed following the experience – and in cooperation with UCSD. Following discussions with LLNL, ORNL, UCSD and

Caltech, the acceptance criterion for the crystals has been set, that the crystals will be uniform to within 3%, as measured with the test bench. IHEP and USTC also will take the responsibility to track the crystals through the production process, and to record the data on accepted crystals into a database.

The test sequence, setup and electronics readout of the Cosmic Ray Stand, and the estimated costs are summarized in Appendix H [55]. The test stand will have a capacity of 40 crystals per day. 43,000 hard cosmic muon events per crystal will be a accumulated for each 48 hours of running, to provide a profile accurate to 1% in each 2 cm section, for each crystal in a batch. This will allow all 16,000 crystal pairs to be tested within three years, with time for repeat runs, cross-checks, and reprocessing and remeasurement of any crystals that fail to meet the specifications.

12 Conclusion: The BaF_2 GEM Calorimeter

The precision BaF_2 crystal calorimeter is the superior choice for GEM. Its enhanced potential for physics discoveries, manufacturability by a strong international team, and its stability in the SSC radiation environment, are now established. Multiple calibration techniques of sufficient precision, which are a concern for any high-precision EM calorimeter system, have been developed by the use and/or extension of proven techniques.

Over the last two decades, large homogeneous crystal calorimeter systems (Crystal Ball, CLEO, CUSB, L3) have been built, and have achieved their high design resolutions. The only limitations have been traced to the calibration quality, which fundamentally rests with the availability of sufficient physics calibration processes, combined with quick precise monitoring methods. For the case of a high precision calorimeter for the SSC, speed and radiation hardness in situ are additional requirements, which – following extensive R&D – have been met by the GEM BaF_2 system. Ongoing developments in China will further improve the intrinsic radiation hardness of the crystals, and will further ensure that all of the design goals for GEM are met. But most importantly, crystals of EXISTING quality can be strictly controlled to meet all of the GEM's requirements.

Based on the established evidence, the BaF_2 EM calorimeter, whose capabilities are well-matched to the Scintillating Fiber hadron calorimeter and precision muon system, will provide GEM with unique discovery potential in the SSC physics program. The

BaF_2 system's ability to find the Intermediate Mass Higgs, and other new particles in this mass range through their decays into electrons and/or photons, cannot be matched by any other EM technology which could be manufactured on a large scale starting in 1993 – at the current state of development, or with forseeable developments in the near-term future.

APPENDIX A.

Requirements for Each GEM Electromagnetic Calorimeter Technology

The GEM Executive Committee reviewed the status of the EM calorimetry R&D Programs, and formulated the following list of requirements for each technology:

A. Requirements for BaF_2 Technology

1. Demonstrate substantial improvement in the radiation resistance of large BaF2 crystals (20-25 cm long) towards the GEM specifications - reach absorption length of at least 60 cm at 220 nm after 1 MRad irradiation with photons, and if possible with high energy hadrons. Present a detailed plan to obtain final GEM quality crystals, along with evidence of manufacturability and cost, including work required to prepare crystals after delivery.

2. As proposed by the Expert Panel, produce small radiation-hard crystals to demonstrate there are no fundamental limitations in making radiation hard BaF_2 crystals (e.g. absorption length $\geq$ 95 cm at 220 nm after 1 MRad)

3. Address in detail questions of preradiation, wrapping, residual non-uniformity, in crystals we can practicably expect to manufacture. Cosmic ray transverse measurements in produced crystals could provide useful data. Provide a detailed practical plan for calibration of the BaF_2 system in-situ: describe the calibration strategy, RFQ layout, and the required calibration time for each proposed technique to achieve the necessary accuracy.

4. Show by MC and by lab tests that the following effects do not destroy the resolution of the BaF2 system (maximum tolerable constant term is 0.6

   - Residual non-uniformity (as installed);
   - Non-uniformity developed by possible further radiation damage of "saturated" crystals and/or by possible annealing; (Note - the expert panel and executive committee are not convinced of the proposal to preradiate the crystals)
   - Accuracy of intercalibration (see point 3);
   - Short term instabilities of readout system;
   - Linearity, linearity calibration and dynamic range of readout system.

B. Requirements for LAr/LKr Technology

1. Demonstrate by beam tests that the stochastic term in the resolution for non-projective geometry is $\leq 7\%/\sqrt{E}$. Determine the angular dependence of this resolution.

2. Produce detailed mechanical design/analysis of the EM barrel and end caps with optimization of gap between barrel and end cap, wall thicknesses, etc.

3. Demonstrate by Monte Carlo simulations, for realistic projective geometry and full angular range (between 90 and 5.7 degrees) the resolution:

$$\leq 7\%/\sqrt{E} + 0.4\%$$

   and physics consequences of the gap between barrel and end cap, wall thicknesses, etc.

APPENDIX B.
BaF_2 Crystal Specifications for GEM

The specifications for BaF_2 crystals that will meet the GEM requirements for the final BaF_2 calorimeter are summarized in this section. The three vital requirements are radiation resistance, dimensional tolerances for a 50 cm long crystal-pair, and UV transmittance.

We have specified the transmittance requirements in terms of the minimum fraction of the light passing through a 25 cm long BaF_2 crystal at specified wavelengths. For simplicity, these specifications include the ~8% loss at the two interfaces between air and BaF_2. The radiation resistance requirements lead to a specification that after a saturated radiation dosage the BaF_2 crystals have more than 95 cm light attenuation length for 220 nm light (at the peak wavelength of the fast scintillation component).

GEM Specifications for BaF_2 Crystals

- **Dimensional Tolerances:**
  - from -300 μm to 0 μm in the transverse dimensions (typical deviations from nominal 100μm)
  - from -400 μm to 0 μm in length
  - less than 50μm in planarity of all faces after coupling two 25 cm long half crystals.
- **Transparency Before Irradiation**, specified in terms of the minimum fraction of the light at specified wavelengths which passes through 25 cm of crystal length:
  - $\geq$ 75% at $\lambda = 200$ nm
  - $\geq$ 80% at $\lambda = 220$ nm
  - $\geq$ 82% at $\lambda = 300$ nm
- **Transparency after 1 MRads Irradiation**, specified in terms of the minimum fraction of the light at specified wavelengths which passes through 25 cm of crystal length:
  - $\geq$ 66% at $\lambda = 200$ nm
  - $\geq$ 70% at $\lambda = 220$ nm
  - $\geq$ 72% at $\lambda = 300$ nm

Note: the dimensional tolerances have been further specified following recent work on the engineering design by J. Heck (ORNL).

For the 30 crystal-pairs to be delivered to Caltech during 1992, according to the MoU signed between SIC, BGRI and the GEM Spokesmen (March 16, 1992) the dimensional tolerances are as given above, and the specifications for transparency after irradiation are:

GEM Specifications for 30 BaF_2 Crystals for Delivery in 1992

- **Transparency after 1 MRads Irradiation**, specified in terms of the minimum fraction of the light at specified wavelengths which passes through 25 cm of crystal length:

- $\geq 45\%$ at $\lambda = 200$ nm
- $\geq 50\%$ at $\lambda = 220$ nm
- $\geq 52\%$ at $\lambda = 300$ nm

APPENDIX C.

LETTER OF INTENT
BY
BARIUM FLUORIDE COLLABORATION
TO
ZHONGNAN OPTICAL INSTRUMENT FACTORY
FOR COLLABORATION ON THE PRECISION MACHINING AND POLISHING OF BARIUM FLUORIDE CRYSTALS

Representing the Barium Fluoride Collaboration:

Dr. Craig R. Wuest
Lawrence Livermore National Laboratory
for
Professor Harvey Newman, Spokesman
for Barium Fluoride Collaboration
California Institute of Technology

Representing the Zhongnan Optical Instrument Factory:

Mr. Zhang Chunyuan,
Zhongnan Optical Instrument Factory
for
Mr. Song Shubin, Chief Director
Zhongnan Optical Instrument Factory

INTRODUCTION

The Barium Fluoride (BaF_2) Collaboration has been formed to build a large Electromagnetic Calorimeter to be installed in the Gamma, Electron, and Muon (GEM) Detector at the Superconducting Super Collider (SSC) in Dallas, Texas, USA. This calorimeter will be built of very pure crystals of scintillating barium fluoride (BaF_2). A similar calorimeter, made from scintillating bismuth-germanium-oxide (BGO) was built in the 1980's using methods developed at Shanghai Institute of Ceramics in collaboration with Laboratoire d' Annecy de Physique des Particules (LAPP). This detector consisted of 11,000 crystals of BGO and was installed in the L3 detector at CERN Laboratory in Geneva, Switzerland.

The successful completion of the BGO calorimeter has encouraged scientists to build a new calorimeter for SSC detector applications. Because of the operating parameters for the SSC, BGO was not deemed suitable and BaF_2 was found to perform well, giving a fast (nanosecond) time response and a resistance to darkening due to radiation damage.

Over the past two years many visits have been made between the Institutes in the West and China. These visits have resulted in a major new effort at Shanghai Institute of Ceramics (SIC) and the Beijing Glass Research Institute (BGRI), to provide sample BaF_2 crystals for studies. These studies include radiation resistance, optical clarity, response to high energy beams of charged particles, etc. The results of these studies show that BaF_2 is a good choice for the SSC. However, a few problems have been found with BaF_2 that require further work. First, BaF_2 crystals produced at SIC and BGRI have been found to be less resistant to radiation than desired. Second, the mechanical processing of BaF_2 crystals was needing improvement and, in fact, could have been contributing to the poor radiation resistance because of the introduction of impurities and superficial mechanical stresses into the crystal during cutting, polishing, and lapping.

Early in 1992, Lawrence Livermore National Laboratory was invited to join the BaF_2 collaboration. At the same time, the Zhongnan Optical Instrument Factory was also asked to participate, specifically to apply its precision machining and polishing techniques to BaF_2 processing. This effort has culminated in the delivery to LLNL of polished crystals from the Zhongnan Optical Instrument Factory, and soon after, by the visit to China by Dr. Craig R. Wuest of LLNL and, also, Mr. Michel Lebeau of LAPP in France.

VISIT TO ZHONGNAN OPTICAL INSTRUMENT FACTORY

A visit to the Zhongnan Optical Instrument Factory was made on July 9, 10, 1992. Visitors included Dr. Wuest, Mr. Lebeau, Professor Z.Z. Dai of BGRI and many researchers from SIC, led by Professor P.J. Li of SIC. Many technical discussions and tours of shops were made and it is clear that the Zhongnan Optical Instrument Factory has many important capabilities for the processing of BaF_2 including sawing, grinding, polishing, lapping and optical coating. In addition, many precision machines are available to characterize BaF_2 crystals. These include optical and non -optical measuring machines for angles and spatial coordinates, flatness monitors, spectrophotometers and polarimeters for measuring stresses in the crystals.

All of these facilities have been used to prepare a very precisely machined pair of BaF_2 crystals, which were sent to LLNL for evaluation. Although the crystals arrived in LLNL damaged, it was still in such a shape to provide measurements and evaluation of surface polish. Initial examination of the crystal is favorable and detailed measurements are underway at LLNL.

LLNL has also been studying new techniques for polishing BaF_2 and also for growing ultra-pure crystals. LLNL's polishing technique closely parallels that of Zhongnan except that a

final polishing step is included using a fine diamond-loaded pitch lap with a silicon fluid or ethylene glycol. This final lap provides a high quality, crystalline surface suitable for optical coating with reflective aluminum.

Technical discussions at Zhongnan included the implementation of the diamond lapping technique for BaF_2 processing, as well as discussions on optical coatings. These discussions resulted in a plan for the preparation of BaF_2 crystals for LLNL an also to produce a completely polished crystal pair to replace the damaged pair in LLNL. Also, a single crystal (one-half (1/2) of a crystal pair) will be coated with reflective aluminum and overcoated with protective silica. The details of these tasks are described in the next section.

SCOPE OF WORK - SHORT TERM PROGRAM THROUGH AUGUST 30, 1992

The program of work agreed upon at the Zhongnan Optical Instrument Factory on July 10, 1992 and at SIC on July 14, 1992 is as follows:

1) Zhongnan Optical Instrument Factory will provide five (5) or more crystal pairs to LLNL as soon as possible, contingent upon the expeditious supply of crystal boules to Zhongnan. SIC will supply small (front) crystals and BGRI will supply large (back) crystals to Zhongnan. SIC already has crystals available. BGRI will grow five crystals as soon as possible. The specification of the crystal pairs is described in the Technical Specification Document prepared by Mr. Jack Heck of Oak Ridge National Laboratory and delivered to Zhongnan by Dr. Craig Wuest of LLNL and Mr. Michel Lebeau of LAPP. This document entitled, "Specification for Barium Fluoride Scintillation Crystals for the SSC EM Calorimeter," is numbered XDE-TS-A6292-01 REV A. Changes to a number of dimensional tolerances, surface flatness, perpendicularity and profile were made in this document, as agreed upon by parties from Zhongnan and LLNL, with consultation by Mr. Lebeau of LAPP, and incorporated into the technical specification. The specific task is outlined in Section 2.0, "Option Two, Cut Individual Crystals," beginning on page 8. The task is modified so that five (5) each Front crystals and five (5) each Back crystals are to be prepared by Zhongnan as specified in Tables 2 and 3 on pages 4 and 5. The crystals are to be rough-cut using dimensions for Theta Row 1 in Tables 2 and 3. The cut crystal is to correspond to the drawing: SK-TS-A6292-01-01, "Left Hand (LH) Front Crystal," which contains the modifications to the specifications as described earlier. These same modifications also apply to drawing SK-TS-6292-01-03, "Left Hand (LH) Back Crystal," as well. These rough-cut crystals will be sent to LLNL as soon as possible.

2) Zhongnan Optical Instrument Factory will provide one (1) crystal pair to LLNL to replace the damaged crystal pair received at LLNL on July 1, 1992. The specification for this crystal pair is the same as for the damaged crystal pair and is an effort to show Zhongnan's capability to provide crystals to final finished specification. This is a fully polished crystal pair, as opposed to the five crystal pairs in job 1), which are rough cut only, and will be polished at LLNL. The crystal pair for this task was delivered to Zhongnan on July 9, 1992 by Professor Z.Z. Dai from BGRI.

3) Zhongnan Optical Instrument Factory will prepare a single crystal, either a front or back crystal half, with a reflective optical coating, consisting of 1250 Å of aluminum with an outer protective layer of 2500 Å of silica (SiO_2). Care should be taken so that the end faces of the crystal are not coated. The four (4) long sides of the crystal only, should be coated. This finished crystal will be sent to LLNL for analysis. It should be noted that all six (6) faces of this crystal should be polished to the best possible finish prior to coating.

The three jobs described above do not require the use of radiation resistant, or especially pure, crystal boules. For the sake of time savings, machining of crystals of lower optical quality is satisfactory as long as high quality of machined and polished surfaces is maintained.

The time for these three jobs to be completed is determined by the availability of crystal boules. SIC has a sufficient number of Front half crystal boules to allow Zhongnan to begin cutting these boules immediately (July 20, 1992). Three weeks is needed by Zhongnan to cut these five crystals. Also, beginning on July 20, 1992 Zhongnan will begin polishing the single crystal pair outlined in Job 2), and the coating of the 1/2 crystal in Job 3). All these jobs will be completed by August 10, 1992 and ready for delivery to LLNL.

BGRI will begin growing Back crystal halves at Beijing for delivery to Zhongnan on August 17, 1992. As Zhongnan cuts these crystals, they should be shipped to LLNL, not waiting for five crystals to be cut before shipping (i.e., partial shipment to LLNL is requested to expedite the assembly of complete crystal pairs). In this way, we can be best prepared to present favorable results to the GEM executive committee at the end of August, 1992.

SCOPE OF WORK - LONG TERM PLANS FOR FISCAL YEAR 1993, BEGINNING OCTOBER 1, 1992

Long term collaboration between the Barium Fluoride Collaboration and the Zhongnan Optical Instrument Factory is highly desired. The ability to form a long term collaboration is dependent upon a number of conditions being met. Some conditions, unfortunately, are beyond our control.

The conditions to be met are: 1) Successful demonstration of radiation resistant BaF_2, 2) Successful demonstration of machining and polishing of large BaF_2 crystal pairs, 3) Successful demonstration of reflective optical coating of BaF_2 , 4) Acceptance of the BaF_2 Electromagnetic calorimeter by the GEM Detector Executive Committee, 5) Continued approval for funding of the SSC by the United States government.

Zhongnan Optical Instrument Factory is called upon to perform tasks in support of items 2) and 3). LLNL, BGRI and SIC are working to satisfy the requirement of item 1). Items 4) and 5) are somewhat beyond our control.

Because of time constraints, we are reducing our short term goal to produce 5 crystal pairs. It is anticipated that in FY93, we would continue this work to complete a full complement of 25 crystal pairs as outlined in the Technical Specification XDE-TS-A6292-01 REV A. - Option One - "Finished BaF_2 Crystal Pairs." These 25 crystal pairs would form a prototype calorimeter.

Assuming all items are described previously are satisfied, we can look forward to the continued collaboration between Zhongnan Optical Instrument Factory and the BaF_2 Collaboration. For the FY93 program, we would begin to expand facilities and operations at Zhongnan, BGRI and SIC to handle full-scale production of 15,000 BaF_2 crystal pairs. Expansion would require detailed analysis of production capabilities of Zhongnan and acquisition and installation of new machines to satisfy the required goals of the BaF_2 collaboration. This goal will likely be the production of 15 crystal pairs per day for a period of three (3) years.

Engineers from Western Institutions would work closely with counterparts in China to implement this production line. In addition, engineers from Zhongnan Optical Instrument Factory would be called upon to help design and produce a crystal coating facility based on the existing four meter coater installed at BGRI.

Collaboration would include cooperation between all BaF_2 collaborators: Zhongnan Optical Instrument Factory, SIC, BGRI, Tsing Hua University, LLNL, Oak Ridge National Laboratory, California Institute of Technology and other BaF_2 participating Institutions. This means a free and open exchange of ideas, information, technology, materials and results among all participants. We can look forward to many publications of our work in scientific, engineering, and technical journals. In addition, the exchange of visitors between all participating members of the BaF_2 collaboration would be expected and encouraged.

Conclusions

The Barium Fluoride collaboration fully intends to continue its work into the future, contingent upon continued support from sponsoring agencies of the United States and Chinese governments. This sponsorship is provided by the U.S. Department of Energy and the Chinese Academy of Sciences (Academia Sinica).

For the short term, our goal is to satisfy the immediate requirements of radiation resistance and precision mechanical processing of BaF_2. With the satisfaction of these goals, it is our hope that the Executive Committee of the GEM Detector at SSC will choose BaF_2 for the material to be used in the Electromagnetic Calorimeter.

As the many events unfold over the next few months, the BaF_2 collaboration will endeavor to keep the personnel at the Zhongnan Optical Instrument Factory fully informed. We look forward to a long and rewarding collaboration with Zhongnan Optical Instrument Factory and with all other Institutes in China.

Executed on this day, Tuesday, July 14, 1992 at Shanghai Institute of Ceramics, Jiading, China.

APPENDIX D.
The BaF_2 Expert Panel, and Results on Radiation Damage, Through July 1992.

A summary of the Panel's conclusions following its meetings in December and January, and the R&D progress on the radiation damage problem made over the last six months are presented below.

Conclusion of the BaF_2 Expert Panel: February 1992.

The principal conclusion of the Panel's February 1992 report is "there is no apparent fundamental reason why BaF_2 can not be made radiation hard" [6]. This fundamental conclusion has been reconfirmed in the Panel's last meeting in August [8], (from their draft report, as the final version is not available at the time of this writing) citing that the color centers are the result of 'point defects' that are associated with impurities, including Oxygen and Hydrogen.

- While it is not possible at this time to guarantee that crystals of sufficient radiation hardness to meet the GEM specifications can be produced within the time frame allowed, the recent progress looks very promising.
- A coordinated, comprehensive plan of research should be (drawn up) to efficiently use all the talent that is available for solving the radiation damage problem... The Panel strongly encourages R&D work to develop the necessary technology to reach this goal.

The BaF_2 Panel's conclusion is based upon the existing data obtained by that time. Some highlights are summarized below:

- The BaF_2 radiation damage caused by photons shows clear saturation. Both transmittance and light output measured after irradiation do not degrade further after initial dosage of a few tens kRad to 100 kRad, depending on the quality of the BaF_2 crystals; (Figures 12 and 14 of [4])
- There is no permanent damage caused by either photons or neutrons. All damage recovers in full after an annealing at 500°C for three hours; (Figures 12 and 17 of

[4])[20].

- There is no spontaneous annealing of the radiation damage of BaF_2 under room temperature measured up to 68 days after irradiation; (Figures 15 and 16 of [4])
- The radiation damage of BaF_2 has no dose rate dependence; (Figure 17 of [4])
- There is evidence that the damage of BaF_2 is caused by formation of color centers, which cause self-absorption of the scintillation light as it is transmitted through the crystal. There is no apparent damage to the scintillation mechanism itself, so that the intrinsic scintillation light yield by the crystal is unaffected (Section 5.4 of [4]).
- Large size (20-25 cm long) BaF_2 crystals produced by SIC in December 1991 have considerably better radiation resistance than the crystals from previous batches. The transmittance of a 20 cm long crystal is ~50% at 220 nm after 1 MRad irradiation which corresponds to a light attenuation length of 35—40 cm. (Figures 18 and 19 of [4]).

In addition to the continuation of the ongoing R&D on radiation hard crystals in China, following up on the improved production methods and understanding of the radiation damage mechanism which has been achieved by the Chinese scientists over the last year, we implemented – as rapidly as possible – the research program recommended by the BaF_2 Expert Panel.

Summary of Progress on Radiation Damage: March - July, 1992

Since January 1992 a great deal has been learned about BaF_2 radiation damage properties, the underlying mechanism leading to light absorption in the UV, and the influence of impurities and microstructural defects on the radiation damage. Some of the main results are summarized below.

- Trace element and microstructural analysis at Charles Evans and Associates shows clearly the difference between crystals produced in December 1991 and that from previous batches [37]. It was discovered that

[20]This fact has been extended by the recent work of Woody *et al.*[10] to include radiation damage from charged hadrons: damage from all types of particles can be completely removed by heating in an inert atmosphere.

- The newer crystals from China have Sr and rare earth concentrations which are much lower, by one to two orders of magnitude, compared to older crystals produced in China; None of the rare earths have been detected in the newer Chinese crystals down to typical limits of 0.01 ppm (depending on the element).
- Impurities are concentrated in microscopic inclusions.
- New crystals show different microstructural properties:
  * Large regions with no inclusions;
  * Fewer total inclusions;
  * Inclusions are clustered together into macroscopic groups, and lie along crystal planes.

- Oxygen, fast cooling and their correlation with damage at SIC and BGRI:
  - Crystals produced under poor vacuum have poor radiation resistance [45];
  - Improper annealing (fast cool down) leads to decreased radiation hardness [46];
  - Crystals with more O_2 show larger structural changes under the microscope [46].

- Studies of the radiation damage mechanism, especially the key roles of O and H, have been carried out by Tongji University in China and the West Va. University in US:
  - OH^- doped crystals, produced by annealing the crystal in humid air at high temperature, show absorption bands both in the UV and in the infrared, at wavelengths which precisely match those computed for interstitial H and substitutional O^- [47];
  - electron paramagnetic resonance (EPR) spectra obtained with OH^- doped crystals show clearly identified O^- and Hydrogen atom signals, which are correlated with the UV absorption bands. Paramagnetic signals seen in small OH^- doped samples are similar to larger undoped crystal samples [48]. These measurements support the key role of oxygen and hydrogen, in combination with preexisting color centers due to other trace impurities (such as rare earths) in the crystals. Another (possibly interrelated) aspect involves Manganese changing its valence state.

It is important to note that the levels of Mn trace impurities (in the range of 0.1 ppm) estimated by the West Virginia Univ. group match the GDMS results obtained by CE&A very well. The UWV group has also noted a possible Cr^{3+} line. It is also interesting to correlate this with the July 22 report from SIC, which shows that the best crystals they have grown use raw materials that have the lowest Cr content: below their detection limit, and below the GDMS limits at CE&A (0.02 - 0.1 ppm).

- A 25 cm crystal kept in the dark at room temperature at Caltech has shown no spontaneous annealing after irradiation with 1 MRad, up to 210 days after irradiation. Data from BNL may show some very slow recovery, from 51% to 56% transmission (220 nm) in a 20 cm crystal, over a period of 7 months. No further recovery was observed in this crystal between 7 and 9 months. (See the reports by R. Zhu (Caltech) and C. Woody (BNL).

- A 25 cm long BaF_2 crystals produced by SIC shows that the light output is reduced to around 40% (due to self-absorption of the scintillation light) after Co^{60} doses up to 1 MRad. The crystal was produced recently at SIC with improved processing techniques, aimed at reduction of oxygen and water. Saturation of the radiation is observed at a dose of around 20 - 50 kRad with photons.

- A small BaF_2 crystal (1" diameter $\times$ 1" long) from SIC was irradiatied by neutrons obtained by proton-induced stripping from a Be target at the University of Lowell Van de Graaff facility. The fluence at typical points in the crystal varied from 5 to 8 $\times 10^{13}$ n/cm^2. The neutron energy spectrum was roughly flat from 0 to 2.2 MeV, with little background of thermal neutrons (0.1% of the flux) and a low associated dose of photons (estimated between 1 and 2 kRad). The absorbence of this crystal as a function of wavelength was measured at BNL by Woody *et al.*. The result, showed that the high fluence of MeV neutrons had little effect. In order to separate out the effects of the associated photon dose, the crystal was annealed at 500°C after neutron dose, and was then reirradiated with 1 kRad of Co^{60} γ's. The absorbence from the run at the Van de Graaff could be explained (within dosimetry errors) by the photon dose alone. It is also noteworthy that the radiation damage is fully annealable.

- First results on the effects of hadrons have been obtained by Woody *et al.*during the last month. Large crystals from Optovac (25 cm), an older 25 cm crystal from SIC (Part of the 1991 Fermilab test matrix) and a 20 cm SIC crystal produced at the end of 1991 were irradiated by placing the crystals near a primary target

at the AGS. After a 2 MegaRad dose of hadrons, followed by a 1 MegaRad dose of photons, the crystal was found to be completely annealable: the damage was removed by heating in an inert atmosphere.

Another important result of this measurement is that the activation of BaF_2 by hadron irradiation is low. Following an irradiation dose of approximately 50 kRads, the induced radioactivity was measured to be 0.8 milliRem/hr on contact.

APPENDIX E.
GEM Barium Fluoride Crystal Calorimeter System: AccSys Technology Proposal, July 27, 1992.

ACCSYS TECHNOLOGY, INC

1177 Quarry Lane
Pleasanton, CA 94566
(415) 462-6949
FAX: (415) 462-6993

GEM Barium Fluoride Crystal Calorimeter Calibration System

The barium fluoride (BaF_2) crystal calorimeter proposal for the GEM detector at the SSC Laboratory will be calibrated on-line using an RFQ linac to bombard a target with an intense pulsed proton beam to produce burst of photons. The present proposal for this RFQ calibration system can be satisfied by the AccSys Model PL-4 linac system operating with an H^- output beam that is stripped to H^0 in a gas neutralizer for transport into the center region of the detector through the magnetic field.

A drawing of the prototype Model PL-4 RFQ linac is shown in Fig. 1. This system, now being tested, is being developed for the U.S. Navy as a neutron generator. It is capable of a peak output current of more than 40 mA. The Navy unit uses an H^+ ion injector, but could be just as easily used with the H^- ion injector shown in Fig. 2. This rf driven H^- ion source is an upgraded version of the one in use at CERN for calibration of the BGO crystal calorimeter of the L3 experiment. A contract has been signed by AccSys with DESY to fabricate this H^- injector for use on the Linac III system at HERA.

As seen in Fig. 2, the ion source and acceleration gaps are mounted inside the grounded vacuum chamber for safety and to allow the hydrogen gas load from the ion source to be easily pumped away. The power from the ion source equipment cabinet to the injector is fed through an insulated tube, allowing the equipment cabinet to be located remotely for easy service and maintenance during operation of the accelerator within an experimental area.

The 35 keV H^- beam extracted from the ion source is transported and focused into the RFQ linac through a low energy beam transport (LEBT) system that uses two solenoid magnet lenses. The calculated beam optics design for the LEBT shows that the beam from the injector can be focussed properly into the RFQ using modest field magnets.

The H^- ion beam from the injector will be accelerated to a final energy of 3.85 MeV using a 3 m long RFQ operating at 425 MHz. This RFQ accelerator, used for the Model PL-4, was originally developed to generate neutrons for non-destructive testing, and was designed to be rugged and reliable. The detailed specification of this system are listed below:

Operation frequency	425 MHz
Accelerated particle species	H^-
Input ion energy	35 keV
Nominal output energy	3.85 MeV
Bunch synchronous phase	-35°
Final synchronous phase	-30°
Peak surface field (E_k)	37.7 kV/m (1.92 E_k)
Design input current	45 mA
Nominal current limit	100 mA
Output beam current (peak)	30 to 40 mA
Normalized input emittance (95 %)	<0.04π cm mrad
Nominal phase-space acceptance	0.115π cm mrad
Normalized output emittance (90 %)	<0.06π cm mrad
Residual vacuum	$<1\times10^{-6}$ Torr
RFQ length	299.5 cm
Peak structure power (theoretical x 1.4)	392 kW
Peak beam power	179 kW minimum
Total peak power	571 kW minimum
Beam pulse length	1 - 2 μsec
Beam repetition rate	150 Hz
Output energy spread (90%)	<±20 keV
Output phase spread (90%)	<±15°

The 3.85 MeV output beam from the RFQ can be focused by three electromagnetic quadrupole magnets and two 45° achromatic bending magnets to form a waist at the gas neutralizer on the outside of the GEM detector. As shown by the beam dynamics calculation in Fig. 3, the neutral H^0 beam exiting the stripper cell would travel the 12 meter flight path through the solenoid and only be about 5 cm in diameter. The actual implementation of this system on the GEM experiment is shown in Fig. 4.

MODEL PL-4 RFQ LINAC

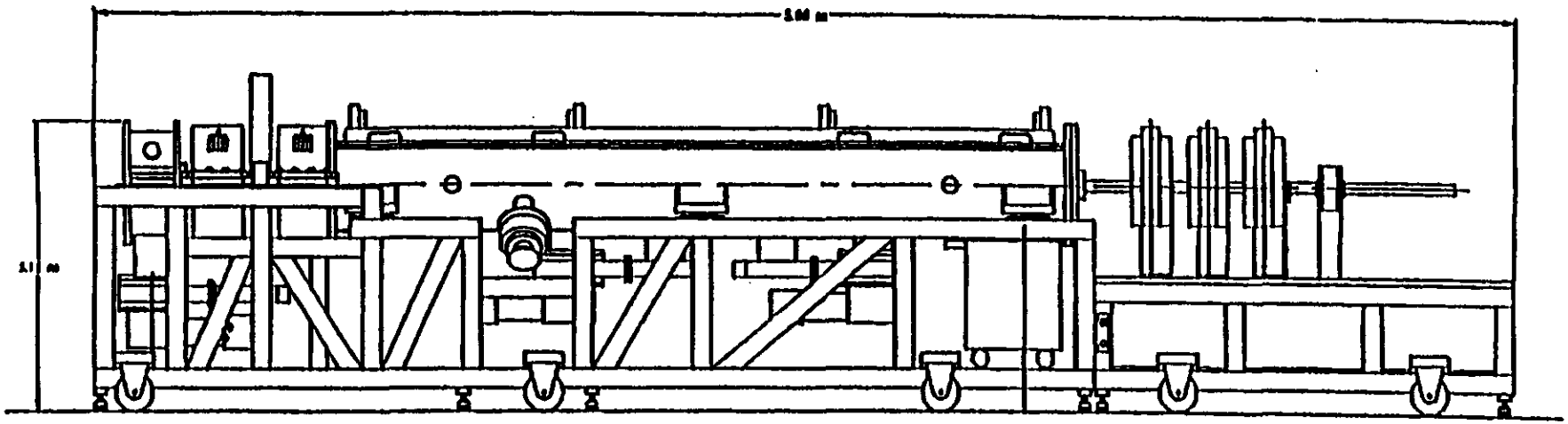

Fig. 1 - Drawing of prototype Model PL-4 linac

ACCSYS TECHNOLOGY INC

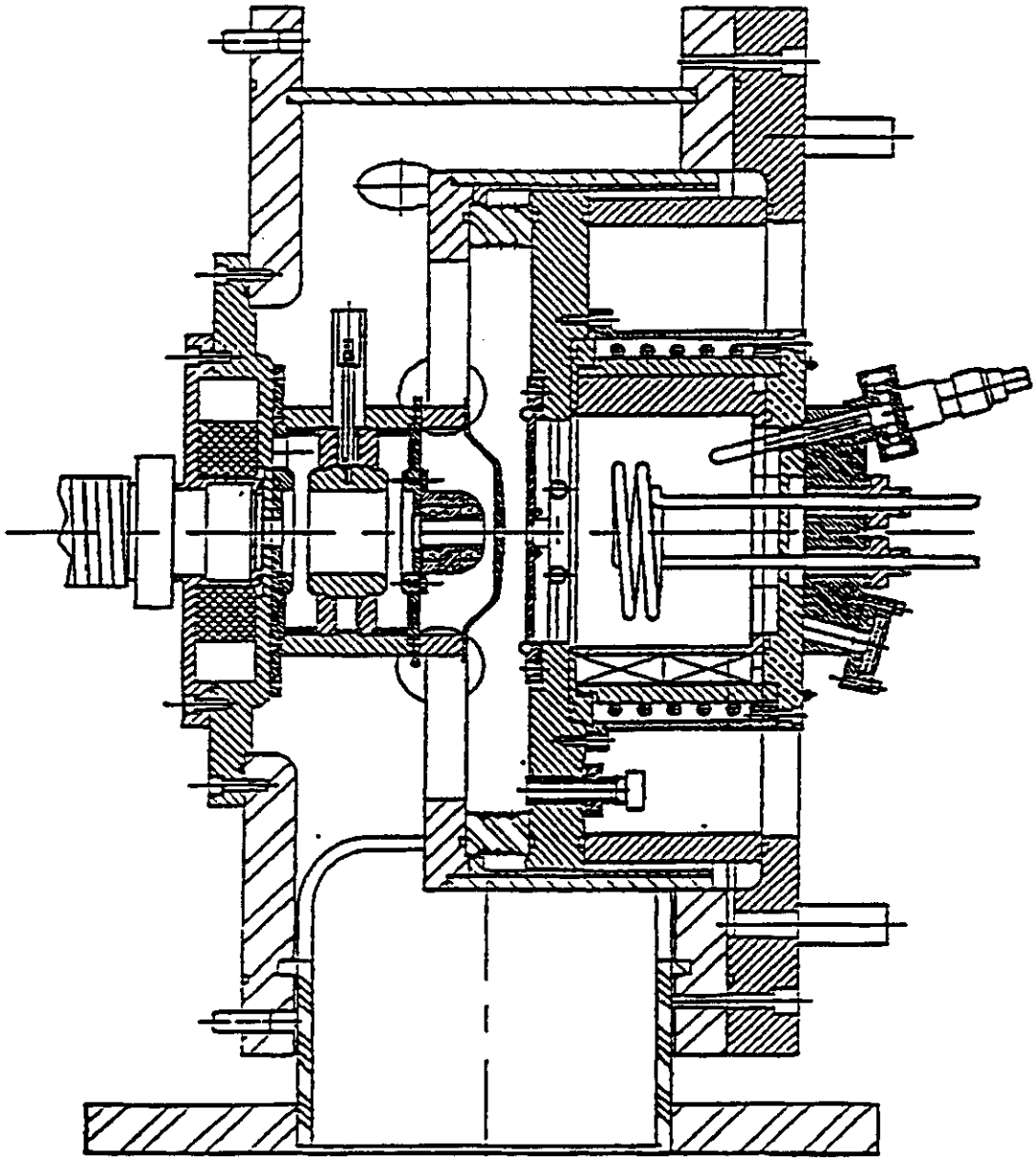

Fig. 2 - RF driven
H^- injector for

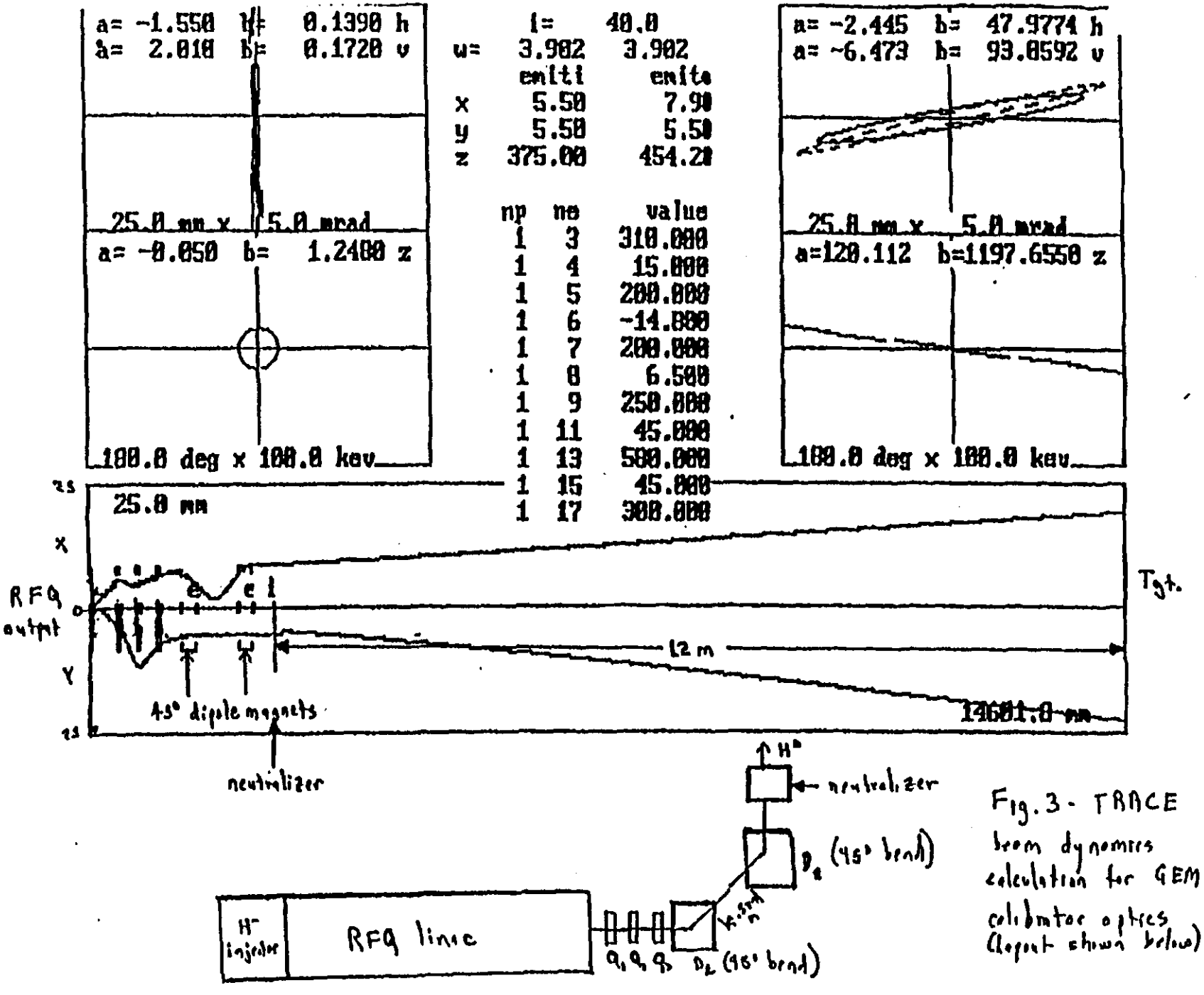

Fig. 3 - TRACE beam dynamics calculation for GEM calibrator optics (layout shown below)

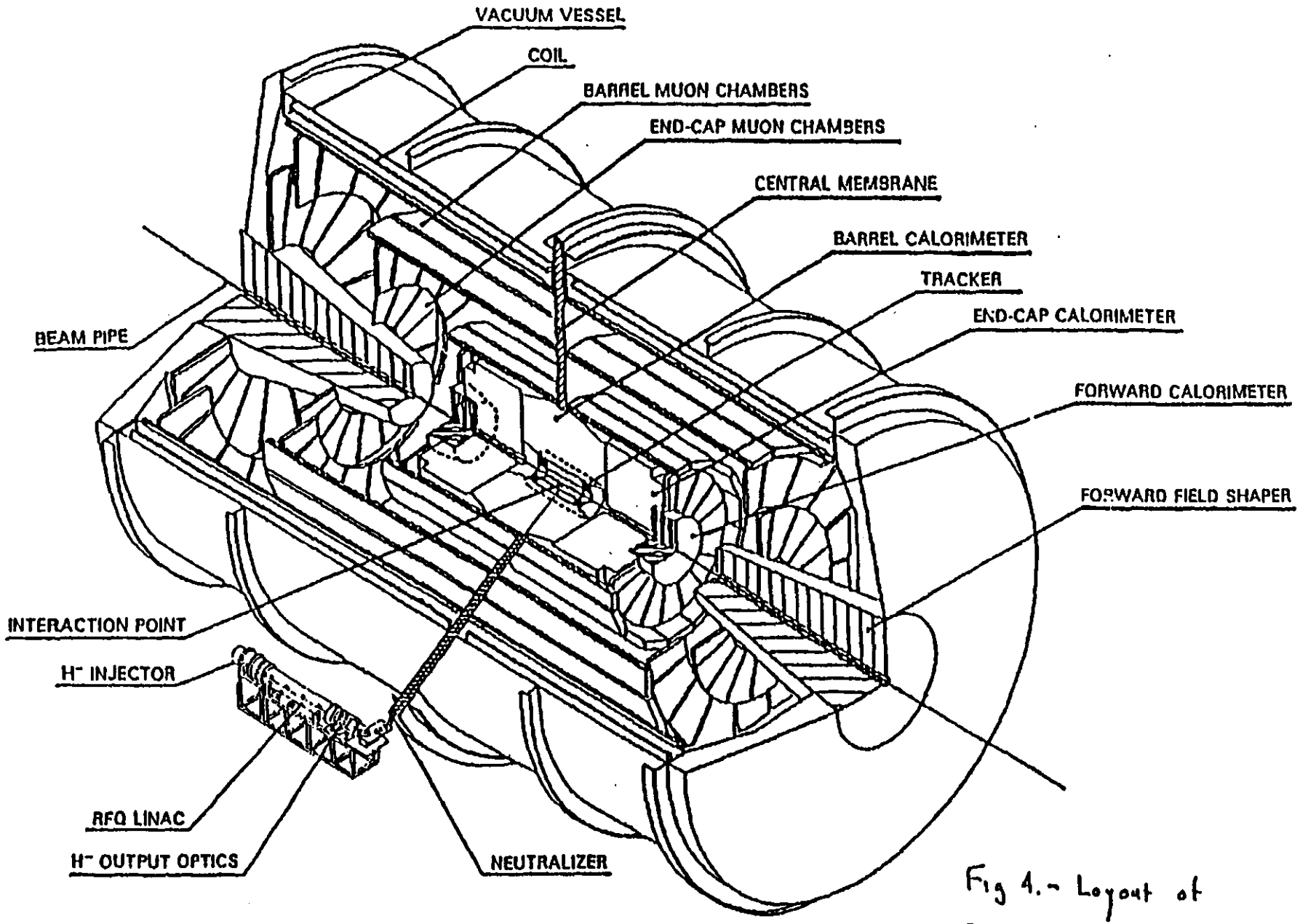

Fig 4.- Layout of GEM experiment with Model PL-4 RFQ Calibrator.

APPENDIX F.
Results From the 1991 BaF_2 Test Beam.

ABSTRACT

We report on the analysis of the 1991 BaF_2 test beam run carried out by GEM physicists at FNAL. Despite inadequacies in this early setup, we have been able to verify the intrinsicly small energy independent term in the BaF_2 energy resolution. The BaF_2 energy is calculated from a simple sum of energies in each crystal. Only small corrections (2%) based on the ratios of energies in the central crystal, the central 9 crystals, and the central 25 crystals are made. The energy resolution is independent of position for beam particles incident upon the central crystal of the matrix.

Experimental Setup

The 1991 BaF_2 test beam run was performed in the neutrino east beam line at FNAL with at 7×7 array of tapered crystal pairs from the first BaF_2 procurement from SIC. Each pair consisted of two 25 cm long crystals bonded together with UV transmitting glue. The transverse dimensions of the crystals, 2×2 cm^2 at the front and 4×4 cm^2 at the back, were smaller than those proposed for GEM. Light from the crystals was detected with photomultiplier tubes connected at the back with UV transmitting silicone grease.

The crystal pairs were stacked in an aluminum box. There was no support structure for the individual crystals. The mechanical tolerances of the crystals were not nearly as good as those specified for GEM. This caused some gaps in the array and required several iterations of loading and unloading the matrix before all the channels were functioning properly. By the time we took data, the grease had seeped under the crystal wrapping causing rather large visible black regions. Due to our attempts to keep the mess to a minimum, some of the grease joints covered only part of the photocathode. In addition, the crystals had very large (1.5 mm) bevels on all the edges including the ones at the glue joint. The combination of these effects led to rather serious nonuniformities in the light output as a function of position along the crystal. The nonuniformities measured with a muon beam going transversely through the crystal were large enough to cause a 0.5% to 0.6% contribution to the constant term in the resolution function.

The phototube output was sent over a long cable to a 12 bit LeCroy fastbus ADC. The gains were set so that the least count in the ADC was about 30 MeV, allowing us to run at beam energies above 100 GeV. It was found late in the data taking that the two lowest order bits of the ADC were not working. After fixing this problem we took data only at 68 GeV. We have not attempted to analyze the data with the bad ADC. There was no calibration system available during the test run. We used a muon trigger to set the voltages to the 10% level. The electron data were used for the calibration.

The beam momentum was measured with a spectrometer composed of bending magnets and drift chambers. Previous experiments had obtained a momentum resolution of 1% in this beam. We improved the beam spectrometer readout to get better momentum resolution. The beam chambers and counters in the beam line were rather thick which is not ideal for an electron beam. It is clear that the beam electrons radiate a good deal in the upstream part of the beam since we had to set the downstream momentum substantially lower than the upstream momentum to get the maximum rate. Based on our measurements we estimate that we were able to improve the beam momentum resolution to 0.5 ± 0.2 %.

Data were taken primarily at 68 GeV, where we had a reasonable rate and the contribution of the stochastic term to the resolution is relatively small. The beam had a spot size of approximately 4×4 cm^2, a momentum spread of around 3 GeV, and an angular spread of 1.7 mrad. Electrons were tagged with a transition radiation detector and pions vetoed in a backing calorimeter.

Event Selection

We attempt to select events which have a well measured beam electron, without biasing our energy resolution measurement. Selection based entirely on beam chamber information is unbiased as long as we get a fairly uniform coverage of the center crystal after cuts. Some selection based on the matching of the position measured in the BaF_2 matrix and that projected from the beam chambers is also used to remove events badly measured in the beam spectrometer.

In the bending plane (x), a beam particle is measured by up to 7 wires upstream of the dipole magnets and by up to 8 wires downstream. In the nonbending direction (y), up to 8 wires are used. Three straight line segments are fit and points are dropped from the fit until $P(\chi^2)$ is greater than 0.04. Single wire resolutions range from 340 to 400 microns. The probability distributions are flat with slight enhancements at high and low probabilities. We require at least 5 hits on the upstream x-segment and on the downstream x-segment. No y-segment is required to maintain reasonable efficiency. We do however use y-segments, which are found, to tune the position resolution in the BaF_2. Cuts are placed on the measured upstream and downstream slopes to remove the tails of the beam. A similar tail removing cut is placed on the positions at the center of the dipole magnets extrapolated from the upstream and downstream segments. These cuts each removed a few % of the beam particles. Next, the x-positions extrapolated to the center of the magnet must match within 2.5 mm. The distribution for this cut is shown in Figure 1. The distribution has a long tail showing that a large fraction of the beam particles are not cleanly measured before the cut. A 4×4 cm^2 counter defined the beam in front of the BaF_2 matrix. We next require that the downstream segment pass through that counter in the bending direction. The distributions both in x and in y are shown in Figure 2. One can see that the beam more than covers the counter in x while the distribution in y is peaked in the middle of the counter. Again we notice that there is a clear tail indicating mismeasured events or events that were triggered by a spurious hit in this counter. Finally, we make a rather restrictive cut on the measured bend angle, which is shown in Figure 3. The average bend is 27.94 mrad. We select the region between 28 and 28.6 mrad. This cut is independent of BaF_2 information so it is unbiased. The reason for choosing this restrictive cut is that the agreement between beam momentum and BaF_2 energy is measurably better in this region. We can only surmise that for smaller bends, there is a higher probability of momentum mismeasurement or of accompanying photons hitting the BaF_2 matrix. To remove pions from the data sample, we have used the energy measurement in a hadron calorimeter behind the matrix. Figure 4 shows the distribution before and after cuts.

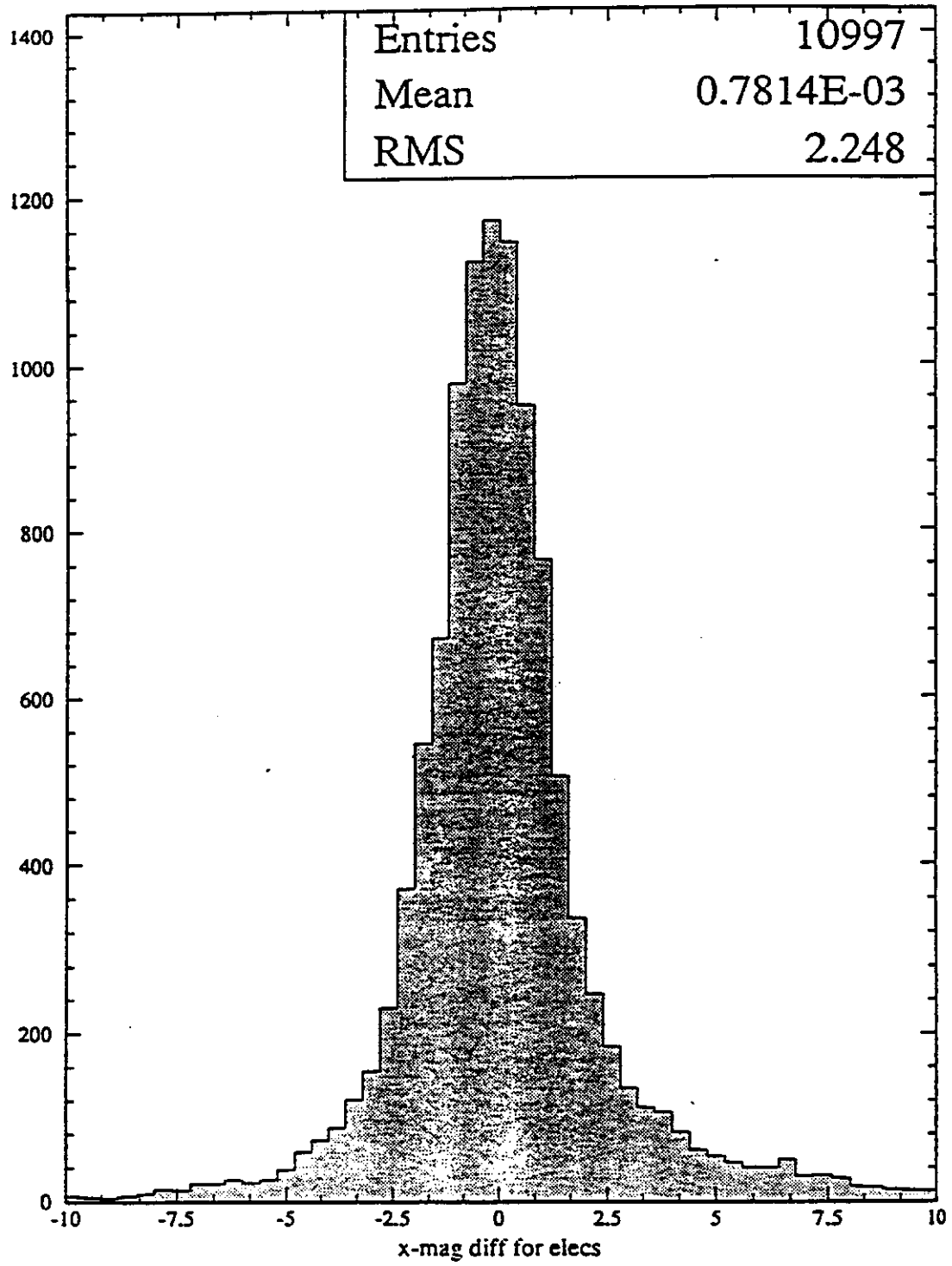

Figure 1: The distribution in the difference between the x-positions at the center of the bending magnet extrapolated from the upstream and downstream segments. This distribution, for electron triggers. shows a rather large fraction of mismeasured events. The corresponding plot for pion triggers is much cleaner.

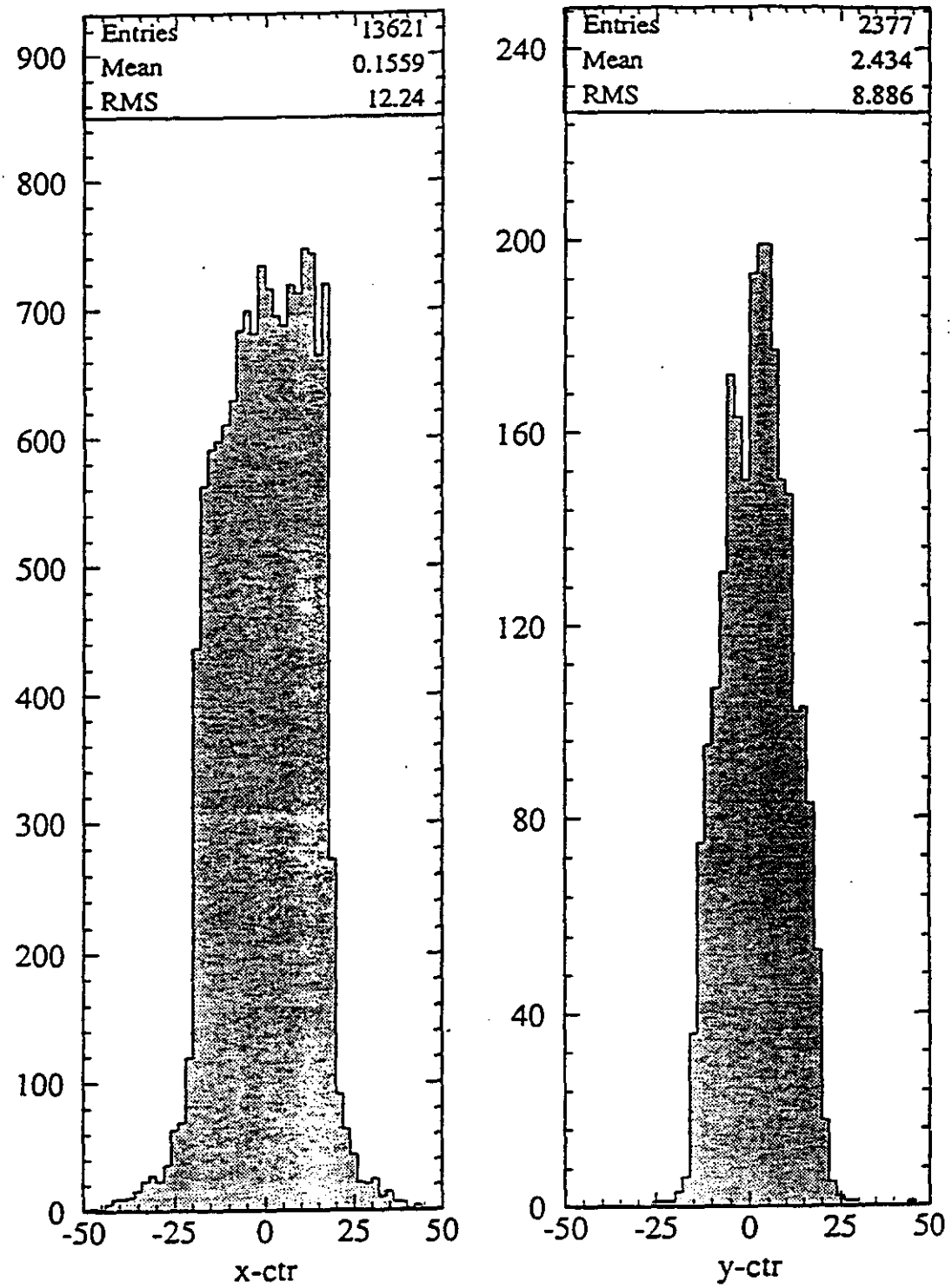

Figure 2: The x and y distributions of the position of the beam track in a 4 × 4 cm^2 trigger counter in front of the BaF_2 matrix. A cut was placed at ±20 mm on the x-position.

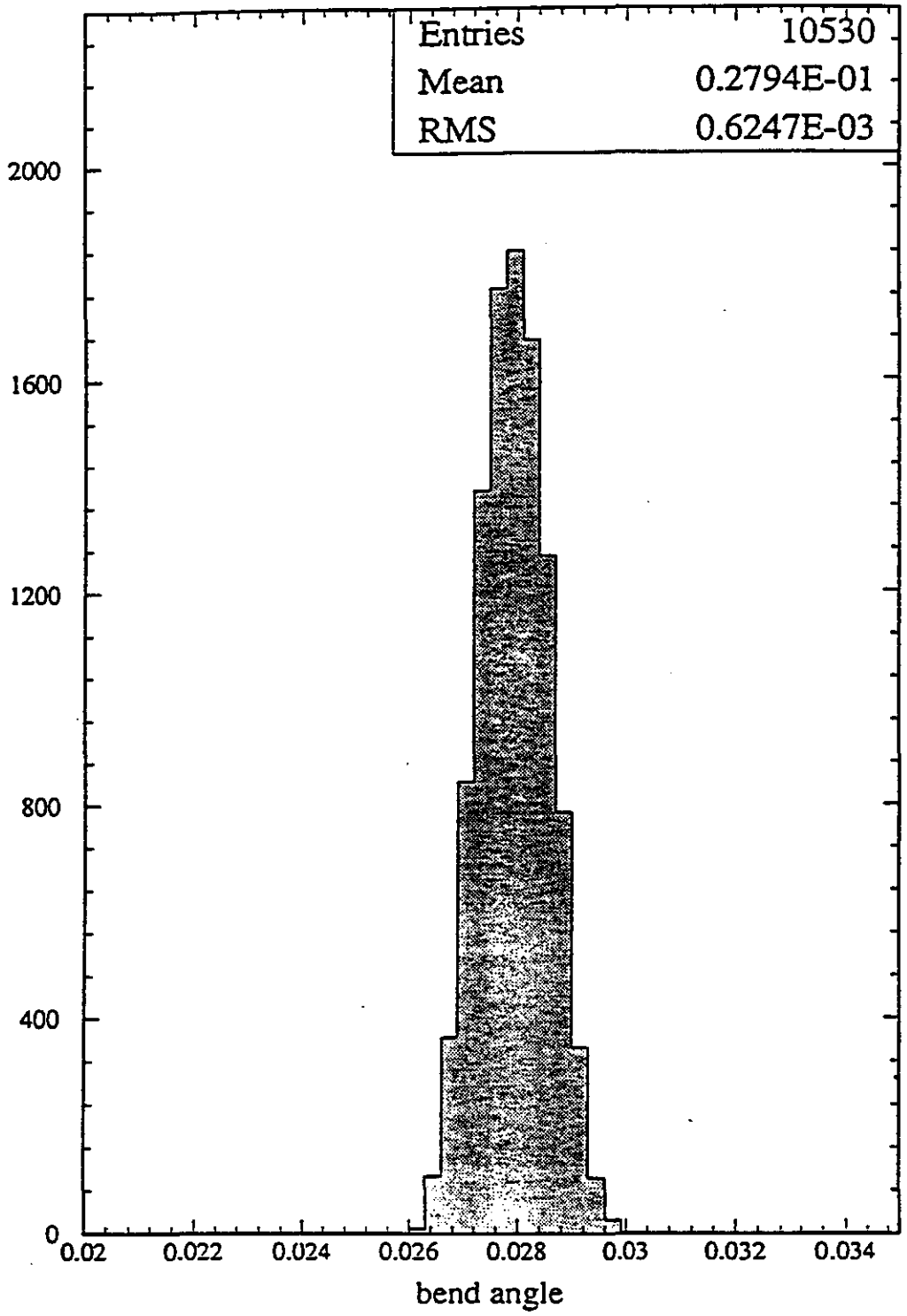

Figure 3: The distribution in the measured bending angle.

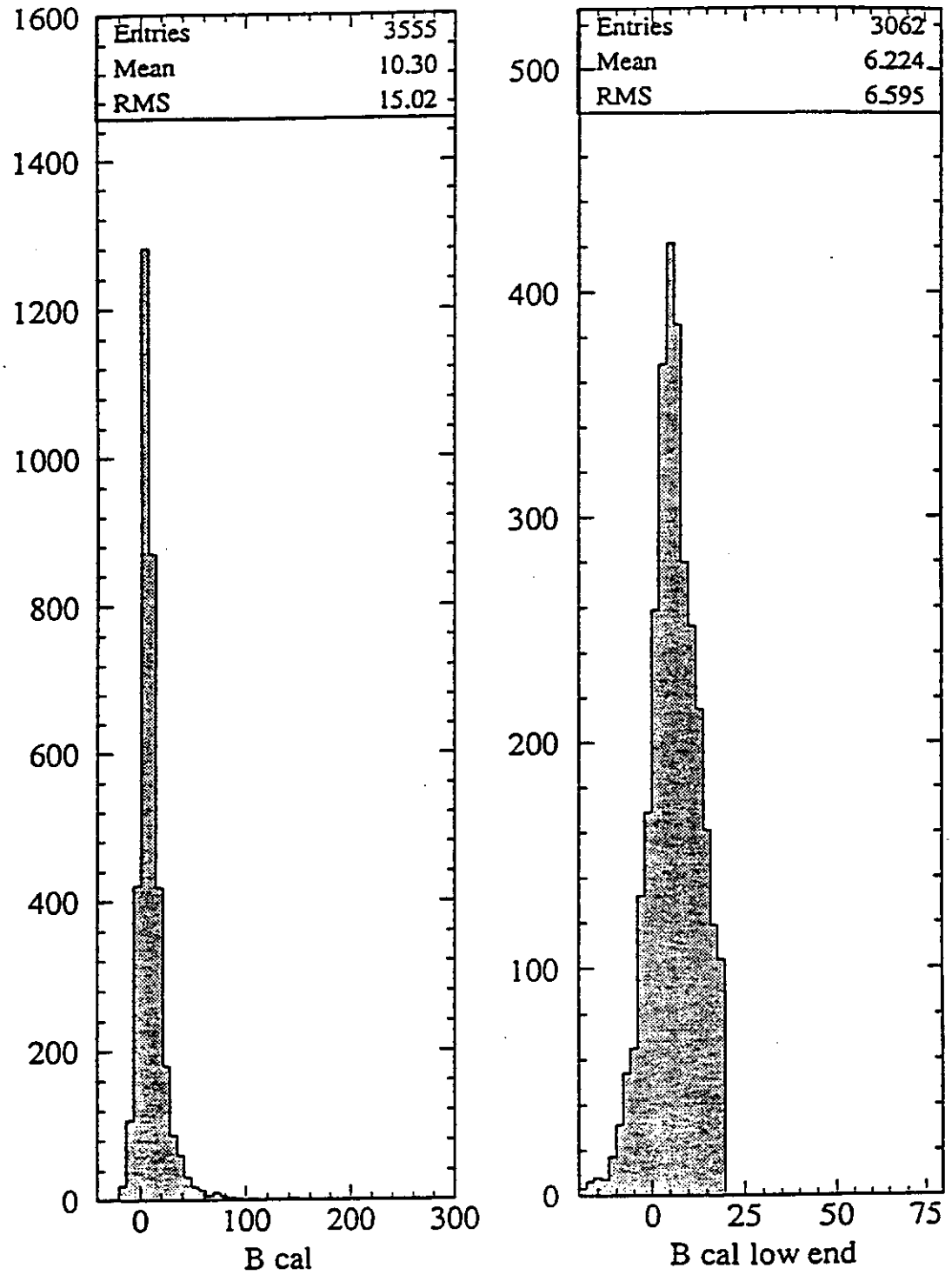

Figure 4: Energy in the backing calorimeter before and after cuts. The units are arbitrary.

After all these cuts, we make a constrained fit to the upstream and downstream points to best determine the momentum. This only slightly improves the agreement between momentum and energy. We cut on the momentum error coming from this constrained fit at 0.17 GeV removing the more poorly measured tracks.

Figure 5 shows the average difference between the position extrapolated from the beam track and the energy weighted average position at shower maximum in the BaF_2 matrix. One sees the usual distribution in which the BaF_2 position is correctly measured by the average at the center of crystals and at the boundaries between crystals but shifts systematically elsewhere. Figure 6 shows the same difference after correction. The size of the error bars gives the position resolution, typically 1 mm, in each bin. The extrapolated beam position resolution makes a significant contribution to this 1 mm. Figure 7 shows the scatter plot of the position in the BaF_2 matrix versus that from the beam chambers. Even after all of the clean beam cuts, there are significant tails in which the two positions disagree by several mm. Since the energy weighted position is quite reliable if there is a single electron in the BaF_2 matrix, this indicates that there is still a portion of the selected beam which is not clean. We cut on the difference to remove some of the remaining problems with the beam. The cut distribution is shown in Figure 8. Again we only cut on the difference in x, at ± 1.9 mm, since no y track is required. The tails in the bending plane are substantially worse than in the nonbending plane. We also require that the BaF_2 matrix has only one local maximum in energy above 300 MeV to remove some events with more than one particle incident. This removes only a few % of events. It is clear that, even after all cuts, some problems with the beam remain and will affect our measurement.

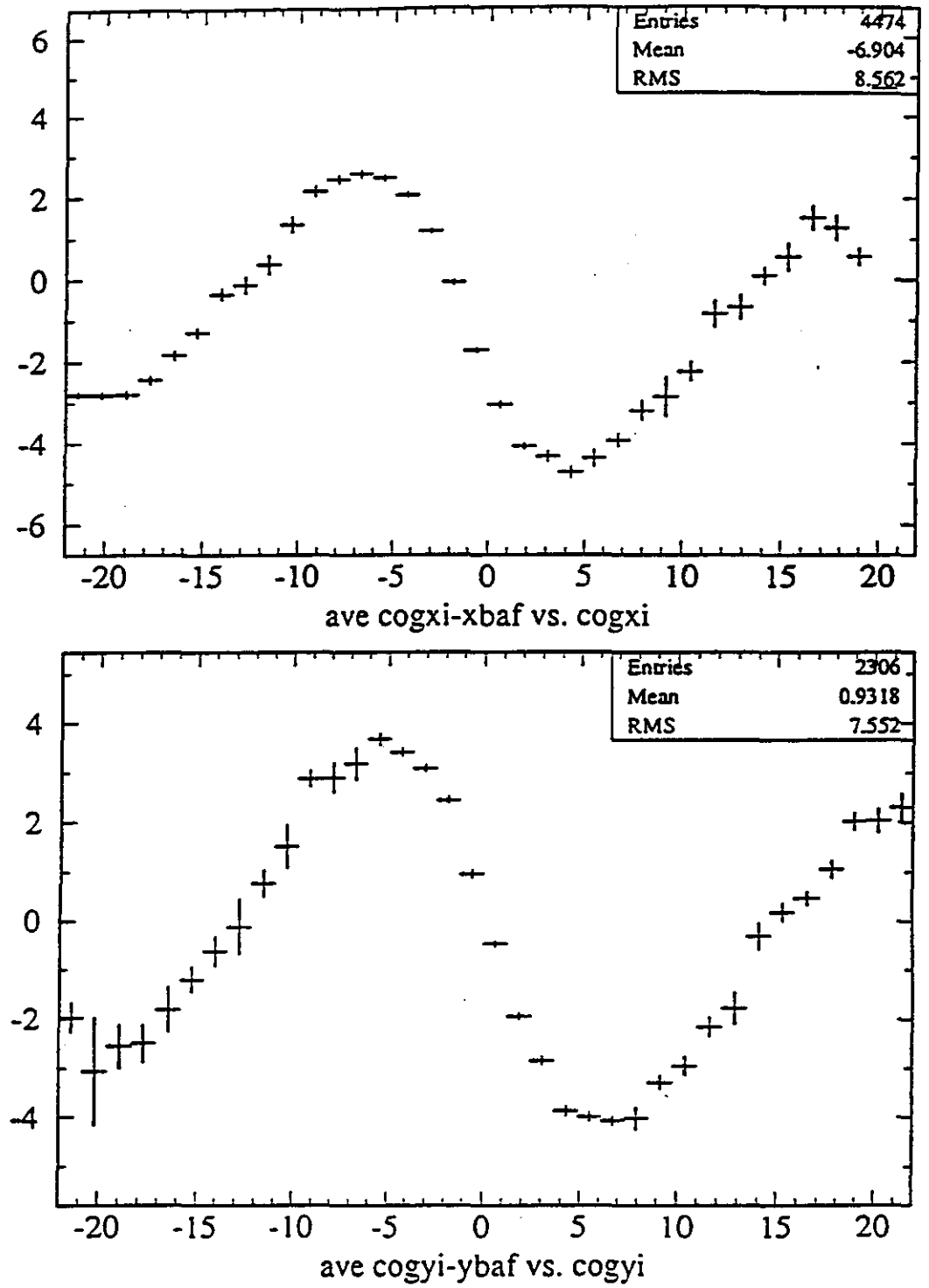

Figure 5: Average difference between BaF_2 position and extrapolated beam track position before polynomial correction.

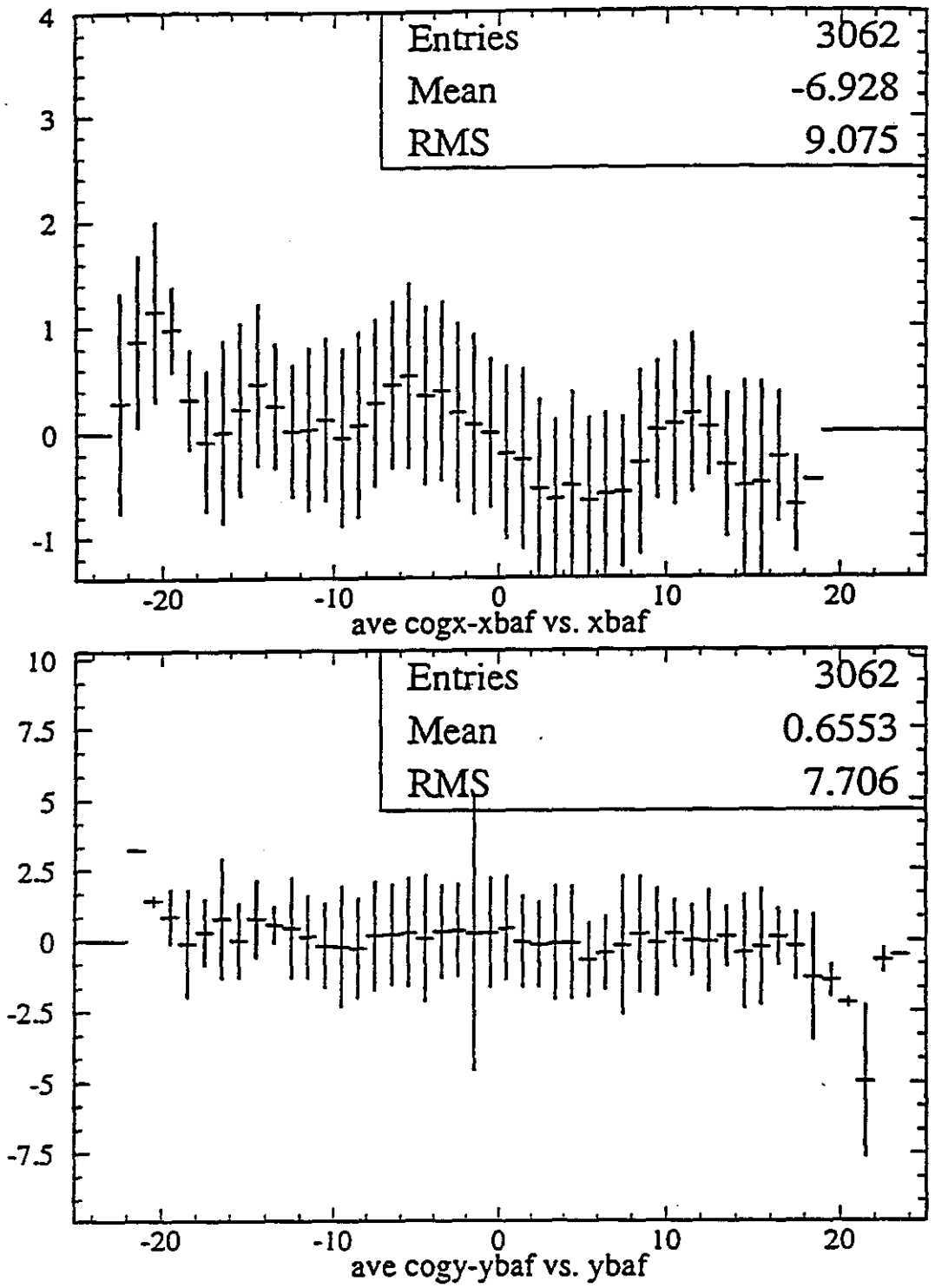

Figure 6: Average difference between BaF_2 position and extrapolated beam track position after polynomial correction. The size of the error bars corresponds to the position resolution in each bin. The extrapolated beam position error makes a significant contribution to this resolution.

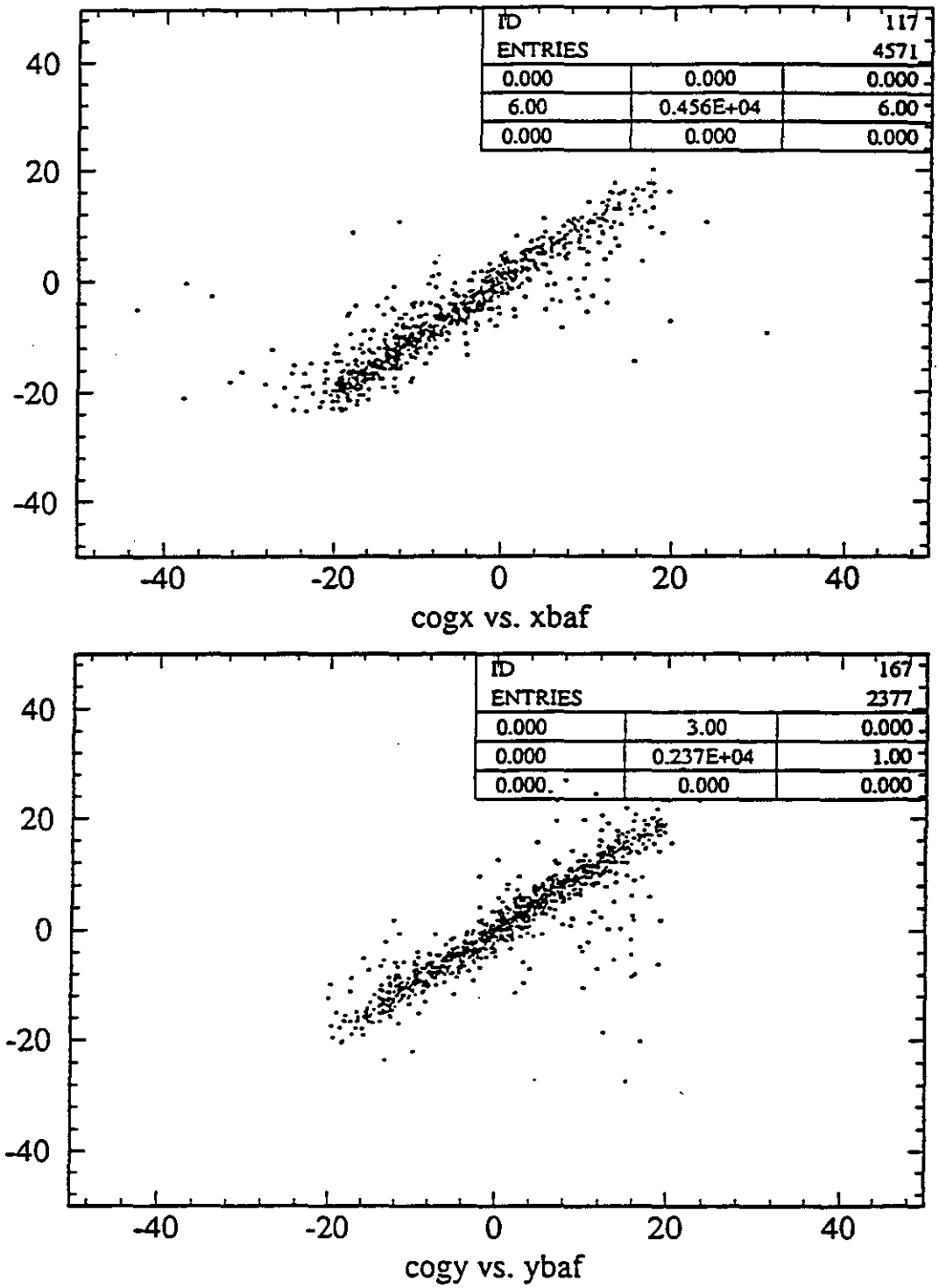

Figure 7: Scatter plot of the position measured by the BaF_2 matrix and the position extrapolated from the beam chambers to shower maximum.

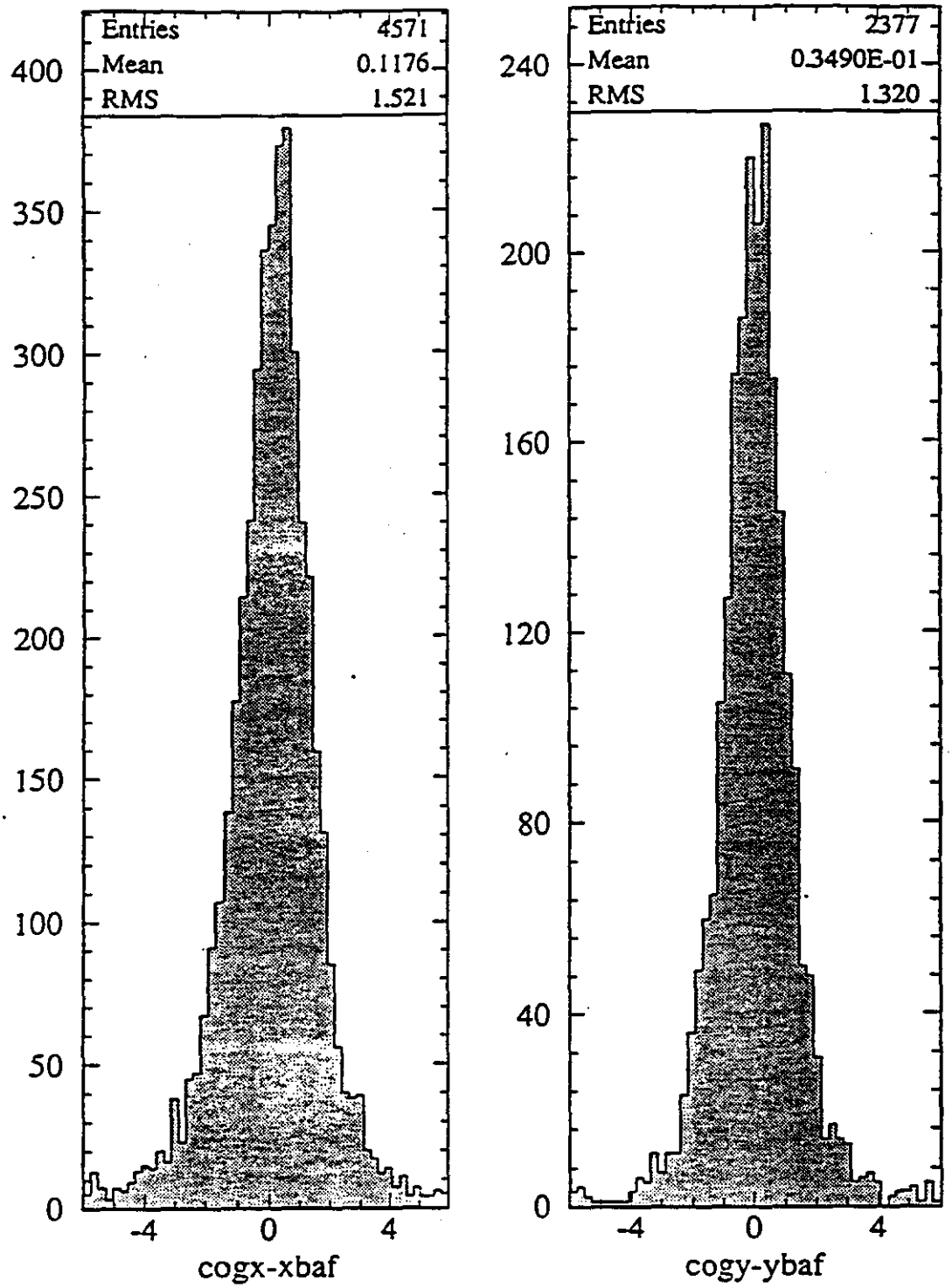

Figure 8: Difference between the BaF_2 measured position and the beam chamber measured position. A cut on the tails helps remove dirty beam background. One can see that there is more spreading in the x direction than in y.

BaF_2 Energy Measurement

The energy in the BaF_2 matrix is computed by adding up the pulse heights above pedestal in each crystal multiplied by a gain factor. The pedestals are determined from random triggers taken during the run. The gain factors, one per crystal pair, are determined from the data themselves by optimizing the agreement between beam momentum and measured energy. Figure 9 shows the raw energy sums in the full matrix, the center 5×5 crystals, and in the center 3×3 crystals. From the averages we can see that most of the energy is contained in the central 9 crystals, with about 7% in the next row of crystals. The gains determined for the outer row of crystals are negative and nearly of the same magnitude as the gains in the inner rows. We find that this is due to the effects of electronic noise in the readout, most probably in the ADC. The total energy in the 49 crystals is therefore lower than in the central 25 by about 450 MeV.

Corrections are applied to this summed energy to get our best BaF_2 energy measurement. By far the largest correction is based on the ratio $(S_{1\times1}/S_{3\times3})$ of the energy in the highest energy crystal to that in the 3×3 array centered on that crystal. If a shower is centered on a crystal, we will find a high maximum energy (75%) and also expect the minimum amount of lost energy in the dead material between crystals. If a shower is near the center of an edge of a crystal we will get less energy (45%) and more energy loss in the dead material. If the shower is near the corner, we get the lowest ratio (25%) and the maximum energy loss in dead material. Figure 10 shows this ratio of energies. We make a simple quadratic correction as shown in Figure 11. The correction is as large as 2%. The bottom of the figure shows the average energy error after corrections. The error bars in that plot show the RMS spread of energies bin by bin. We can see that the correction is quite effective and that the resolution after correction does not depend much on position. We point out that this is a simple BaF_2 based correction.

In addition to this, we apply one other rather small correction on the BaF_2 energy. This is based on the ratio $(S_{1\times1}/S_{3\times3})$ of the energy in a 3×3 array of crystals to that in a 5×5 array. The maximum size is 0.3%. We also apply a small correction to the beam momentum which is based on the average disagreement between momentum and BaF_2 energy. We correct according to the average energy error versus the x position at the center of the magnet from the upstream and downstream x-segments. This correction is less than 0.2%.

We have looked for additional dependence of the energy error on many other variables and found nothing significant. These include the x and y positions measured in the BaF_2, the slopes of the track segments, the bending angle, and the event number in the run. In particular we found no measurable time dependence

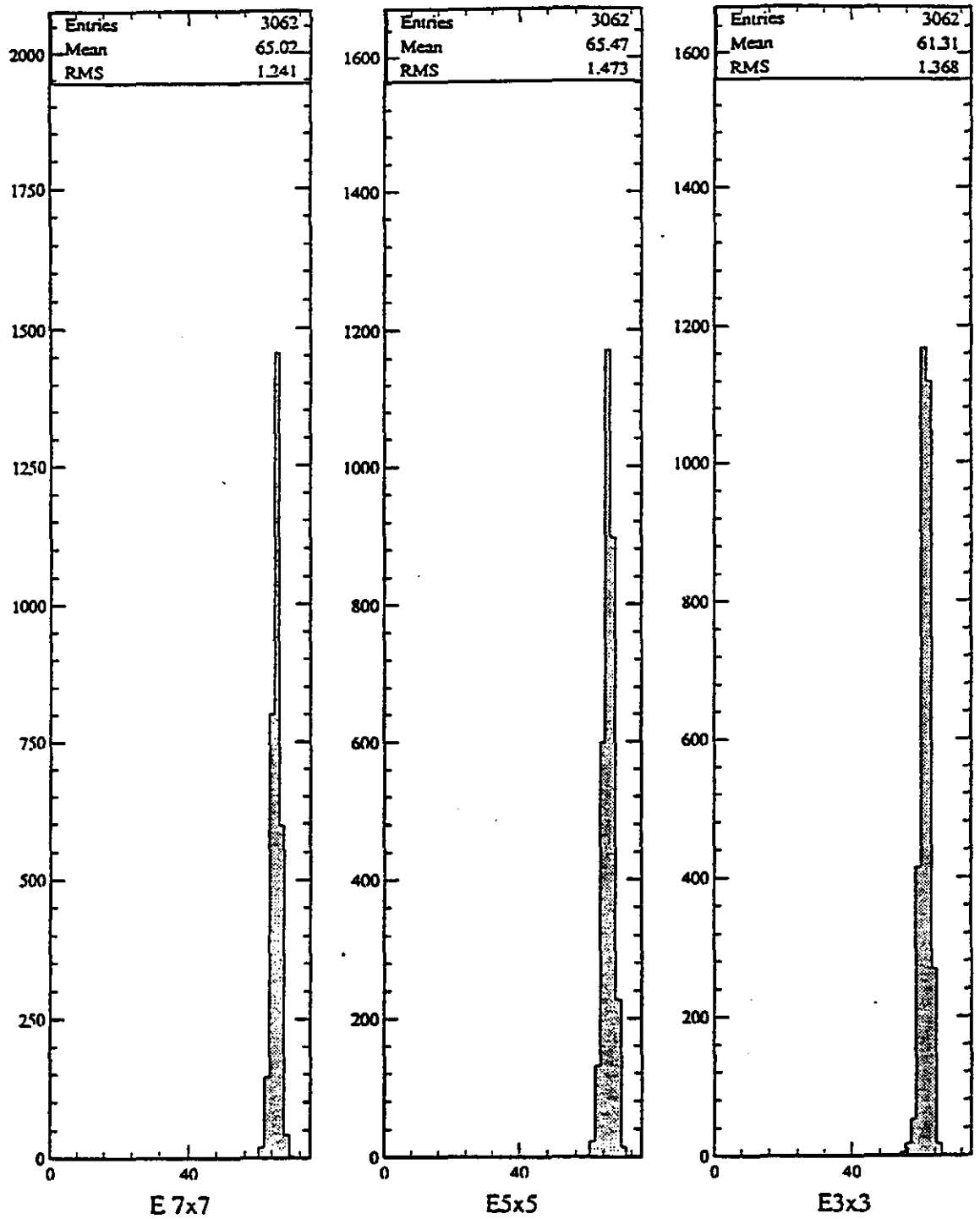

Figure 9: The raw sum of energy in the full 49 crystal array, the central 25 crystals, and in the center 9 crystals.

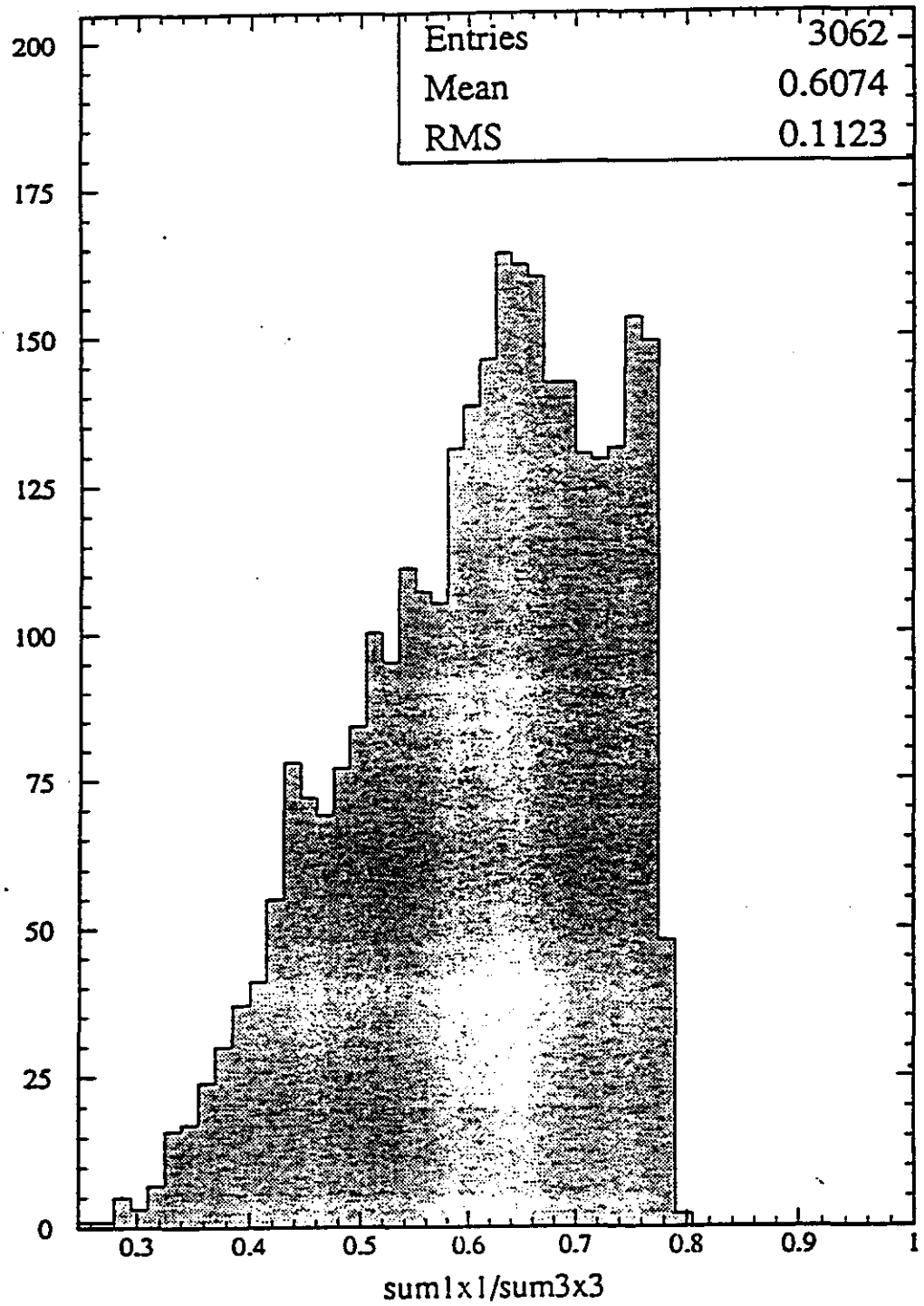

Figure 10: The ratio, $S_{1\times1}/S_{3\times3}$. of energy in the highest energy crystal to the energy in the 9 crystals centered on that crystal.

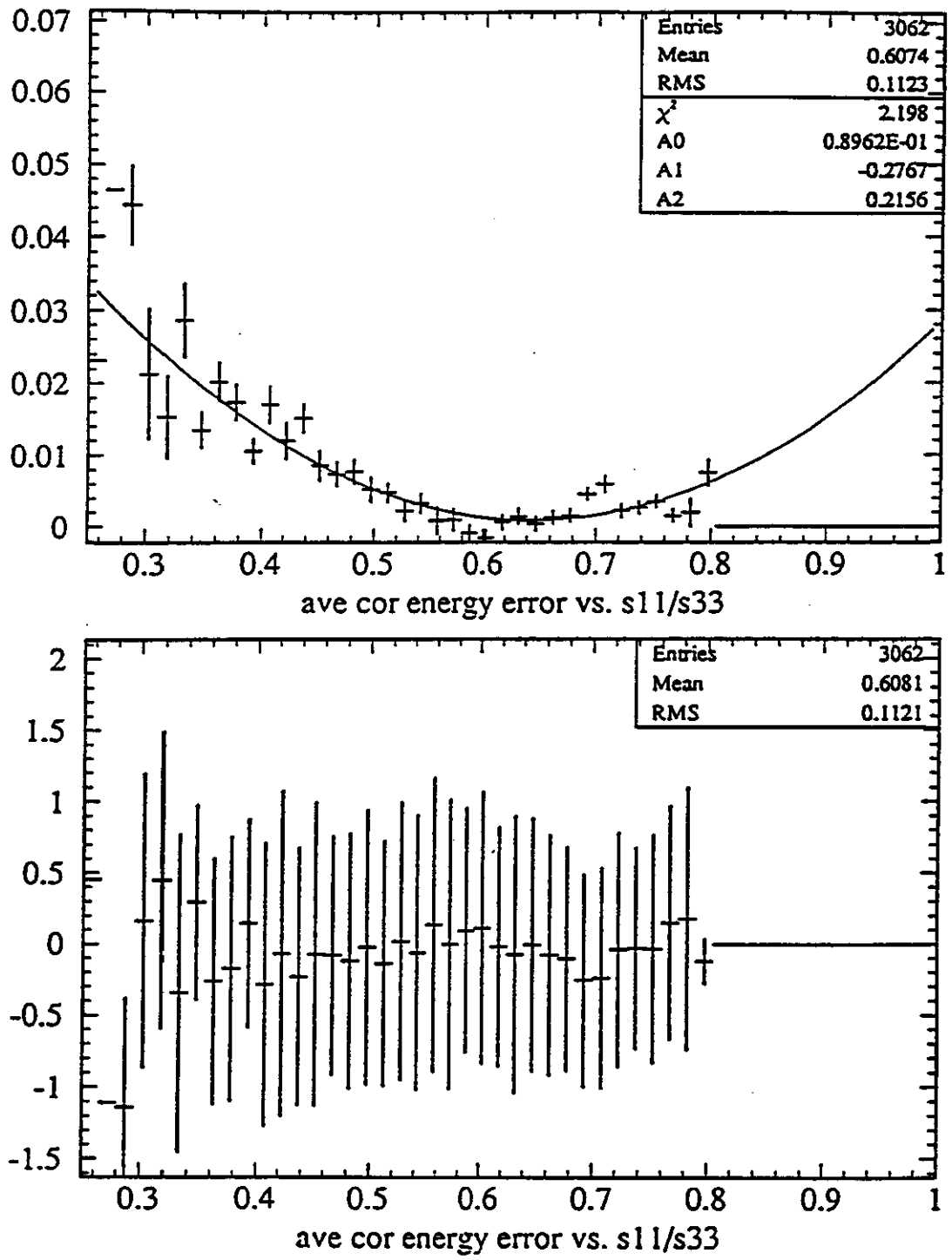

Figure 11: The first graph shows the average fractional energy error versus $S_{1\times1}/S_{3\times3}$. The simple quadratic fit shown is used as a correction. The second graph shows the energy error after correction. The error bars in the second graph give the RMS spread of energy in each bin. The energy spread is seen to be nearly independent of position. The correction is very good except in the lowest three bins where there is very little data (see previous figure).

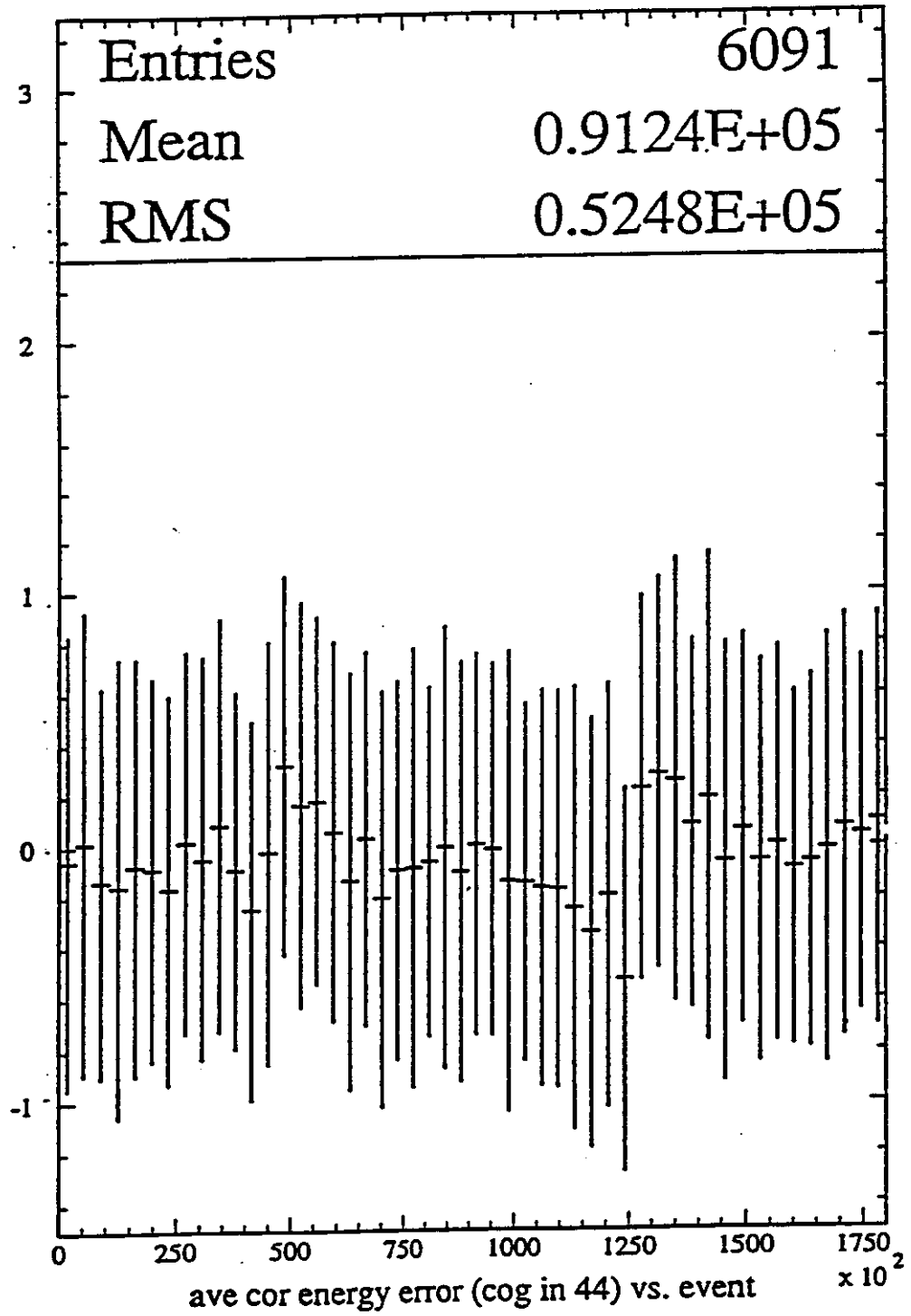

Figure 12: Average measured energy error versus event number over a 16 hour long set of runs. No time dependence is seen.

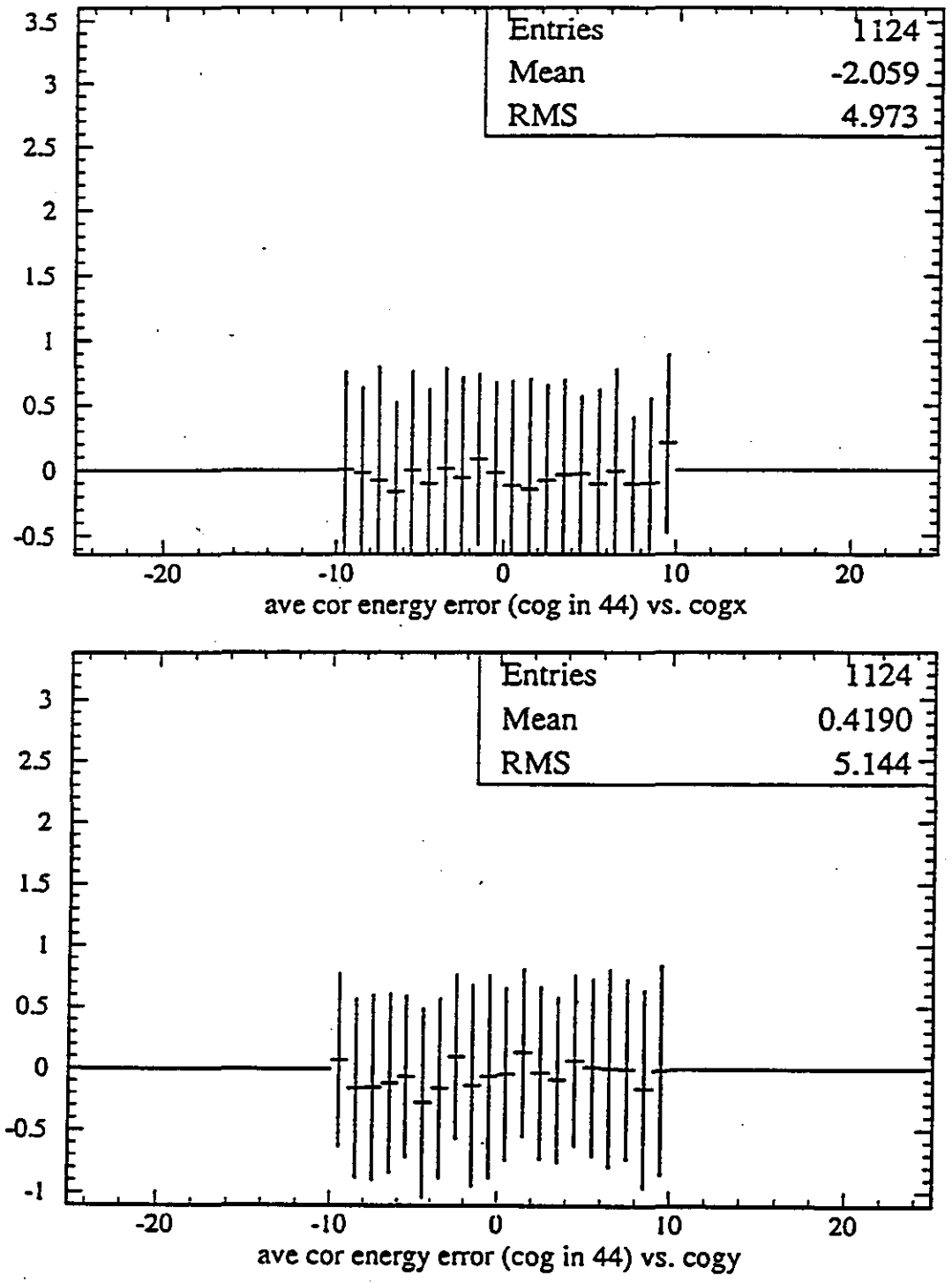

Figure 13: Average measured energy error versus x and y position in the BaF_2. The error bars shown correspond to the energy resolution in each bin.

to the energy output as shown in Figure 12. The dependence of the energy upon the measured position in the BaF_2 is shown in Figure 13. After this very simple correction of 2% or less there is no measurable position dependence and the resolution also does not depend on position.

Results on Resolution

In the study of the energy resolution, we correct the BaF_2 energy by the difference between the measured beam momentum and the nominal beam energy. In this way we can simply compare this corrected BaF_2 energy to 68 GeV. Figure 14 shows the distribution of energies measured for those events incident upon the center crystal of the matrix. There is a sharp peak at 68 GeV with a small tail toward low measured energy.

We fit a gaussian to the peak within ± 1.5 GeV (2.28σ) of the mean. The fit and distribution are shown in Figure 15. The standard deviation from the gaussian fit is 0.657 GeV which is 0.97% of 68 GeV but 1.0% of the mean beam energy. The gaussian is a good fit to the data in this region. This energy resolution only improves slightly if cuts on the y-segment in the beam chambers are made. If we do not limit outselves to the particles entering the center crystal, the same analysis gives a resolution of 1.2%. This resolution has not been optimized and suffers from the effects of electronic noise and shower containment as described below.

We have measured the resolution due to electronic noise by using the same analysis to calculate the energy in (random) pedestal triggers. As stated earlier, the effect of common mode electronic noise has been reduced by effectively using the outer row of crystals to subtract the noise from the center 25 crystals. This same subtraction is used for the pedestal events. The result is an RMS contribution to the resolution of 0.4% at 68 GeV. The pedestal widths in the ADC were 1 channel RMS which would cause a noise level 5 to 25 times higher, depending on correlations between channels, if no common mode noise correction were made. This noise is very simple to cure either with an ADC with more than 12 bits or with a high gain and a low gain readout channel.

We estimate that the beam spectrometer resolution, including the effects of multiple particles in the the beam, is 0.5 ± 0.2 %. After subtracting the resolution in the beam momentum measurement and the effect of very simple electronic noise, we find that the measured BaF_2 resolution is $0.77^{+0.12}_{-0.18}$ %.

From the uniformity measurements made with the muon beam, we know that the nonuniformity of light collection in these crystals made a significant contribution to the energy resolution. Our best estimate of this contribution is 0.6%, and it is definitely not less than 0.5%, based on measurements in the beam with muons transverse to the crystals. These nonuniformities will not be present in the GEM detector.

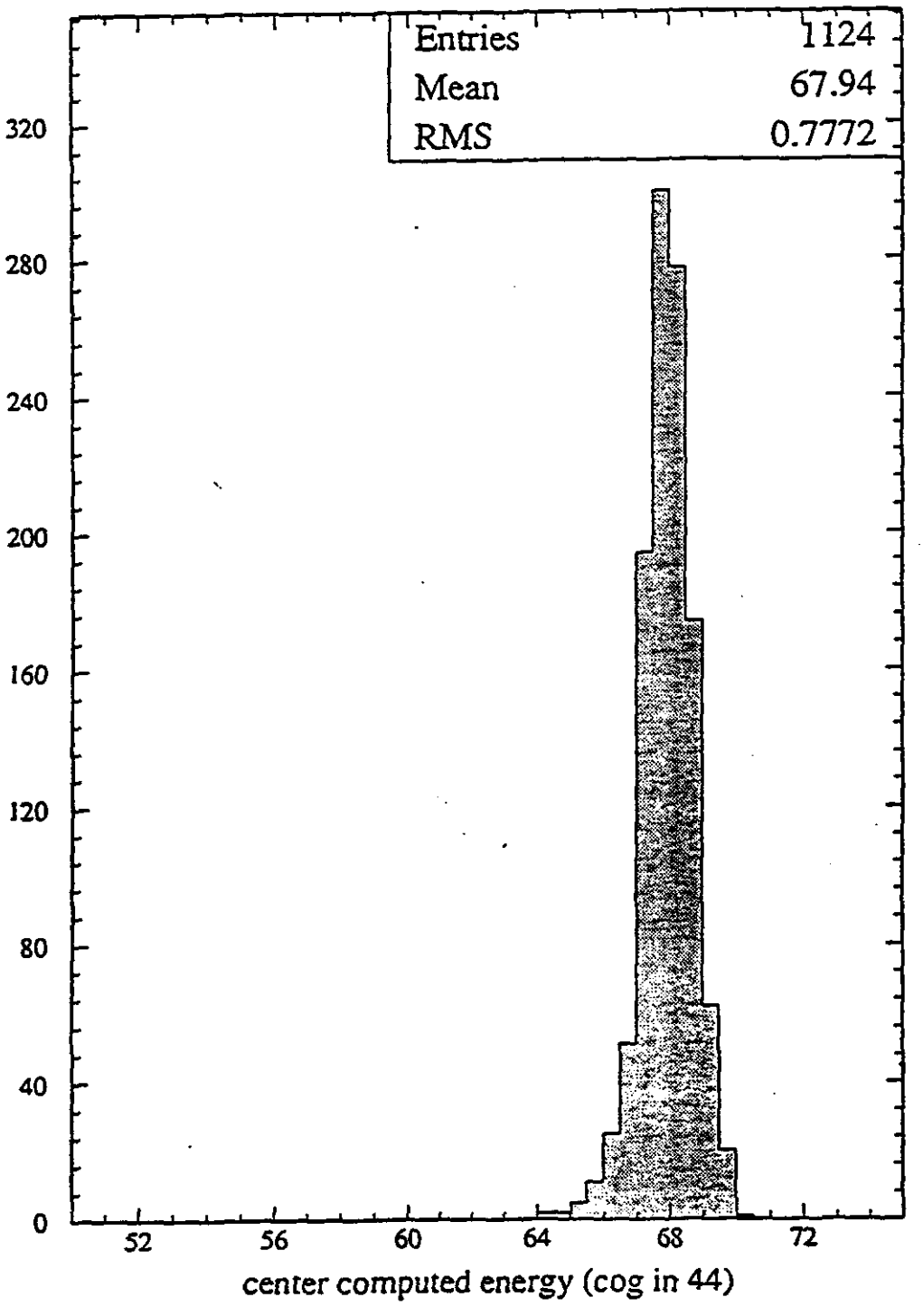

Figure 14: The distribution of fully corrected energies for electrons incident upon the central crystal of the matrix.

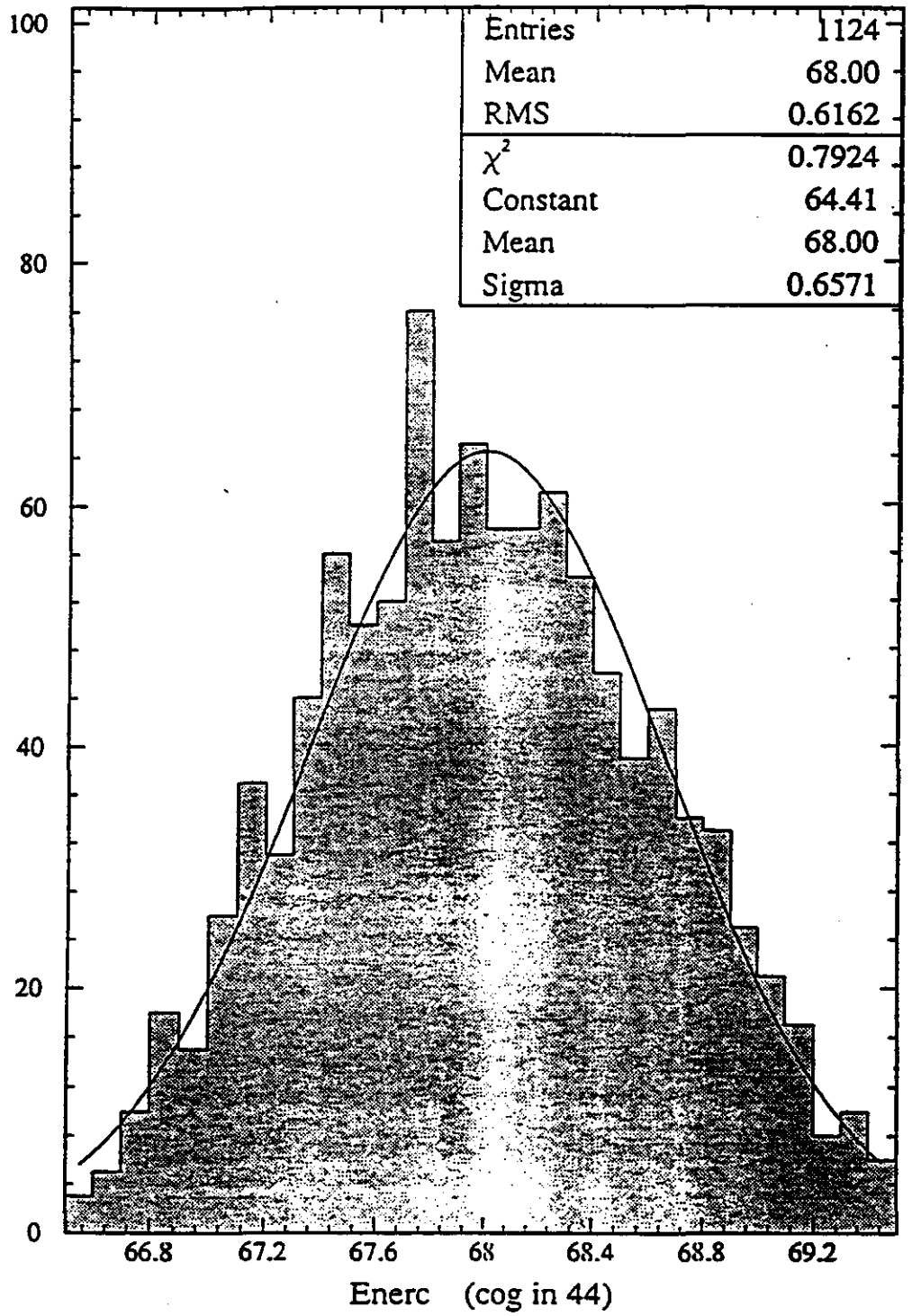

Figure 15: A gaussian fit to the corrected energy distribution over a range of ±1.5 GeV (2.28 σ). The mean energy is 68.00 GeV and the standard deviation is 0.657 GeV. The gaussian describes the data well.

Conclusion

The first BaF_2 test beam run has been carried out successfully entirely by GEM physicists. We have verified the small intrinsic constant term in the BaF_2 resolution despite serious inadequacies in the 1991 BaF_2 test beam setup. We measure a BaF_2 resolution of

$$\frac{\sigma_E}{E} = 0.77^{+0.12}_{-0.18}\ \% \tag{1}$$

which is in agreement with the 0.6% energy resolution expected for BaF_2 in GEM. If we remove the effect of the measured nonuniformities, the BaF_2 resolution must lie in the range from 0 to 0.7%. We expect to be able to make substantial improvements in out next test beam run with improved crystals, a larger size matrix, better beam measurements, thiner beam chambers and counters, a calibration system, and better electronics.

APPENDIX G.

ON OPTICAL BLEACHING OF BARIUM FLUORIDE CRYSTALS[1]

Da-an Ma and Ren-yuan Zhu

Lauritsen Laboratory
California Institute of Technology
Pasadena, CA 91125

September 1, 1992

Abstract

This report presents results on optical bleaching for 25 cm long BaF_2 crystals to be used in constructing the GEM BaF_2 calorimeter at the SSC. A practical scenario of implementing optical bleaching *in situ* and the requirements on the light sources used to bleach the entire GEM BaF_2 calorimeter are presented.

1 Introduction

Barium fluoride (BaF_2) crystals are being considered by the GEM Collaboration, to be used in constructing a precision electromagnetic calorimeter at the SSC [1]. The key issue of using this crystal at the SSC is its radiation resistance [2]. An Expert Panel was assigned by the SSC laboratory to review the radiation damage problem of BaF_2. The Panel met in December 1991 and again in January 1992 following a site visit to the Shanghai Institute of Ceramics (SIC) and Beijing Glass Research Institute (BGRI) by selected Panel members and the GEM Spokesmen. The principal conclusion of the Panel's February 1992 report is "there is no

[1]Work supported in part by U.S. Department of Energy Contract No.DE-AC03-81-ER40050.

apparent fundamental reason why BaF_2 can not be made radiation hard" [3].

The conclusion from the BaF_2 Panel is based upon existing data obtained by that time. Some highlights are summarized below:

- The BaF_2 radiation damage caused by photons shows clear saturation. Both transmittance and light output measured after irradiation do not degrade further after initial dosage of a few tens kRad to 100 kRad, depending on the quality of the BaF_2 crystals; (Figures 12 and 14 of [2])
- There is no permanent damage caused by either photons or neutrons. All damage recovers in full after an annealing at 500°C for three hours; (Figures 12 and 17 of [2])
- There is very slow spontaneous annealing of the transmittance at 220 nm of BaF_2 under room temperature measured up to 68 days after 1 MRad irradiation; (Figures 15 and 16 of [2])
- The radiation damage of BaF_2 has no dose rate dependence; (Figure 17 of [2])
- There is evidence that the damage of BaF_2 is caused by formation of color centers, which cause self-absorption of the scintillation light as it is transmitted through the crystal. There is no apparent damage to the scintillation mechanism itself, so that the intrinsic scintillation light yield by the crystal is not affected (Section 5.4 of [2]).
- Large size (20-25 cm long) BaF_2 crystals produced by SIC in December 1991 have considerably better radiation resistance than the crystals from previous batches. The transmittance of two 20 cm long crystals is ~50% at 220 nm after 1 MRad irradiation which corresponds to a light attenuation length (LAL) [5] of around 34 cm. (Figures 18 and 19 of [2])

The radiation resistance specification, proposed by the BaF_2 Collaboration, is the light attenuation length of longer than 95 cm for 25 cm long crystals after 1 MRad irradiation [2]. This specification is based upon a study of the influence of the light attenuation length on the crystal's light response uniformity, and thus

on the energy resolution [2]. It was also assumed that a stable high precision crystal calorimeter could be built by using pre-irradiated crystals of this quality. The stability is due to the saturation of the radiation damage, and the very slow spontaneous recovery rate of the transmittance at the wavelength of BaF_2's fast scintillation component (220 nm), at room temperature.

After six months, the Panel had its final meeting in early August, 1992. The R&D progress up to the meeting date was evaluated. The progress in quality of production BaF_2 crystals, however, did not match the specification of the BaF_2 Collaboration. The main conclusions of Panel's August meeting are [4]:

- With the knowledge presently available, preirradiation is not a viable solution to the radiation damage problem of BaF_2;
- The only solution is to use annealing of the crystal by exposure to light *in situ*. Such a method could make a calorimeter satisfying GEM's specifications using present production crystals.

Following Panel's recommendation, an extensive R&D was carried out at Caltech. This report presents result of optical bleaching for 25 cm long BaF_2 crystals produced by SIC. A practical scenario of implementing optical bleaching *in situ* and the requirements on the light sources used to bleach the entire GEM BaF_2 calorimeter are presented.

2 Experiment

2.1 Samples

Several 25 cm long BaF_2 crystals produced by SIC were tested. One crystal SIC302 was produced at the end of 1991 with a light attenuation length of 34 cm after 1 MRad irradiation. The other sample SIC402 is the latest crystal produced by SIC which has a light attenuation length of 41 cm after 1 Mrad irradiation. Table 1 lists the dimension, transmittance (T) at 200 nm and corresponding light attenuation length (λ) for these two crystals, where the subscript 0 and 1M refer to before and after 1 Mrad ^{60}Co γ-ray irradiation. The progress in crystal's quality is clearly shown in the increase of T_{1M} and λ_{1M}.

Note, the sample SIC402 was irradiated to 1 MRad by using a ^{60}Co source at SIC, and was consequently bleached to a saturation by using a high pressure mercury lamp whose irradiance spectrum covers 270 to 440 nm [6]. Before the first irradiation, the transmittance of SIC402 was measured at SIC to be 86% [6]. It is clear that the optical bleaching did not remove all color centers produced by the irradiation.

Table 1: Properties of Two SIC Samples

Sample	Dimension (cm)	T_0 (%)	λ_0 (cm)	T_{1M} (%)	λ_{1M} (cm)
SIC302	$3^2 \times 25 \times 4^2$	87.2	780	43.3	34
SIC402	$3.6^2 \times 25 \times 4.6^2$	78.0	174	48.6	41

2.2 Experimental Setup

The light from a monochromator (BAUSCH & LOMB, Grating 1200 Grove/mm) was shot through the large end of the tapered 25 cm long BaF_2 crystal. To investigate the optical bleaching speed no reflector was placed at any surface of the crystal. The experimental setup was kept in dark. The monochromator was set to have a bandwidth around 10 nm with a rectangular light spot with a dimension of 0.8" (height) × 1" (width).

Light with different wavelengths was used in the experiment. The crystal was illuminated with the light, and the transmittance of the crystal was measured frequently until a saturated value was reached. The same procedure was repeated for red light (700 nm), green light (500 nm), blue light (400 nm) and UV light (300 nm).

2.3 Calibration of the Light Intensity

The calibration of the light intensity was carried out by using a Hamamatsu Si-diode with known quantum efficiency. Apertures with different diameter (5, 7.5 and 10 mm) were used to verify the uniformity of the light intensity from the

monochromator. It was found that the photo-current is proportional to the area of the aperture to within 5% for the cases of 5 and 7.5 mm. This indicates that the light intensity in this area has a good uniformity.

Table 2 lists the intensity of the light (mW/cm^2), and the corresponding photon flux (photon/cm^2/s), at the position where the light entering the crystal, for wavelengths of 300, 400, 500 and 700 nm. For convenience, the photon energy (eV), the integrated energy density of the light per hour (J/cm^2/hour) and the integrated photon density per hour are also listed.

Table 2: Light Intensity of Monochromator

Wavelength (nm)	300	400	500	700
Photon Energy (eV)	4.1	3.1	2.5	1.8
I (mW/cm^2)	0.21	0.85	1.5	1.0
F (10^{15} photons/cm^2/s)	0.32	1.7	3.8	3.5
P (J/cm^2/hour)	0.76	3.1	5.4	3.6
N (10^{18} photons/cm^2/hour)	1.2	6.1	13.7	12.6

3 The Wavelength Dependence

Sample SIC302 was first illuminated with a red light (700 nm). After 30 hours of illumination, the light attenuation length saturated at 100 cm. The bleaching light then was changed to 500 nm — the light attenuation length changed very little in 5 hours. It was further changed to 400 nm. After another 10 hours, the light attenuation length saturates again at 180 cm. The light finally changed to 300 nm, the light attenuation length was saturated after around 10 hours.

Table 3 lists the measured transmittance (T) at 220 nm, corresponding light attenuation length (λ), color center density ($1/\lambda$) and color center density normalized to after 1 MRad irradiation (λ_{1M}/λ). Figure 1 shows the transmittance spectra measured. The transmittance at 220 nm (T), its corresponding light attenuation length (λ) and color center density ($1/\lambda$) are plotted as a function of time in

Figure 2.

This result indicates that there is a wavelength threshold of bleaching light below which a different type of color center in SIC crystal can be effectively bleached. This threshold is between 400 to 500 nm. In the next study, we will determine the threshold, and we can use the bleaching light source with wave length of just a little shorter than this threshold, but longer than 400 nm. By doing so, the effect to our solar blind phototube will be reduced to a minimum.

By using the calibration in Table 2, this data also show that 108 J/cm^2 of 700 nm light plus 31 J/cm^2 of 400 nm light are required to bleach the crystal to 180 cm. The time needed to bleach the crystal to the **mid point, defined as 0.5/(saturated LAL)**, is 4.5 hours for 700 nm and 1 hour for 400 nm. The corresponding energy density needed is 16 J/cm^2 and 3.1 J/cm^2 respectively for light of 700 and 400 nm.

Table 3: Bleach SIC302 with Different Wavelengths

Time (hours)	T(%)	λ (cm)	$1/\lambda$ (1/m)	λ_{1M}/λ
Before Irradiation				
	87.2	779	0.13	
1 MRad Irradiation by ^{60}Co γ-ray				
	43.5	34.5	2.9	1.00
Under 700 nm Red Light				
0.	43.5	34.5	2.9	1.00
2.	47.6	39.3	2.5	0.88
4.5	54.6	50.1	2.0	0.69
14.5	63.6	72.2	1.4	0.45
24.	67.1	85.3	1.2	0.40
30.	70.	99.6	1.0	0.35
35.	69.5	97.1	1.0	0.35
Under 500 nm Green Light				
35.5	71.	105.6	0.95	0.33
37.	71.2	106.9	0.94	0.32
39.5	71.3	107.5	0.93	0.32
43.	71.3	107.5	0.93	0.32
Under 400 nm Blue Light				
43.5	72.4	115.0	0.87	0.30
44.5	76.2	150.3	0.67	0.23
54.5	78.9	190.	0.53	0.18
64.	78.5	183.	0.55	0.19
65.	78.3	180.	0.56	0.19
Under 300 nm UV Light				
66.	79.1	194.	0.52	0.18
67.	78.7	186	0.54	0.19
75.	79.5	202	0.50	0.17
89.5	80.4	221	0.45	0.16
95.	81.1	240	0.42	0.15

4 Bleach BaF_2 Crystals with 400 nm Light

As shown in Section 3, the 400 nm is a good wavelength which can be used in an effective optical bleaching for BaF_2 crystals. In order to determine the exact light energy density required to bleach color centers caused by 1 MRad irradiation, we re-irradiated SIC302 to 1 MRad after the test described in Section 3, and tested bleaching by using 400 nm light again.

Table 4 lists the measured transmittance (T) at 220 nm, corresponding light attenuation length (λ), color center density ($1/\lambda$) and color center density normalized to after 1 MRad irradiation (λ_{1M}/λ). Figure 3 shows the transmittance spectra measured. The transmittance at 220 nm (T), its corresponding light attenuation length (λ) and color center density ($1/\lambda$) are plotted as a function of time in Figure 4.

Table 4: Bleach SIC302 with 400 nm Light

Time (hours)	T(%)	λ (cm)	$1/\lambda$ (1/m)	λ_{1M}/λ
0.	43.3	34	2.9	1.00
0.5	58.7	59	1.7	0.50
1.0	64.6	76	1.3	0.46
1.5	67.9	89	1.1	0.39
2.5	71.8	111	0.90	0.31
4.5	74.6	133	0.75	0.26
12.0	78.5	182	0.55	0.19
13.0	78.0	175	0.57	0.20

A test with the latest 25 cm long BaF_2 crystal SIC402, which was delivered in August 1992, produced a similar result, as shown in Table 5, Figure 5 and Figure 6. In summary, both SIC302 and SIC402 have been bleached to a saturated light attenuation length of 180 cm in around 10 hours. This indicates an energy density of 31 J/cm^2 for 400 nm light, or photon density of 6.1 x 10^{19} photons/cm^2, is enough to bleach current 25 cm long crystals from saturated damage to 180 cm.

Less than 1.5 hour is needed to bleach current production crystals to the mid point defined in section 3, which corresponds to 4.5 J/cm^2 or 9 $\times 10^{18}$ photons/cm^2.

Table 5: Bleach SIC402 with 400 nm Light

Time (hours)	T(%)	λ (cm)	$1/\lambda$ (1/m)	λ_{1M}/λ
0.	48.6	41	2.5	1.00
1.0	61.6	66	1.5	0.61
1.5	66.8	85	1.2	0.48
3.5	72.4	115	0.87	0.35
6.5	76.9	159	0.63	0.26
8.5	77.7	170	0.59	0.24
9.5	77.8	173	0.58	0.23
18.5	78.4	181	0.55	0.22

5 Color Center Density: Annihilation and Creation

It is important to understand the dynamic process of the annihilation and creation of optically bleachable color centers.

5.1 Color Center Annihilation

From the data presented in Section 4, it is straight forward to mathematically formulate the process of color center annihilation. The annihilation speed is proportional to the existing bleachable color center density (D) and the light intensity used:

$$dD = -aIDdt \tag{1}$$

where a is a constant in a unit of cm^2/mW/hour, I is the light intensity in a unit of mW/cm^2, and t is the time in a unit of hour. Equation 1 can be solved with a

solution of

$$D = D_0 \, e^{-aIt} \tag{2}$$

By using Table 5, we determined a = 0.85 $cm^2/mW/hour$.

5.2 Color Center Creation

Table 6 lists the transmittance (T) at 220 nm, corresponding light attenuation length (λ), total color center density ($1/\lambda$) and optical bleachable color center density (D) for sample SIC402. These data were obtained by reirradiate SIC402 after 1 MRad irradiation followed by a complete optical bleaching.

Table 6: Transmittance and LAL of SIC402 after Irradiation

Dosage	0 Rad	1 kRad	100 kRad	1 MRad
Transmittance (%)	78.4	63.8	49.2	48.6
λ (cm)	181	73	42	41
$1/\lambda$ (1/m)	0.55	1.4	2.4	2.5
D (1/m)	0	0.85	1.85	1.95

The creation speed of optically bleachable color center density (D) is proportional to the existing trap density (D_{all} -D) and to the radition dose rate, where D_{all} is the total densityof traps related to the optically bleachable color centers in the crystal (1.95/m for current production BaF_2 crystals from SIC).

$$dD = (D_{all} - D) \, bRdt \tag{3}$$

where b is a constant in a unit of 1/kRad, R is the radiation dose rate in a unit of kRad/hour, and t is the time in a unit of hour. Equation 3 can also be solved with a solution of

$$D = D_{all} \, (1 - e^{-bRt}) \tag{4}$$

By using Table 6, we determined b = 0.57 /kRad.

5.3 Color Center Dynamics

In general, annihilation and creation may exist at the same time. We have

$$dD = -aIDdt + (D_{all} - D)\, bRdt \tag{5}$$

The solution of Equation 5 is

$$D = \frac{bRD_{all}}{aI + bR}\,[1 - e^{-(aI+bR)t}] \tag{6}$$

For each values of I and R, an equilibrium between annihilation and creation will be established at an optical bleachable color center density of

$$D = \frac{bRD_{all}}{aI + bR} \tag{7}$$

6 A Realistic Scenario of Optical Bleaching

6.1 The Scenario

It should be noticed that the bleaching using 400 nm does not provide a complete recovery for BaF_2 crystals, i.e the light attenuation length (λ) will not recover to the status of before irradiation, or after a thermal annealing [8]. A realistic scenario of *in situ* bleaching by using 400 nm light thus includes:

- Pre-irradiation;
- Pre-bleaching; and
- *in situ* bleaching.

Note, the pre-irradiation discussed here is different to what discussed extensively by the BaF_2 Expert Panel [3, 4]. The purpose of this pre-irradiation is to activate those deep colo· centers which can not be bleached by using 400 nm light. The detailed dosage needed for pre-irradiation should be investigated in near future.

The pre-bleaching can be carried out with a powerful blue lamp for naked crystals. This is to provide a starting light attenuation length of around 180 cm for current

production BaF_2 crystals. The optical coating and light response uniformity measurement should be carried out after pre-bleaching. The crystal after this initial treatment will have a maximum light attenuation length around 180 cm and will not request a dark room for handling.

Recent Monte Carlo study by K. Shmakov [9] shows that the requirement on *in situ* bleaching should keep the light attenuation length between 110 to 180 cm. By doing so, the light response uniformity and thus the high energy resolution of BaF_2 crystal calorimeter will not be compromised.

6.2 Energy Density Required for *in situ* Bleaching

There are two possible approaches for *in situ* optical bleaching:

- bleaching when needed; and
- bleaching during run.

We discuss in details the energy density required for these two approaches in the rest of this section.

6.2.1 Bleaching when Needed

By using Equation 2, we can calculate the energy density of 400 nm light needed to bleach a BaF_2 crystal from λ_1 to λ_2:

$$\begin{aligned} I(t_2 - t_1) &= \frac{\ln(D_1/D_2)}{a} \\ &= 1.12 \ \ln \frac{1/\lambda_1 - 0.55}{1/\lambda_2 - 0.55} \end{aligned} \tag{8}$$

Assuming $\lambda_1 = 110$ cm and $\lambda_2 = 160$ cm, we have $I\Delta t = 6.3$ J/cm^2, where $\Delta t = t_2 - t_1$. Equation 9 can be used to calculate power needed for any working interval of the light attenuation length.

Since the sum of equivalent surface area of all crystals of GEM BaF_2 calorimeter is around 200,000 cm^2 (calculated at the middle of the crystal), 1.2 MJ is needed

to bleach all crystals from 110 cm to 160 cm. This means that a light source with an effective power of 600 W would do the job in 30 minutes through 16,000 fibers to each crystal.

Note, this energy density needed will be reduced by a factor of around 3 if the crystals were wrapped with reflector to allow multiple bounsings inside the crystal.

By using Equation 4, we can calculate the value of the time interval (Δt) in which the light attenuation length degradats from λ_1 to λ_2:

$$\begin{aligned} \Delta t &= \frac{1}{bR} \ln \frac{D_{all} - D_1}{D_{all} - D_2} \\ &= \frac{1.8}{R} \ln \frac{2.5 - 1/\lambda_1}{2.5 - 1/\lambda_2} \end{aligned} \tag{9}$$

Assuming $\lambda_1 = 160$ cm and $\lambda_2 = 110$ cm, we have $\Delta t = 0.30/R$ hours. The Equation 10 thus can be used to calculate the time interval in which the BaF_2 crystal will stay in the working interval of the light attenuation length between λ_1 and λ_2, provided a radiation dose map is known.

In the worst case of $|\eta| = 2.5$ at the SSC, the dose rate is around 0.4 kRad/hour at standard luminosity. This indicates *in situ* bleaching needs to be carried out less than one hour at $\eta = 2.5$ and every 15 and 7.5 hours at $\eta = 0$ and 1. Assuming a physics run has a beam time of 8 hours at the SSC, this approach seems applicable for the BaF_2 barrel constructed with current production crystals at the standard SSC luminosity, but has limitation for end caps and high luminosity, i.e. 10^{34} cm^{-2} s^{-1}. BaF_2 crystals with better quality, i.e. low total trap density D_{all} and b are needed, if this approach is to be used *in situ*.

Note, if a powerful laser with short pulse is used, this approach may be adequate for current production BaF_2 crystals, even at high luminosity. Some eximer lasers, e.g. 351 nm laser with xenon fluoride gas should be investigated.

6.2.2 Bleaching during Run

An alternative approach is to implement the bleaching light constantly on crystals during run. Because of the solar blindness, the proposed readout device for BaF_2 crystals would not see the bleaching light at 400 nm. In this approach, crystals

are assumes to work at a particular light attenuation length, i.e. at a **working point** (λ_w), which is the equilibrium point described in Equation 7.

By using Equation 7, we can calculate the intensity of 400 nm light needed to compensate the radiation dose *in situ*, so that a stable light attenuation length (λ_w) can be maintained.

$$\begin{aligned} I &= \frac{bR\,(D_{all} - D_w)}{aD_W} \\ &= 0.67R\,\frac{2.5 - 1/\lambda_w}{1/\lambda_w - 0.55} \end{aligned} \tag{10}$$

Assuming the applied light intensity is a factor of k of the value defined by Equation 11, the real light attenuation length can be calculated by using Equation 7.

$$D = \frac{D_{all}}{1 + k(D_{all}/D_w - 1)} \tag{11}$$

For current production BaF_2 crystals and the defined working light attenuation length of 150 cm, we have the real light attenuation length of

$$1/\lambda_{real} = \frac{1.95}{1 + 15.3k} + 0.55 \tag{12}$$

The real working light attenuation length can be calculated as 169 cm for k = 3 and 111 cm for k = 0.3. It is thus clear that the deviation of the intensity of the bleaching light does not compromise the high resolution of BaF_2 crystal calorimwter.

Assuming a working point of λ = 150 cm, the required light intensity is 10.5 R mW/cm^2, where R is the dose rate in unit of kRad/hour. The required light intensity thus is proportional to the dose rate and is also related to light attenuation length of working point. Table 7 lists the dose rate and the required light intensity as a function of rapidity for GEM BaF_2 calorimeter.

In this approach, the maximum total power required for barrel is around 52 W, while the two endcaps need 100 W. An effective light source of 150 W thus will be enough to maintain 150 cm light attenuation length for entire BaF_2 calorimeter. As discussed in Section 6.2.1, this intensity can be reduced by a factor of around 3, if the multi-bounsing between reflectors were taking into account.

Table 7: Light Intensity Needed to Maintain BaF_2 at $\lambda = 150$ cm

$\|\eta\|$	0	1	2.5
Dose Rate (kRad/hour)	0.02	0.04	0.4
I (mW/cm^2)	0.21	0.42	4.2

6.3 Implementation of Optical Bleaching through Fibers

The bleaching light can be introduced to the crystal through an optical fiber. An 800 W average power can be transmitted through a 1 mm fiber [7]. This corresponds to 12.5 W for a 125 μm fiber, which greatly exceeds the power needed in either approaches discussed in this section. From Table 7, we conclude that an 125 μm fiber can accommodate the power needed at $\eta = 2.5$, if the "bleaching during run" approach is chosen. This is true even at high luminosity of 10^{34} cm^{-2} s^{-1}.

A detailed design on transfering 400 nm light to BaF_2 crystals through optical firbers has been started, and the first indication is no obvious technical difficulty in implementing the optical fiber.

7 Conclusion

We have studied optical bleaching of current production quality BaF_2 crystals by using a monochromator with well calibrated light intensity. The study shows a BaF_2 calorimeter can be built with current production crystals from China. With an effective 150 W light source, the entire BaF_2 calorimeter can be set to work at 150 cm light attenuation length. The key issue of radiation damage problem of BaF_2 crystals thus is solved.

The main conclusions of this study are:

- Light of 400 nm wavelength was found to be more effective than the 500 nm light in optical bleaching of BaF_2 crystals;
- By using 400 nm light, the saturated light attenuation length is found to be

around 180 cm for two current production BaF_2 crystals;

- A maximum of effective 150 W of optical power at 400 nm is needed to bleach all BaF_2 crystals in GEM calorimeter during run at the standard SSC luminosity, and to keep the light attenuation length of all BaF_2 crystals at around 150 cm;
- The deviation caused by a factor of three deviation of the intensity of the bleaching light does not compromise the energy resolution of the BaF_2 calorimeter;
- By using 400 nm light, 6.3 J/cm^2 is needed to bleach the crystal from λ = 110 cm to 160 cm. To completely bleach the whole GEM BaF_2 crystal calorimeter, the total energy needed is 1.2 MJ , which can be accommodated by an effective 700 W light source in 30 minutes;
- Taking into account of multi-bounsings of the bleaching light inside the crystals, all powers and energies reported in this report are expected to be reduced by a factor of around 3;
- Further improvement of crystal quality, i.e. reducing D_{all} would certainly help to reduce the requirement on the power of the light source.

8 Acknowledgement

The authors wish to thank Prof. Z.W. Yin and P.J. Li for providing BaF_2 sample for this work, and Drs. H. Kobrak, C. Wuest, Y. Kamyshkov and J. Branson for many useful discussions.

References

[1] GEM Collaboration, Letter of Intent to the SSCL, November 30, 1991.

[2] R.Y. Zhu, CALT-68-1767 and GEM TN-92-48, January 1992.

[3] S. Majewski *et al.*, BaF_2 Expert Panel Report, February 1992.

[4] S. Majewski *et al.*, BaF_2 Expert Panel Report, August 1992.

[5] D.A. Ma and R.Y. Zhu, **CALT-68-1811** and **GEM TN-92-148**, August 1992.

[6] Z.W. Yin, private communication,

[7] C. Wuest, private communication, according to LLNL's Laser Isotope Separation Program.

[8] R.Y. Zhu *et al.*, *Nucl. Instr. and Meth.* **B61** (1991) 61.

[9] K. Shmakov, *talk in GEM calorimeter meeting*, August 9, 1992.

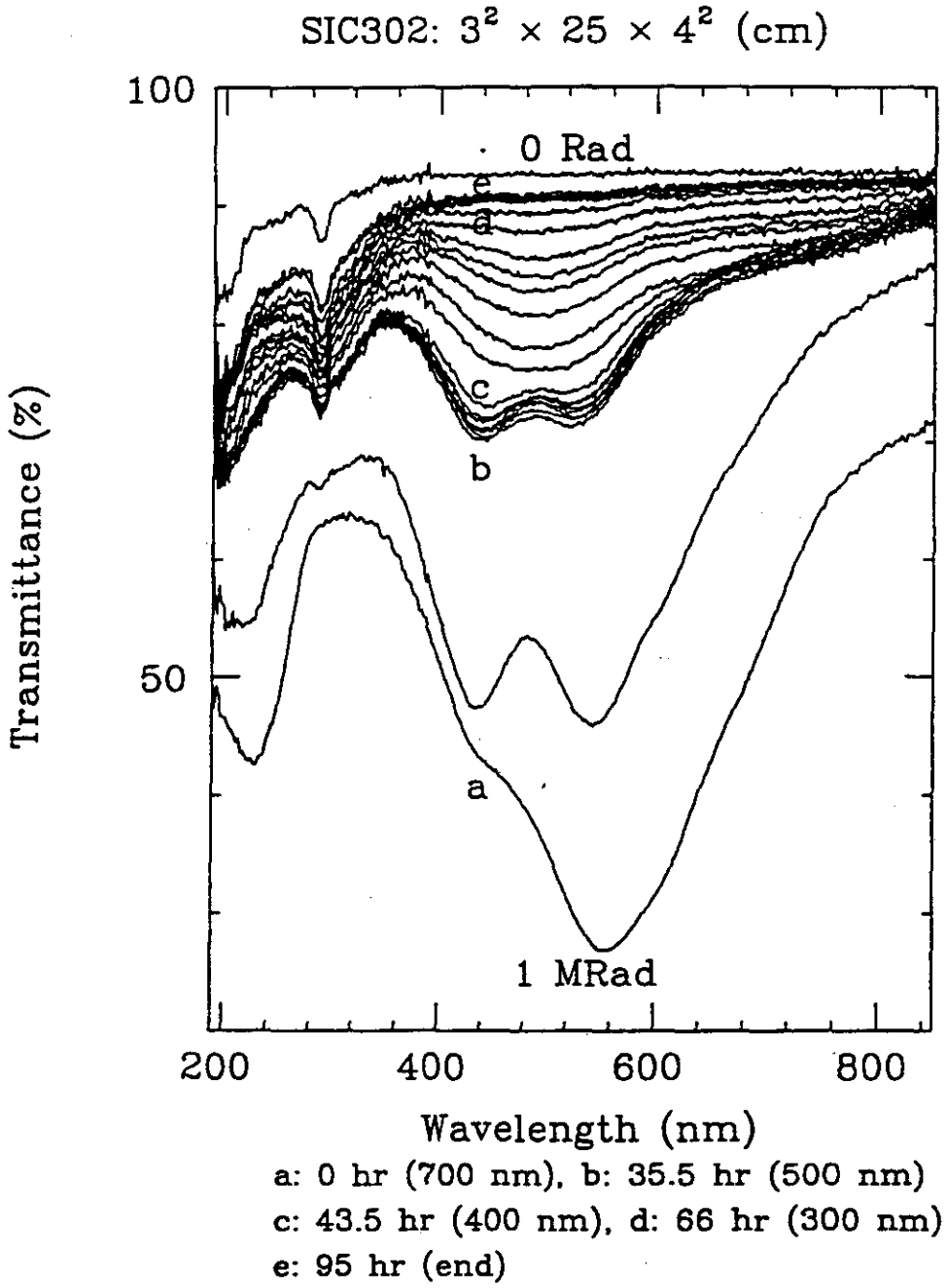

Figure 1: Transmittance of SIC302 are plotted as a function of wavelength under optical bleaching with different wavelengths.

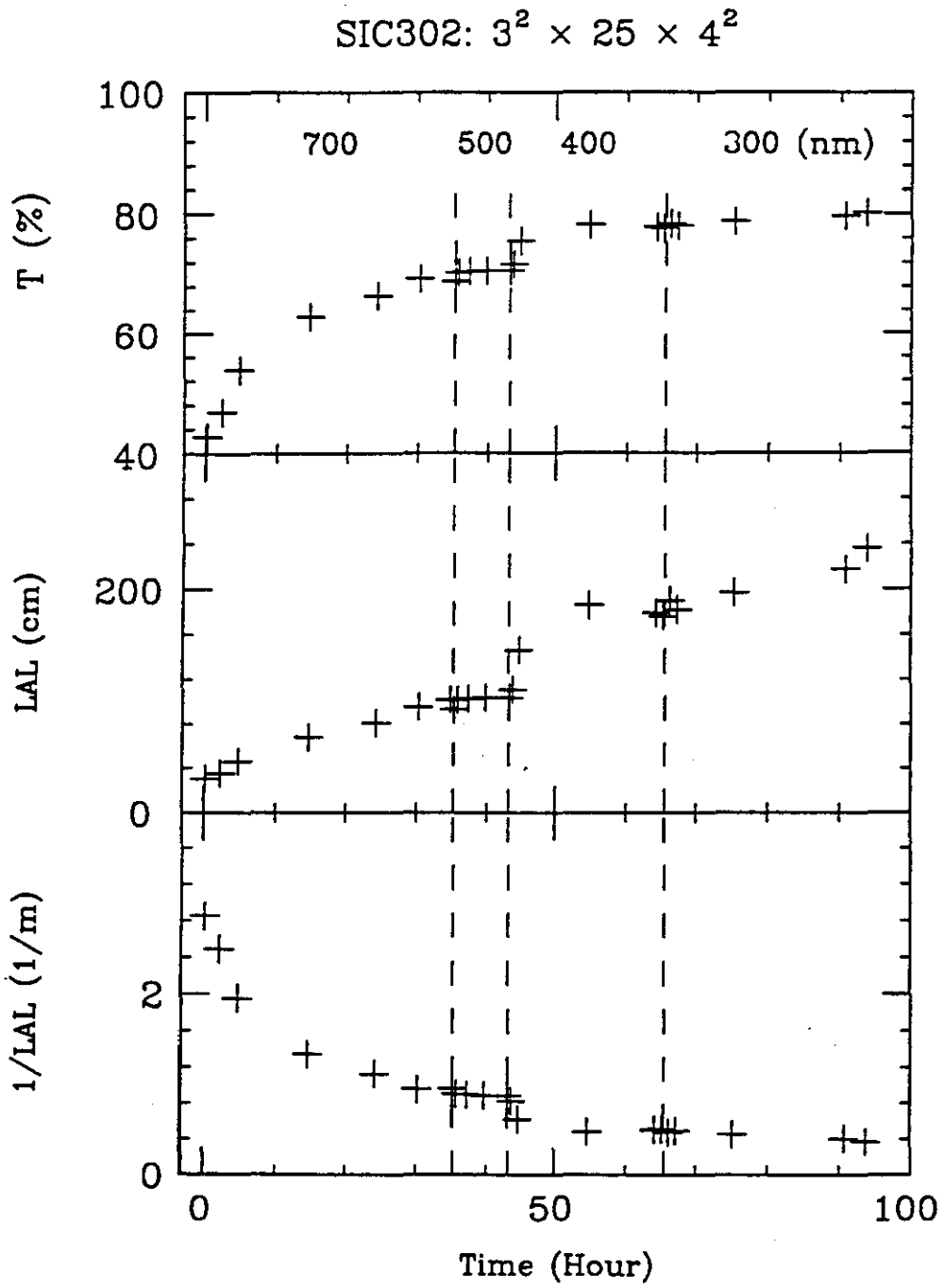

Figure 2: Transmittance (a), light attenuation length (b) and color center density (c) of SIC302 are plotted as a function of time under optical annealing with different wavelength.

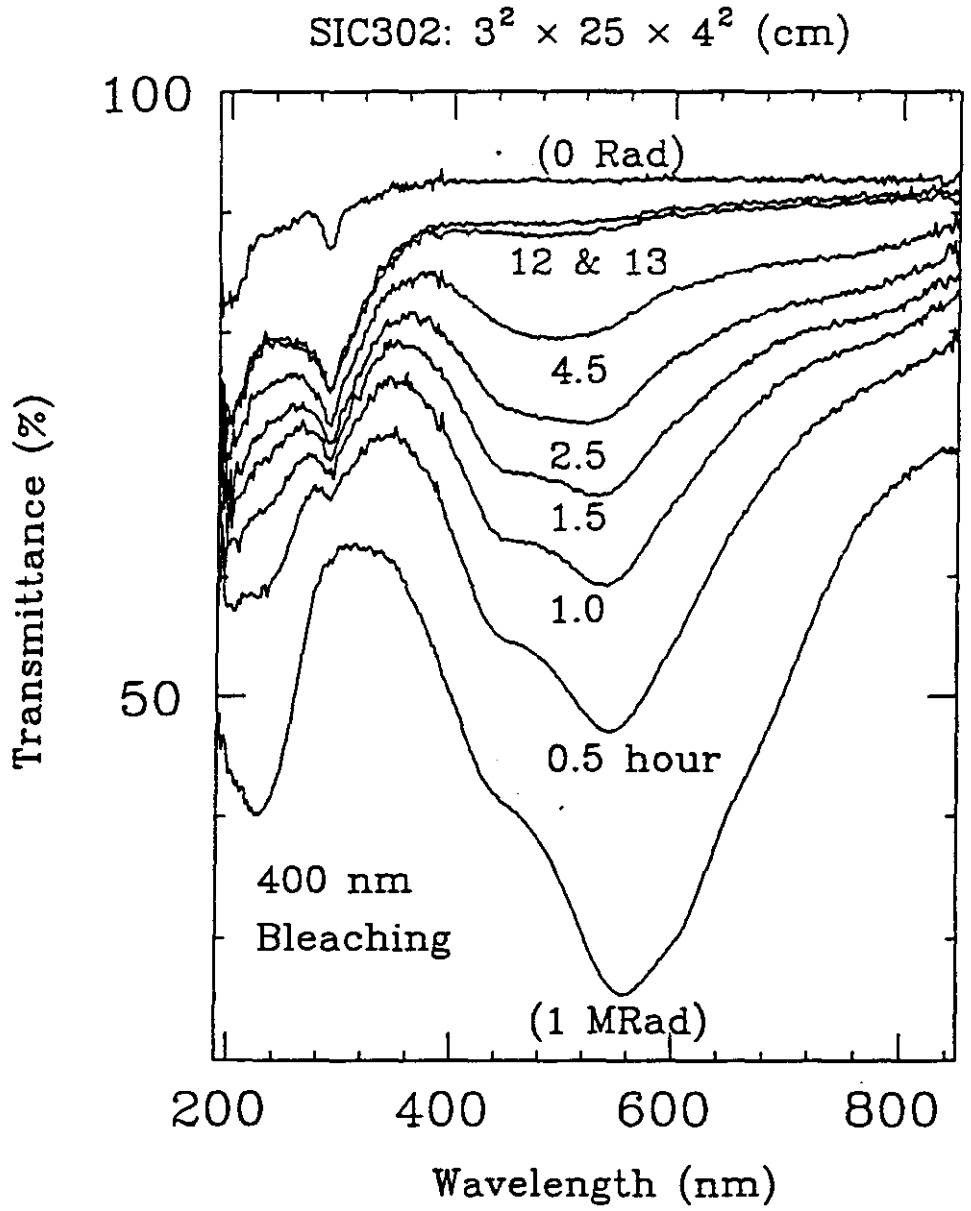

Figure 3: Transmittance of SIC302 are plotted as a function of wavelength under optical bleaching with 400 nm light.

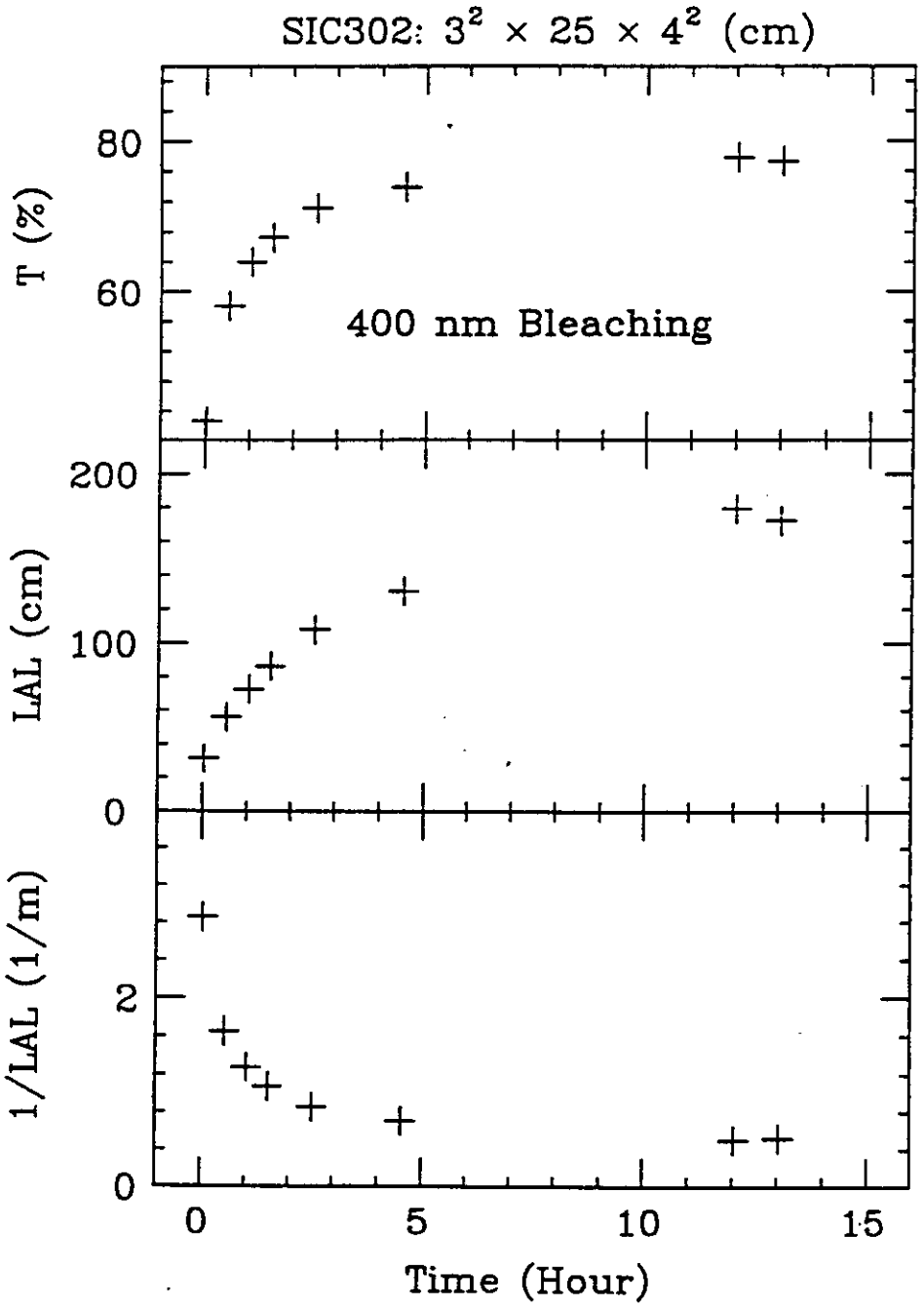

Figure 4: Transmittance (a), light attenuation length (b) and color center density (c) of SIC302 are plotted as a function of time under optical annealing with 400 nm light.

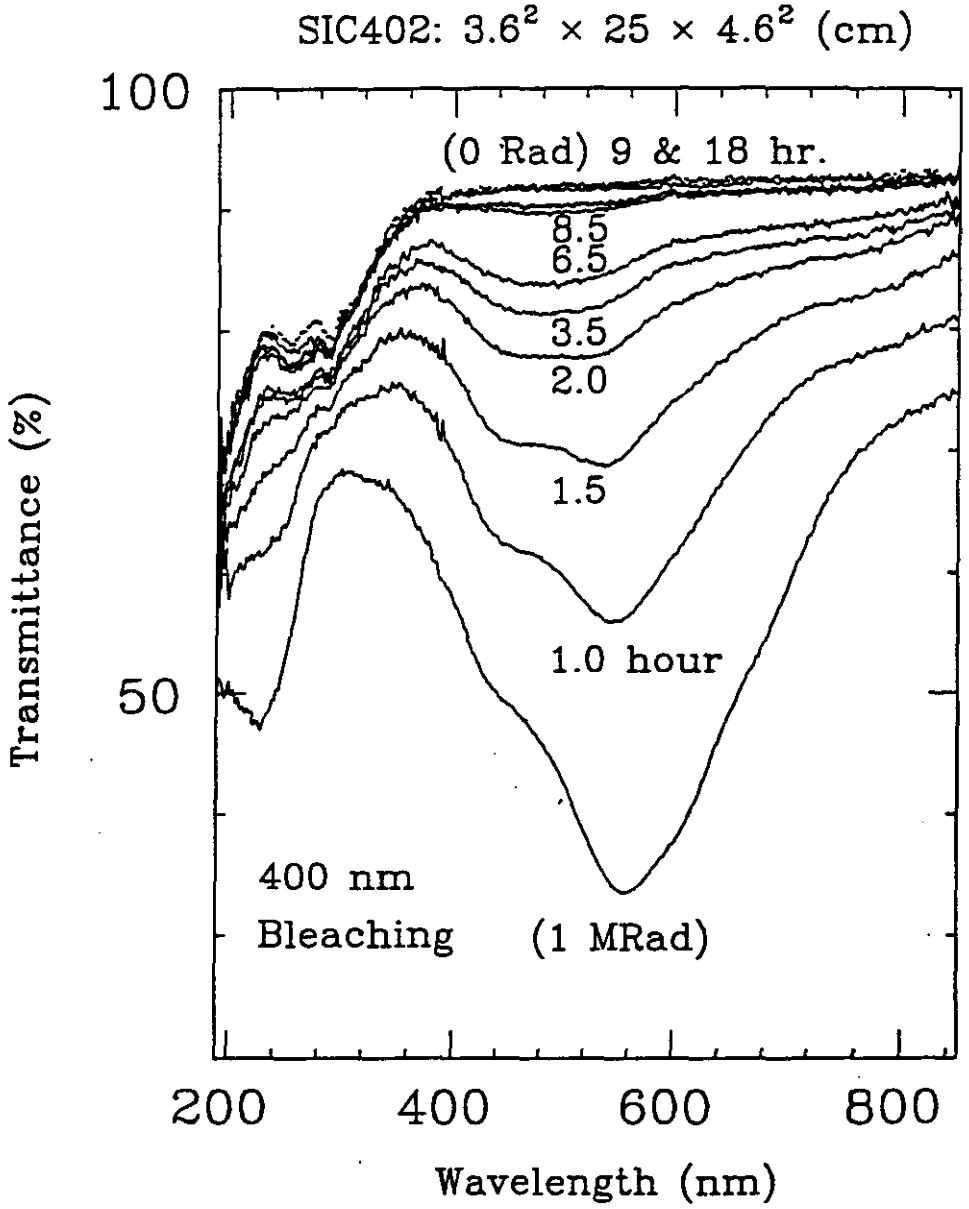

Figure 5: Transmittance of SIC402 are plotted as a function of wavelength under optical bleaching with 400 nm light.

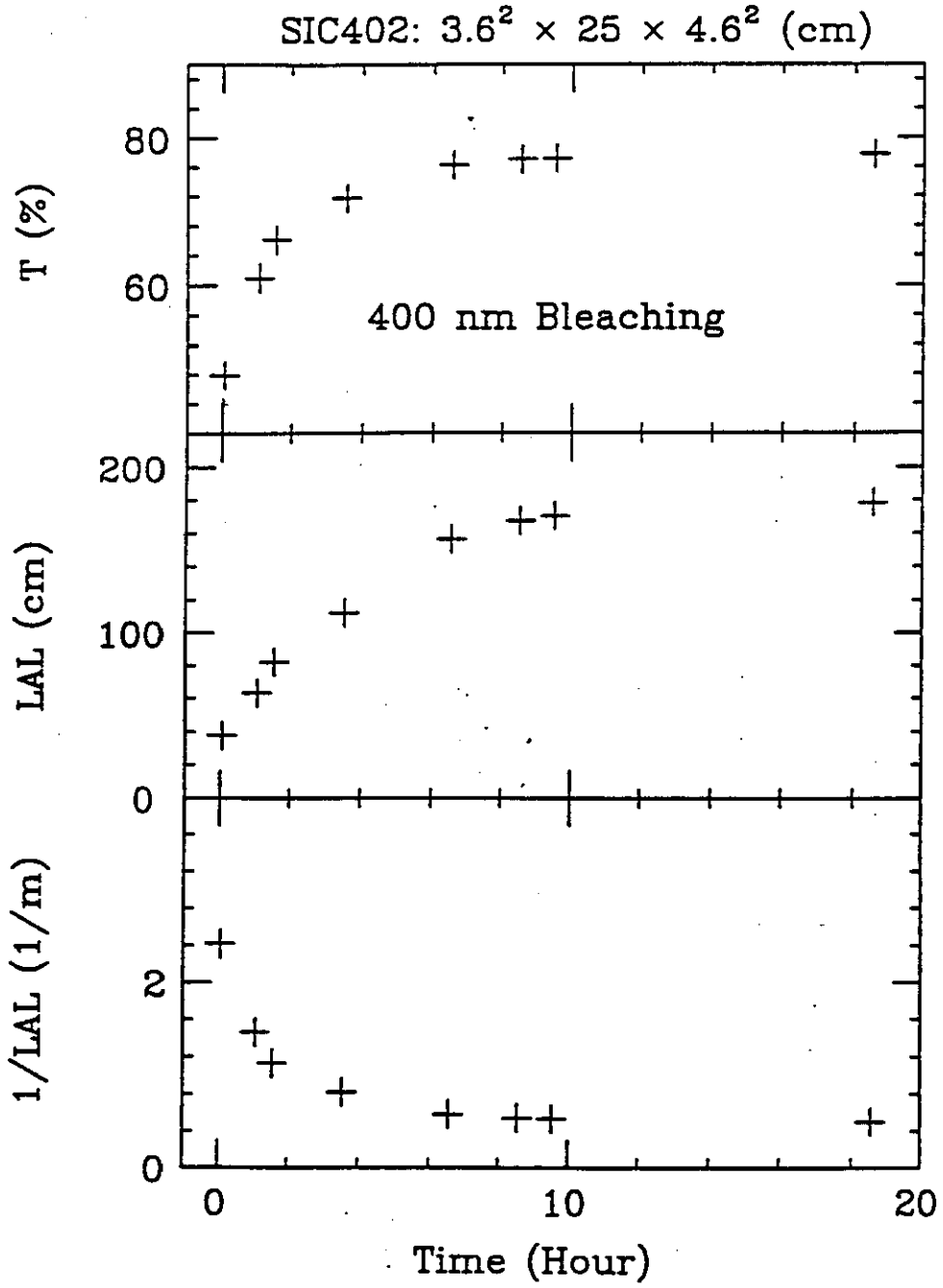

Figure 6: Transmittance (a), light attenuation length (b) and color center density (c) of SIC402 are plotted as a function of time under optical annealing with 400 nm light.

APPENDIX H.

Constructing Cosmic Ray Test Stand at IHEP & USTC for GEM BaF_2 Calorimeter

Institute of High Energy Physics
and
University of Science & Technology of China

August 30, 1992

1 Goal

In constructing GEM's precision barium fluoride (BaF_2) crystal calorimeter, crystal quality control and acceptance test for each crystal must be performed before assembling. Items to be tested include crystal's light yield and light response uniformity. Those crystals with uniformity better than 3% will be accepted and recorded in database. The crystals of GEM BaF_2 calorimeter will be produced by Shanghai Institute of Ceramics (SIC) at Shanghai, China, and Beijing Glass Research Institute (BGRI) at Beijing, China. We propose to establish cosmic ray test stands at Institute of High Energy Physics (IHEP) and University of Science and Technology of China (USTC) to carry out this task.

2 Method

We propose to test each BaF_2 crystal by using cosmic muon with minimum ionization in crystal. Each crystal is divided to 25 sections along axial length. These sections

cover the whole length of crystal (50 cm). Scintillator counters and two layers of steel will be used to select hard muons and to reject soft muons and shower photons. 8 layers of drift chambers will be used to determine the exact track of cosmic muons and thus the path length of the muon traversing the crystal with 1% precision. The light response uniformity along the crystal axis thus can be determined by normalizing the observed pulse height to the path length measured.

43,000 hard cosmic muon events per crystal will be accumulated in 48 hours. A histogram of 1730 entries/section can give section response with precision better than 1%. We plan to establish an ability to test 16,000 crystals in 3 years. Taking into account the possible repeated test, a 40 crystals/day capability is needed.

3 Test Apparatus

We plan to install two test apparatus: one in IHEP, Beijing, and the other in USTC, Hefei. We also suggest to install the same apparatus at SSCL to do on site test. The proposed test apparatus will be similar to the Cosmic Ray Stand at UCSD, as shown in Figure 1.

The trigger will be provided by 3 layers of scintillation counters (SC1, SC2 and SC3). Scintillation counters and two layers of steel of 10 cm thick will be used to select hard muons with energy greater than 500 MeV and to reject soft muons and shower photons.

The muon track will be measured by 8 layers of drift chambers (1X, 1Y ... 4X, 4Y). Each layer has 2 sublayers to resolve left-right ambiguity. To determine the track length in crystal better than 1%, it is necessary to determine the track angle with precision better than 1%. The scintillators and chambers will have the size of 60 $\times$ 100 cm^2 to accommodate 100 crystals in 5 layers. Each crystal has a PMT attached. The electronics and DAQ of the test apparatus is shown in Figure 2. The DAQ should be able to deal with 9 Hz event rate and will accumulate 900 MB data every bunch in 40 hours.

4 Data Processing

The data processing of cosmic test stand consists of he following aspects:

1. Muon track reconstruction;
2. Crystal pulse height normalization and histograming;
3. Fit each histogram to Landau or Gaussian distribution;
4. Calculation of crystal's light response uniformity.

   All data will be recorded on data base to be used by off-line analysis.

5 Time Schedule and Manpower

The time schedule and manpower to perform this task are listed below. Many of the personnel mentioned have been working on high energy physics experiments at Beijing, U.S. and Europe with experiences on scintillation counter, chamber, DAQ and off-line analysis.

We plan to build cosmic test stand in one year, starting from 1993, and to test crystals in 3 years starting from 1994. The manpower devoted to this task are:

- Construction phase:
  - IHEP: 1 professor (GUO, Ya-nan), 3 associate professors, 2 engineers and 4 students;
  - USTC: 1 professor (HAN, Rong-dian), 3 associate professors, 2 engineers and 5 students.
- Routine Test Phase
  - IHEP: 1 professor, 1 associate professors, 1 engineer, 1 student and 3 technicians;
  - USTC: 1 professor, 1 associate professors, 1 engineer, 2 students and 2 technicians.

6 Cost

Table 1 lists equipment and manpower cost per apparatus. The cost of manpower includes only engineers and technicians. The cost of 7 man-years each of physicists students are contributions from IHEP and USTC.

Table 1: Material and Manpower Cost per Apparatus

Phase	Item		U.S. Cost (k$)	China Cost (k$)
1	Crystal Box		25.5	22.0
1	PMTs and Bases		100.0	100.0
1	HV System		40.0	40.0
1	Scintillation Counter & Rack		19.0	11.5
1	Drift Chamber		85.0	75.0
1	DAQ		39.5	24.0
1	Subtotal		309.0	272.5
Phase	title	Manyears	U.S. Cost (k$)	China Cost (k$)
1	Engineer	1	118	12
1	Technician	1	108	12
1	Subtotal	2	226	24
2	Engineer	1.5	177	18
2	Technician	9	972	108
2	Subtotal	10.5	1149	126
Total			1681.0	422.5
Contingency			478.6	55
Grand Total			2159.6	477.5

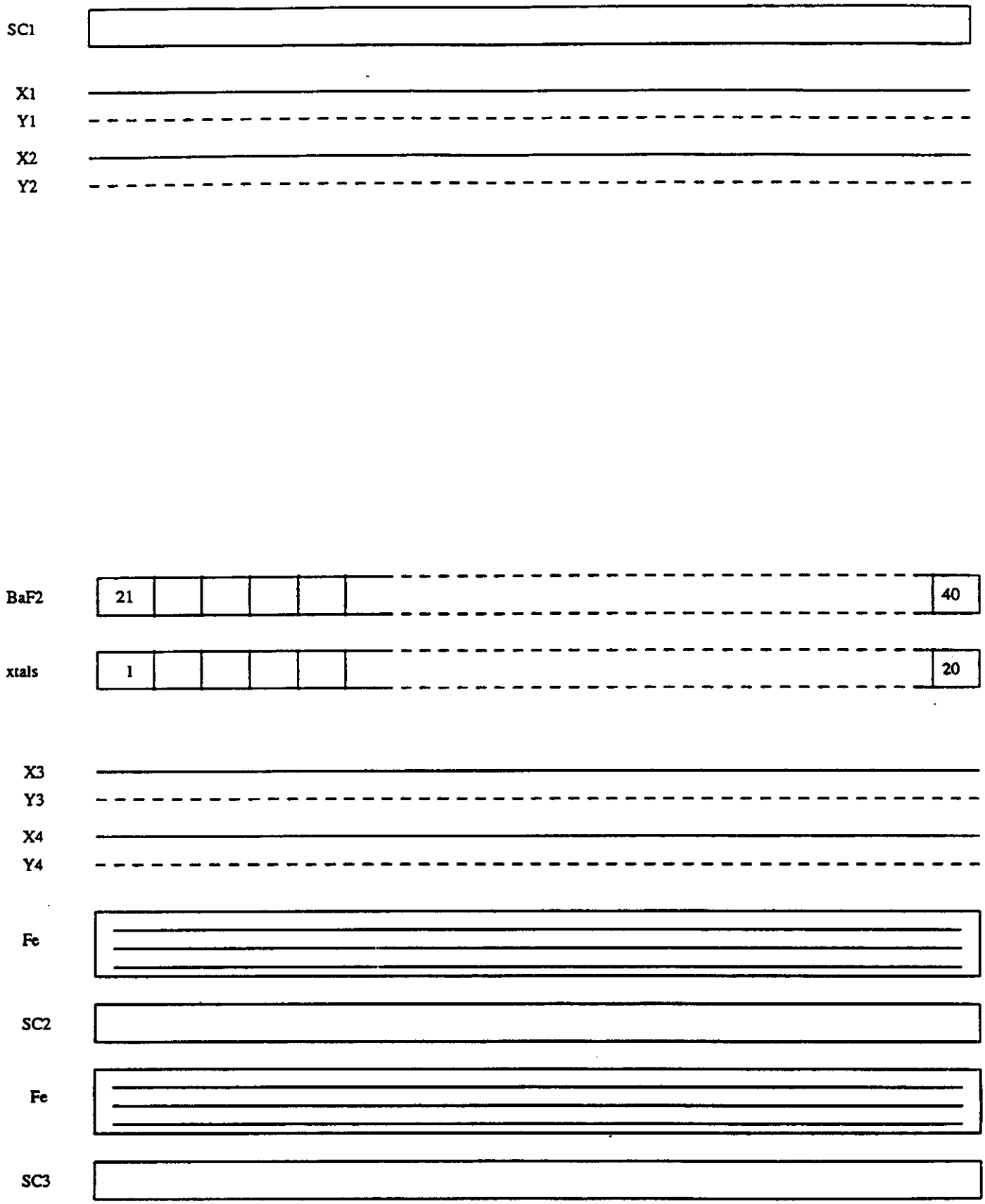

Fig.1 BaF2 Cosmic Ray Test Apparatus

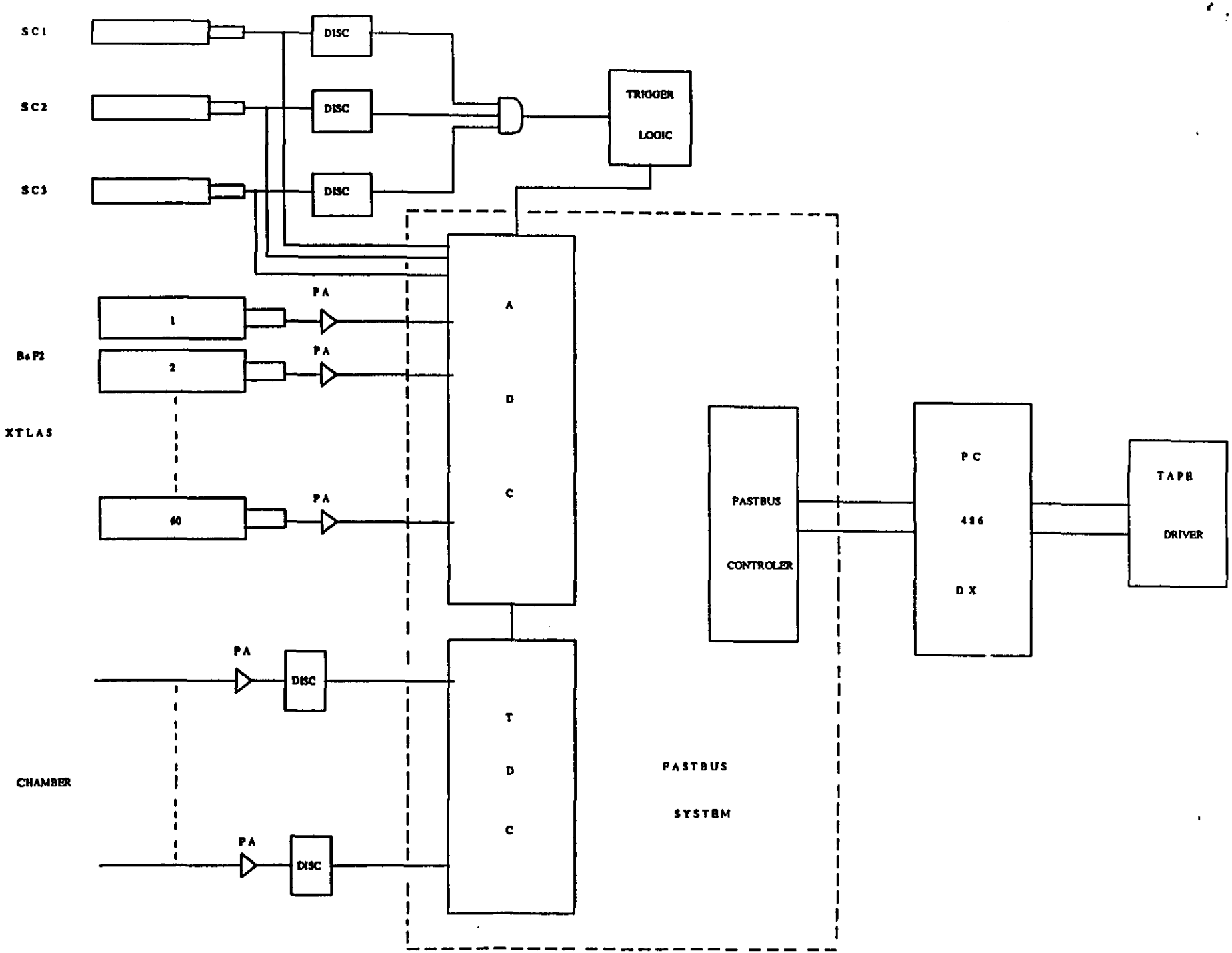

Fig.2 Electronics and DAQ of BaF2 Test Apparatus

References

[1] L3 Collaboration, *Nucl. Instr. and Meth.* **A289** (1990) 35.

[2] R.Y. Zhu and H. Yamammoto, *Intermediate Mass Higgs Searches With the GEM Detector*, CALT 68-1802 and GEM Internal Note GEM-TN-92-126, July, 1992.

[3] GEM Collaboration, Letter of Intent Submitted to the the SSC Laboratory, November 30, 1991.

[4] R.Y. Zhu, *On the Quality Requirements For The BaF_2 Crystals*, GEM Internal note **GEM TN-92-48 Rev A.**, January 1992.

[5] K. Shmakov and Y. Kamyshkov, Talks presented at GEM Calorimeter and Collaboration meetings. See GEM Technical Notes, including GEM TN-92-84 (Tucson Calorimeter Group Meeting).

[6] S. Majewski *et al.*, BaF_2 Expert Panel Report, February 1992.

[7] Y. Kamyshkov *et al.*, *Monte Carlo for BaF_2 at ORNL*, Progress Report, July 31, 1992; August 1992 Report (in preparation).

[8] S. Majewski *et al.*, BaF_2 Expert Panel Report, August 1992 (final version in progress at the time of this writing).

[9] C. Woody *et al.*, measurements of BaF_2 crystals at BNL, following exposure with MeV neutrons, described in *Irradiation Report for Brookhaven National Laboratory*, University of Mass. at Lowell, April 29, 1992.

[10] C. Woody *et al.*, *Progress Report on Radiation Damage Studies of BaF_2 for GEM at BNL*, July 24, 1992.

[11] Z. W. Yin and J. T.He, papers presented at the Shanghai BaF_2 Workshop, May 1991.

[12] C. Woody, *A Report on Radiation Damage in Barium Fluoride to the GEM Collaboration*, December 4, 1991.

[13] M. Murashita *et al.*, Nucl. Inst. Meth. **A243** (1986) 67.

[14] S. Wu *et al.*, in CERN Green Book *ECFA Workshop on LEP 200*, Aachen, September, 1986.

[15] GEM Detector Barium Fluoride EM Calorimeter Design/Costing Update, Caltech/ORNL/LLNL Report, July 23, 1992.

[16] M. Lavel *et al.*, *Nucl. Instr. and Meth.* **A206** (1983) 169;
P. Schotanus *et al.*, *Nucl. Instr. and Meth.* **A259** (1987) 586; and *IEEE–NS* **34** (1987) 76.

[17] P. Schotanus *et al.*, *Nucl. Instr. and Meth.* **A238** (1985) 564; and Kobayashi *et al.*, *Nucl. Instr. and Meth.* **A270** (1988) 106.

[18] K. R. Shi *et al.Proposal for Welding a* 7×7 *Cell Supporting Structure for the GEM Detector Barium Fluoride EM Calorimeter*

[19] C. Wuest, B. Fuchs, and W. Kway, *Barium Fluoride Research and Development at Livermore National Lab*, July 24, 1992.

[20] M. Merk, *Study of Bhabha Scattering at the* Z^0 *Resonance Using the L3 Detector*, Nijmegen Ph. D. Thesis, 1992 (Unpublished).

[21] Hamamatsu Photonics K.K., *R4406 specification.*

[22] S. Suzuki, talk given in *Symposium on Detector Research and Development for the SSC*, Fort Worth, Texas, October 15—18 (1990).

[23] Hamamatsu, *Proposals to Develop a Remote Processed Proximity Focused Phototube*, March and June, 1992.

[24] H. Weisberg *et al.*, *Photodetectors for* BaF_2 *Calorimetry at the SSC*, 1992 DoE/SBIR Proposal.

[25] The ATT preamplifier has 1200 electron noise for an input capacitance of 10 pf. See M. Levi, in *Symposium on Detector Research and Development for the SSC*, Fort Worth, Texas, October 15—18 (1990) 3.

[26] P. Denes, BaF_2 *Update; General Readout Considerations*, Princeton University, July 1992.

[27] R.Y. Zhu, **CALT-68-1693**, in *ECFA LHC Workshop* Volume III, Aachen (1990) 411.

[28] The nominal gain of R4406 is 4 in the Hammamatsu specification. The reason of its lower gain, compared to the gain of 12 of Hammamatsu's standard R2148 triode, is due to the processing technology used. At present, the K-Cs-Te cathode has been evaporated inside the closed triode envelope. This contaminates the dynode. The lower gain of R4406 is due to the lower efficiency of the secondary electron emission from the K-Cs-Te contaminated dynode. By using a remote transfer technology in a large vacuum tank, this contamination will be eliminated. It is therefore expected (as indicated by Hammamatsu themselves) that R4406 triodes produced in future, under standard production conditions, will have a nominal gain of 12.

[29] J. Branson, Talk At the GEM Calorimeter Meeting at Tucson, GEM TN 92-84, March 1992; Report in preparation.

[30] K. Arisaka *et al.*, *KTeV Design Report*, Fermilab, January 22, 1992.

[31] R. Zhu, Talk presented at the August 9, 1992 Calorimter Group Meeting; H. Yamamoto, GEM Note in preparation, August 1992.

[32] Y. Kubota *et al.*, *The CLEO II Detector*, CLNS 91/1122, 1991.

[33] J. Wenniger, *Measurement of the Electroweak Paramters of the Z^0 with the Reaction* $e^+e^- \rightarrow e^+e^-(\gamma)$ (in French), University of Geneva Ph. D. Thesis No. 2544, 1992 (Unpublished).

[34] W. Ruchstuhl and J. Wenniger, L3 Internal Note 766 (1990).

[35] H. Newman, in GEM Technical Note TN 92-84, March, 1992.

[36] A. Bay *et al.*, *The Xenon Monitor of the L3 Electromagnetic Calorimeter*, University of Geneva Preprint UGVA-DPNC 1992/01-150, submitted to Nucl. Instr. and Meth.

[37] M. Strathman, Report on material characterization of BaF_2 samples to the BaF_2 Expert Panel, June 1992.

[38] M. Strathman, Report on material characterization and light-induced annealing of BaF_2 samples to the BaF_2 Expert Panel, August 3, 1992.

[39] S. Stoll, private communication. BNL report in preparation, August 1992.

[40] R.Y. Zhu *et al.*, *Super Collider I*, Plenum Press, ed. McAshan, (1989) 587;
H. Ma *et al.*, *Nucl. Instr. and Meth.* **A274** (1989) 113; and *Nucl. Instr. and Meth.* **A281** (1989) 469.

[41] R. Hamm *et al.*, *An SSC Electromagnetic Calorimeter Calibration Source*, Final SBIR Project Report to the Dept. of Energy, AccSys Technology Inc., Pleasanton, California, August, 1991.

[42] R. Zhu and U. Chaturvedi, *Final Acceptance Test of the L3 RFQ System*, Caltech/World Lab Internal Report, October, 1991.

[43] R.Y. Zhu, *Physics Requirements On The Precision of Electromagnetic Calorimeter at SSC*, GEM TN-91-06, August 1991.

[44] H. Bergstroem *et al.*, Penn State Preprint PSU/TH/63, March, 1990.

[45] G. Chen *et al.*, GEM Internal note **GEM TN-92-78**, March 1992.

[46] P.J. Li *et al.*, GEM Internal note **GEM TN-92-77**, March 1992;
Z.W. Yin, Talk given in First East Asia/Pacific – US Symposium on SSC, May 1992
Progress Report on the Work on BaF_2 Crystals, SIC, July 22, 1992.

[47] L.M. Wang *et al.*, *The Optical and Radiation Damage Properties of Barium Fluoride Crystals*, talk presented in Shanghai BaF_2 Workshop, Shanghai, May 1991.
L.Y. Chen *et al.*, *The Radiation Damage of BaF_2 Crystals*, talk prepared for GEM BaF_2 Panel meeting, Shanghai, December 1991.

[48] L. Halliburtoon *et al.*, Identification and Chracterization of Radiation-Induced Point Defects in BaF_2, University of West Virginia Optoelectronics Group Technical Reports, April - June 1992.

[49] *A Precision BaF_2 Crystal Calorimeter for the Superconducting Supercollider*, Subsystem R&D Proposal and Progress Report, September, 1991.

[50] F. Ajzenberg-Selove, *Nucl. Phys.* **A475** (1987) 1; and H. B. Willard *et al. Phys. Rev.* **85** (1952) 849.

[51] C. Wuest and G. J. Mauger, *Effects of Light Exposure on Irradiated Barium Fluoride Crystals*, LLNL Report, August 27, 1992.

[52] D.A. Ma and R.Y. Zhu, *Light Attenuation Length of Barium Fluoride Crystals*, **CALT-68-1811** and GEM TN-92-149, August 1992.

[53] D.A. Ma and R.Y. Zhu, *On Optical Bleaching of Barium Fluoride Crystals*, **CALT-68-1812** and GEM TN-92-149, August 1992.

[54] R.Y. Zhu, *Calibration with $Z \rightarrow e^+e^-$ at the SSC*, talk given in GEM Calorimeter meeting, August 9, 1992.

[55] Institute of High Energy Physics, and University of Science & Technology of China Proposal, *Constructing A Cosmic Ray Stand at IHEP & USTC for the GEM BaF_2 Calorimeter*, August 30, 1992.